

Appl. No. : 09/849,869
Filed : May 4, 2001

REMARKS

Claims 1-86 are pending in the present application. The Examiner indicated that Claims 1-15 and 17-86 have been withdrawn as being drawn to a non-elected invention, and refers to the Election made in Paper No. 23.

In the Response to Restriction Requirement filed on June 6, 2003 (Paper No. 23), Applicants elected Group CCXXIV. In particular, Applicants elected Claims 57 to 61 and 66-83. The claims were elected in so far as they relate to SEQ ID NO: 16. While SEQ ID NO: 16 is disclosed in Claim 16, Applicants did not elect Claim 16 for examination. Thus, Applicants request examination of the elected claims: Claims 57-61 and 66-83.

Despite the confusion over the elected claims, Applicants have addressed the portions of the Office Action that have general relevance.

First, the Examiner objected to text missing from the continuing data in line 7 of page 1. The specification has been amended to include the complete priority information.

The Examiner also objected to the labeling of Figure 1A. The captions of the three panels of Figure 1A have been amended to read Fig. 1A, Fig. 1B and Fig. 1C. Replacement figures are attached. The Brief Description of the Figures and other relevant portions of the specification have been amended accordingly. These amendments were made solely to conform the specification to the revised numbering of Figure 1 and do not add new matter.

Discussion of Rejection Relating to Utility

The Examiner argued that MrgX1 (SEQ ID NO: 16) lacks an apparent or disclosed specific and substantial credible utility. Applicants respectfully disagree.

The Standard

According to the Utility Examination Guidelines ("Utility Guidelines"; 66 Fed. Reg. 1092 (2001)), an application complies with the utility requirement of 35 U.S.C. §101 if it asserts at least one "specific, substantial, and credible utility." Each of the requirements is addressed separately below.

Applicants draw the Examiner's attention to the fact that the utility discussed below for the claimed receptor directly parallels the caveat in Example 12 in the utility guidelines training materials, which indicates that the use of a receptor as a marker to identify specific sub-

populations of cells is a substantial utility, where the value of the identification is recognized in the art. As described below, the utility of identifying specific sub-populations of pain sensing neurons in the dorsal root ganglia was clearly recognized in the art at the time the invention was made. Thus, Applicants' claimed utility meets the requisite standard under 35 U.S.C. §101.

Applicants Have Demonstrated a Specific Utility

The Utility Guidelines explain that a "specific" utility is one that is specific to the subject matter claimed, in contrast to a general utility that would be applicable to the broad class of the invention. Here, the specification indicates that probes based on the Mrg receptors can be used to identify nociceptive neurons within the dorsal root ganglia, and more specifically can be used to identify a particular sub-population of nociceptive neurons that express the lectin IB4 (IB4⁺; page 39, lines 22-26). The ability to identify sub-populations of nociceptive neurons is based on the specific expression pattern of the Mrg receptors. This is a utility that is particular to the claimed receptors and is not applicable to polypeptides or even receptors in general. Thus, applicants submit that a specific utility has been provided.

Applicants have Demonstrated a Substantial Utility

Applicants have provided a real-world use and thus have disclosed a substantial utility. As discussed above, the specification indicates that the claimed molecule can be used as a marker to identify a particular sub-population of nociceptive neurons within the dorsal root ganglia, those that are IB4⁺. The benefits of being able to identify specific sub-populations of nociceptive neurons within the dorsal root ganglia are well recognized in the art.

Applicants' disclose in the specification that all of the Mrg receptors they examined were expressed in wild type DRG but not in DRG from mice that lacked the neurogenin gene (Ngn^{-/-}) (see, e.g. Figure 2A of the specification). This indicated that the Mrg receptors are specifically expressed in nociceptive neurons. Expression of Mrg receptors was not detected in any other tissue of the body or in any other region of the nervous system that had been examined at the time of filing.

In addition, the specification discloses that the receptors are specifically expressed in TrkA⁺ nociceptive neurons within the DRG, and more specifically in a subset of nociceptive neurons that express the lectin IB4 (IB4⁺). This particular subclass of nociceptive neurons is

known to be therapeutically important. For example, a review of nociceptors by Caterina and Julius (Curr. Opin. Neurobiology 9:525-530 (1999), courtesy copy attached), demonstrates that IB4⁺ neurons are involved in chronic pain transmission (page 525, column 1, through page 526, first column). IB4⁺ neurons have also been found to be involved in neuropathic pain (Malmberg et al. Science 278:279-283 (1997), of record).

The utility of using markers to identify the sub-populations of neurons in the DRG, such as those involved in pain sensation is clear and is well recognized in the art. For example, Petruska et al. (J. Neurophysiology 84:2365-2379 (2000), courtesy copy attached), teach that interpretation of data from studies of the DRG is confounded by the various types of sensory cell bodies. Petruska, et al. state that the advantage of being able to study the nociceptive sub-populations of neurons is manifest (page 2365, second column).

In another example, the ability to identify IB4⁺ neurons allowed Bennet et al. (J. Neuroscience 18:3059-3072 (1998), courtesy copy attached) to study the viability of neurotrophin administration for the treatment of peripheral neuropathy with GDNF. Boucher et al. (Science 290:124-127 (2000), courtesy copy attached) demonstrate that GDNF has potent analgesic properties in neuropathic pain states.

The therapeutic benefit of being able to identify or target IB4⁺ neurons is made explicit by Vulchanova et al. (Neuroscience 108:143-145 (2001), abstract attached), who demonstrated that a toxin conjugated to IB4 can be used to kill IB4⁺ neurons and thereby decrease sensitivity to noxious stimuli. The ability to target IB4⁺ neurons based on Mrg expression, as disclosed in the present application, would facilitate such therapeutic applications.

For all of these reasons, one of skill in the art would recognize the substantial utility of using Mrg receptors as markers to identify specific, therapeutically important, sub-populations of neurons in the DRG.

Applicants have Demonstrated a Credible Utility

An assertion of utility is "credible" unless (A) the logic underlying the assertion is seriously flawed, or (B) the facts upon which the assertion is based are inconsistent with the logic underlying the assertion. Further, as stated in the Utility Guidelines, a credible utility is assessed from the standpoint of whether a person of ordinary skill in the art would accept that the recited or disclosed invention is currently available for such use.

Appl. No. : 09/849,869
Filed : May 4, 2001

As discussed above, the facts provided in the specification as filed are consistent with the logic underlying the assertion that Mrg receptors can be used to identify nociceptive neurons within the DRG. Thus, the application provides a credible utility.

Discussion of Rejections Under 35 U.S.C. §102

The Examiner found that MrgX1 (SEQ ID NO: 16) is anticipated by Ahmad et al. (WO 99/32519) because the present application is not entitled to priority under 35 U.S.C. §120. In reaching this conclusion, the Examiner indicated that the priority application (09/704,707) can not meet the requirements of 35 U.S.C. §112, first paragraph, where the present application, which is a continuation-in-part of the priority application, was found not to meet the requirements of §112.

In view of the arguments presented above, Applicants submit that the rejection under §101 and the related rejection under 35 U.S.C. §112 are improper. As the same utility is disclosed in the priority application 09/704,707, Applicant's submit that they are entitled to this priority under 35 U.S.C. §120 and that as a result, WO99/3519 is not available as prior art under 35 U.S.C. §102(b).

Appl. No. : 09/849,869
Filed : May 4, 2001

CONCLUSION

Applicant's respectfully request examination of all the elected claims. Further, they submit that in view of the arguments above, the elected claims are in condition for allowance. If the Examiner believes that a telephonic conference would be helpful, he is invited to contact the undersigned at the telephone number provided below.

Respectfully submitted,

KNOBBE, MARTENS, OLSON & BEAR, LLP

Dated: October 21, 2003

By:



Andrew N. Merickel
Registration No. 53,317
Attorney of Record
Customer No. 20,995
(415) 954-4114

W:\DOCS\ANM\ANM-6041.DOC
102103

A Distinct Subgroup of Small DRG Cells Express GDNF Receptor Components and GDNF Is Protective for These Neurons after Nerve Injury

David L. H. Bennett,¹ Gregory J. Michael,² Navin Ramachandran,¹ John B. Munson,³ Sharon Averill,² Qiao Yan,⁴ Stephen B. McMahon,¹ and John V. Priestley²

¹Department of Physiology, United Medical and Dental Schools (St. Thomas' Campus), London, SE1 7EH, United Kingdom, ²Department of Anatomy, Queen Mary and Westfield College, London, E1 4NS, United Kingdom, ³Department of Neuroscience, University of Florida College of Medicine, Gainesville, Florida 32610, and ⁴Department of Neuroscience, Amgen Inc., Thousand Oaks, California 91320

Several lines of evidence suggest that neurotrophin administration may be of some therapeutic benefit in the treatment of peripheral neuropathy. However, a third of sensory neurons do not express receptors for the neurotrophins. These neurons are of small diameter and can be identified by the binding of the lectin IB4 and the expression of the enzyme thiamine monophosphatase (TMP). Here we show that these neurons express the receptor components for glial-derived neurotrophic factor (GDNF) signaling (RET, GFR α -1, and GFR α -2). In lumbar dorsal root ganglia, virtually all IB4-labeled cells express RET mRNA, and the majority of these cells (79%) also express GFR α -1, GFR α -2, or GFR α -1 plus GFR α -2.

GDNF, but not nerve growth factor (NGF), can prevent several axotomy-induced changes in these neurons, including the downregulation of IB4 binding, TMP activity, and somatostatin expression. GDNF also prevents the slowing of conduction velocity that normally occurs after axotomy in a population of small diameter DRG cells and the A-fiber sprouting into lamina II of the dorsal horn. GDNF therefore may be useful in the treatment of peripheral neuropathies and may protect peripheral neurons that are refractory to neurotrophin treatment.

Key words: IB4; *trkA*; RET; somatostatin; GFR α -1; GFR α -2; axotomy; C-fibers; nociception; pain; sprouting; spinal cord

In the adult animal, specific dorsal root ganglion (DRG) cell populations require particular neurotrophins for their phenotypic maintenance (Verge et al., 1996). The *trk* receptors in general are expressed in a nonoverlapping manner by sensory neurons in combination with the low-affinity neurotrophin receptor p75 (Wright and Snider, 1995). Large diameter DRG cells mostly possess myelinated axons and respond principally to low threshold stimuli. These neurons express *trkB* or *trkC* or both (McMahon et al., 1994). Small diameter DRG cells, in contrast, have unmyelinated axons and are principally nociceptors and thermoreceptors. Half of this group (40% of total DRG cells) constitutively synthesize neuropeptides and express *trkA* (Averill et al., 1995; Molliver et al., 1995). The other half of the small diameter DRG cells (35% of total DRG cells) possess cell surface glycoconjugates that can be identified by binding of the lectin Isolectin B4 from *Griffonia simplicifolia* (IB4) (Silverman and Kruger, 1990). They also express the enzyme thiamine monophosphatase (TMP). During development these cells are dependent on NGF for survival (Silos-Santiago et al., 1995). During the postnatal

period, however, these cells downregulate *trkA* expression (Bennett et al., 1996a; Molliver and Snider, 1997). It is this population that in the adult does not express detectable levels of the low-affinity neurotrophin receptor p75 nor any known *trk* receptor (McMahon et al., 1994; Averill et al., 1995; Molliver et al., 1995; Wright and Snider, 1995). In this study we have examined the possibility that GDNF exerts a trophic action on these neurons.

GDNF is a member of the transforming growth factor- β (TGF- β) superfamily (Lin et al., 1993) and is related to neurturin (Kotzbauer et al., 1996). GDNF has been demonstrated to have potent survival-promoting effects on midbrain dopaminergic neurons (Beck et al., 1995; Bowenkamp et al., 1995) and motoneurons (Henderson et al., 1994; Oppenheim et al., 1995; Yan et al., 1995). There is growing evidence that GDNF can have a trophic action on sensory neurons. In GDNF-deficient mice there is a significant reduction in the number of spinal sensory neurons (Moore et al., 1996). During the late embryonic and postnatal period, the survival of a subpopulation of DRG cells is supported by this factor *in vitro* (Buj-Bello et al., 1995), and those neurons that are supported are IB4 binding (Molliver et al., 1997). GDNF can also prevent the death of axotomized developing sensory neurons *in vivo* (Matheson et al., 1997).

The receptor for GDNF is thought to be a complex of GFR α -1 (Jing et al., 1996; Treanor et al., 1996; GFR α Nomenclature Committee, 1997), which acts as a ligand binding domain, and RET, which acts as the signal transducing domain (Durbec et al., 1996; Trupp et al., 1996). Neurturin also appears to use RET for signaling, but operates via another GPI-linked binding protein termed GFR α -2 (Baloh et al., 1997; Buj-Bello et al., 1997; GFR α Nomenclature Committee, 1997; Klein et al., 1997). GDNF may

Received Dec. 8, 1997; revised Jan. 23, 1998; accepted Jan. 28, 1998.

This work was funded by the Medical Research Council of Great Britain. D.L.H.B. is supported by the Special Trustees of Guy's and St. Thomas' Hospitals. We acknowledge the expert technical assistance of C. Abel and S. Hamilton. We also thank Genentech for the provision of rhNGF and Amgen for the provision of rhGDNF; H. S. Phillips and R. D. Klein for the provision of the GFR α -2 sequence; and Dr. D. O. Clary, Dr. T. Görcs, and Professor J. M. Polak for the provision of the *trkA*, somatostatin, and CGRP antisera, respectively.

D.L.H.B. and G.J.M. contributed equally to this work.

Correspondence should be addressed to Professor S. B. McMahon, Department of Physiology, St. Thomas' Hospital Medical School, Lambeth Palace Road, London SE1 7EH, UK.

Copyright © 1998 Society for Neuroscience 0270-6474/98/183059-14\$05.00/0

also be able to act via GFR α -2, particularly in the presence of RET (Sanicola et al., 1997). In this study, we have examined the expression of these GDNF receptor subunits within adult sensory neurons.

One means of studying the trophic requirements of different subgroups of sensory neurons has been to determine to what extent injury-induced changes can be reversed by the administration of exogenous trophic factors (Verge et al., 1995, 1996). The second aim of the present work was to investigate the efficacy of GDNF in reversing such axotomy-induced changes in adult sensory neurons.

MATERIALS AND METHODS

Animal surgery. Adult male Wistar rats underwent unilateral sciatic nerve section combined with an intrathecal infusion of recombinant human GDNF (rhGDNF), rhNGF or control buffer. The sciatic nerve was exposed under pentobarbitone anesthesia (40 mg/kg, i.p., with sterile precautions) and ligated 20 mm distal to the obturator tendon. Concurrently a small laminectomy was performed between L6 and S1 vertebrae, and the dura was cut. A SILASTIC tube of 0.6 mm outer diameter was introduced intrathecally so that its tip lay at the level of the lumbar enlargement of the spinal cord. The intrathecal tubing was attached to an Alzet miniosmotic pump (type 2002; Alzet, Alza Corporation, Palo Alto, CA) delivering at a rate of 0.5 μ l/hr. Animals received either a control infusion ($n = 4$; saline with rat serum albumin, 1 mg/ml) or this vehicle plus rhGDNF ($n = 4$ at 12 μ g/d; $n = 3$ at 1.2 μ g/d) or rhNGF ($n = 3$ at 12 μ g/d; $n = 3$ at 1.2 μ g/d). Another group of animals underwent axotomy with either control infusion ($n = 4$) or GDNF treatment ($n = 4$ at 12 μ g/d; $n = 3$ at 1.2 μ g/d). Twelve days later the left sciatic nerve was re-exposed and injected with 4 μ l of 1% B-subunit of cholera toxin (CTB) (List Biological Labs, Campbell, CA) in distilled water, using a micropipette glued to a Hamilton syringe. Animals were perfused with heparinized saline followed by 4% paraformaldehyde 14 d after sciatic section. Another group of normal animals ($n = 5$) was labeled with CTB in the same manner but did not undergo sciatic axotomy. After perfusion the left and right L4 and L5 DRGs were removed as well as L3–L6 segments of the spinal cord. Pins were placed in the right side of the spinal cord at the border between L3/L4, L4/L5, and L5/L6 to ease identification of the spinal levels during analysis. Tissues were post-fixed in 4% paraformaldehyde for 2 hr, after which they were transferred to 15% sucrose overnight. One group of animals ($n = 4$) was perfused in the same manner and used for *in situ* hybridization. Another group of naive animals ($n = 3$) was used to provide control values for IB4, somatostatin, calcitonin gene-related peptide (CGRP), and TMP staining.

Electrophysiological analysis was performed on five different groups of animals: normal intact animals ($n = 4$); animals in which the tibial nerve had been cut and tied 2 weeks previously and with an intrathecal cannula delivering 1 mg/ml normal rat serum albumin in saline at 12 μ l/d ($n = 5$); animals with tibial nerve axotomy and continuous intrathecal delivery of rhGDNF (12 μ g/d; $n = 3$), rhNGF (12 μ g/d; $n = 3$), or rhGDNF and rhNGF (12 μ g/d each; $n = 4$). This surgery was performed under pentobarbitone anesthesia and with sterile precautions.

Staining procedures. Sections of DRG and spinal cord were cut at a thickness of 15 and 20 μ m, respectively. Sections of DRG were cut serially onto slides so that each slide contained an ordered series of sections throughout the ganglia, at a separation of at least 150 μ m between sections. When the spinal cord was cut, every fifth section was mounted serially onto slides. Every slide therefore had a series of sections through the L4 and L5 region of spinal cord at a separation of at least 800 μ m between sections. For immunostaining, primary antisera were rabbit anti-CGRP (1:2000, gift of Professor J. M. Polak), rabbit anti-somatostatin (1:2000, gift of Dr. T. Görcs), goat anti-CTB (1:2000, List), and biotinylated IB4 (10 μ g/ml, Sigma). Secondary antisera were FITC- or TRITC-conjugated anti-rabbit or anti-goat IgG (1:200, Jackson Labs) or FITC-conjugated Extr-Avidin (1:200, Sigma). Histochemistry for TMP was also performed as described previously (McMahon, 1986).

Analyses of colocalization of RET immunoreactivity with other DRG products were performed on 8 μ m cryostat sections using dual-labeling immunofluorescence. The production and staining characteristics of the RET antiserum have already been described (Molliver et al., 1997). RET immunostaining was combined sequentially with markers described above as well as sheep anti-CGRP (1:2000, Affinity) and anti-rabbit trkA

(Averill et al., 1995). Indirect tyramide signal amplification (TSA, New England Nuclear) was used for the first reaction when staining with two rabbit antisera as described previously (Michael et al., 1997). The lack of cross-reactivity is thought to be caused by the fact that the primary antiserum is highly diluted compared with when it is used in indirect immunofluorescence without amplification (e.g., trkA 1:100,000 vs 1:4000), and therefore the second series reactions do not detect it. This was verified by a lack of staining in control single-labeled preparations using indirect immunofluorescence and the antiserum dilutions used for TSA.

For combined fluorescence histochemistry with *in situ* hybridization, cryostat sections (6–8 μ m) were cut and thaw-mounted onto Superfrost Plus slides (BDH Chemicals, Poole, UK). Immunocytochemistry and/or lectin binding histochemistry was performed before *in situ* hybridization (Michael and Priestley, 1996b; Michael et al., 1997). Sections were incubated for 40–48 hr at room temperature with trkA antibody (4 μ g/ml), N52 monoclonal antibody to phosphorylated heavy chain neurofilament (1:400, Sigma), or biotinylated IB4 (10 μ g/ml) diluted in diethylpyrocabonate (DEPC)-treated PBS containing 0.2% Triton X-100, 0.1% sodium azide, 0.5 mM dithiothreitol, and 100 U/ml RNasin (Promega, Madison, WI). Lectin binding buffer also contained 0.1 mM $MnCl_2$, 0.1 mM $MgCl_2$, and 0.1 mM $CaCl_2$. Sections were washed in DEPC PBS and incubated for 4 hr in tetramethyl rhodamine isothiocyanate (TRITC)-conjugated secondary antibodies (1:200, Jackson Laboratory, Bar Harbor, ME) or fluorescein isothiocyanate (FITC)-conjugated Extr-Avidin (1:200, Sigma) diluted in the same buffer without added divalent cations. After additional washes in DEPC PBS, sections were processed through prehybridization steps, hybridized to 35 S-dATP end-labeled oligonucleotides, and washed as described previously (Michael and Priestley, 1996a). Slides were dipped in autoradiographic emulsion (Amersham, Arlington Heights, IL) and developed after 4–6 weeks. After the slides were coverslipped with PBS glycerol (1:3 containing 2.5% 1,4-diazobicyclo-(2,2,2)-octane), fluorescent labeling and silver grains were visualized using epifluorescence microscopy combined with either epipolarized illumination or dark-field illumination. The oligonucleotides used for probes were complementary to nucleotides 996–1029 of the rat GFR α -1 sequence (Jing et al., 1996) and nucleotides 161–194 of the rat RET sequence (Canzian et al., 1995), and for GFR α -2 the oligonucleotide sequence cctggactgatgtttgtcgtgactctgtgaagc was used (Klein et al., 1997).

Controls for the specificity of *in situ* hybridization included adding a 100-fold excess of unlabeled oligonucleotide to hybridization buffer, which effectively competed all specific binding of radiolabeled probe. Use of the GFR α -1, GFR α -2, and RET to label sections of rat brain yielded patterns of hybridization identical to reported patterns (Trupp et al., 1997) (our unpublished observations). All probes were synthesized to be of the same size and G+C base content and produced reproducible and characteristic patterns of labeling.

Image analysis. After *in situ* hybridization, cells that had silver grains over the cell cytoplasm at least five times background were counted as positive. For quantitation of *in situ* hybridization, counts of cells labeled for RET, GFR α -1, and GFR α -2 and coexpressed cell markers were conducted on ganglia from at least four animals, with separation between analyzed sections being at least 100 μ m. At least 1500 cells were counted for each probe/peptide combination. For counts of the percentage of cell profiles expressing CGRP, somatostatin, IB4 binding, and TMP activity after different treatments, six sections were randomly selected for each marker for each animal in each group. In each section the total number of cell profiles was counted using dark-field illumination, and then the number of positively stained cell profiles was counted.

For image analysis of IB4, TMP, CGRP, and CTB staining within the dorsal horn, four randomly selected sections of L4/5 spinal cord were used from each animal. Two sections were selected from L4 and two sections were selected from L5 to ensure that the analysis was not biased toward one region of the lumbar enlargement. For analysis of IB4, CGRP, and TMP staining, images of spinal cord sections were captured directly off the microscope at 25 \times objective magnification using a Grunig FA87 digital camera with integrating framestore. The image was then thresholded to a set level to reveal the labeling. Four boxes of size 27 \times 27 μ m were placed over lamina II of the axotomized side (within the sciatic territory) and in equivalent positions on the contralateral (i.e., intact sciatic) side of the sections. The area occupied by labeled terminals was then calculated for each box. A similar method was used for analysis of CTB staining, but in this case the four boxes were placed over lamina III of the sciatic-labeled territory and four were placed dorsal to the

lamina III-boxes in lamina II outer. The area occupied by CTB-stained terminals within each of these boxes was then calculated.

This image analysis system was similarly used for cell size distribution analyses of RET, GFR α -1, and GFR α -2. Images of DRG sections were captured directly off the microscope as described above. Cell profiles were outlined using a hand-held mouse from which the cell area was calculated. For the RET analysis 1128 profiles were drawn, for the GFR α -1 analysis 990 profiles were drawn, and for the GFR α -2 analysis 567 profiles were drawn. Cell size distribution analyses were also performed on normal L4/5 ganglia ($n = 4$ animals), axotomized ganglia ($n = 4$ animals), and ganglia that had undergone axotomy in combination with GDNF treatment ($12 \mu\text{g/d}$; $n = 4$). Twelve sections that had been cut at a thickness of $15 \mu\text{m}$ and stained with toluidine blue were selected for each animal. The selected section was then divided into quadrants, and all the profiles within a randomly selected quadrant were outlined. In total 2033 profiles were drawn in the normal group, 2256 in the axotomy group, and 1875 in the axotomy plus GDNF group.

Trophic factor effects on electrophysiological properties of axotomized C-fibers. As an independent measure of the efficacy of trophic factors, we studied the electrophysiological properties of damaged C-fibers. The conduction velocity (CV) distribution of C-fibers projecting through the tibial nerve was measured in urethane-anesthetized animals (1.25 gm/kg , i.p.) in terminal experiments. Fine strands of the L5 dorsal root were dissected and mounted on recording electrodes. The tibial nerve was continuously electrically stimulated at 2 Hz with square wave current pulses: 5 mA, 1 msec. The evoked activity on the root filament was amplified and filtered by conventional means, and the averages of 64–128 responses were constructed (see Fig. 9). In these averages it was possible to determine the latency of individual fibers. All fibers conducting at less than 2 m/sec were included in analysis. Typically 3–10 C-fibers were found in each strand. A sample of approximately 50 individual C-fibers was measured in each animal, from which the conduction velocity distribution was computed. Distributions from three to five animals in each experimental group were averaged and plotted as cumulative sums (e.g., see Fig. 9). The distributions of CVs were statistically compared using the Kolmogorov–Smirnov test.

RESULTS

GDNF receptor expression within sensory neurons

Abundant labeling for RET, GFR α -1, and GFR α -2 mRNAs was observed in lumbar DRG cells (Fig. 1), with 64 ± 4.4 , 40.6 ± 1.5 , and $32.8 \pm 1.0\%$ of DRG cell profiles labeled, respectively. Cells of all sizes showed labeling, but GFR α -2 and RET mRNAs were expressed by proportionally more small and intermediate-sized cells (Figs. 1, 2).

To identify the cell types that were labeled, *in situ* hybridization was combined with immunocytochemistry for markers that are widely used to characterize three main DRG subpopulations (Averill et al., 1995). Strikingly, a high level of expression of all three GDNF receptor components (RET, GFR α -1, and GFR α -2) was found in cells labeled with the lectin IB4 (Fig. 2, Table 1), a marker for small neurons that do not express any of the trk receptors (Averill et al., 1995; Molliver et al., 1995). In the case of RET, virtually all IB4 cells express RET mRNA (95%), and the IB4 cells account for a very high percentage of the RET population (79%) (Table 1). In contrast to RET, GFR α -1 and GFR α -2 mRNAs are each expressed in only approximately half of the IB4 cells (46 and 55%, respectively) (Table 1). To determine whether GFR α -1 and GFR α -2 are expressed by the same IB4 cells, serial sections were triple-labeled for trkA, IB4, and GFR α -1 or GFR α -2 mRNAs (Fig. 3). This analysis revealed that the RET/IB4 cells can be subdivided into four, roughly equally sized subgroups, based on their expression of the GFR α subunits: GFR α -1 alone (21% of IB4 cells), GFR α -2 alone (28%), both GFR α -1 and GFR α -2 (30%), and neither GFR α -1 nor GFR α -2 (21%).

In contrast to the high expression of GDNF receptor components in the IB4 cells, expression was low in the second subpopu-

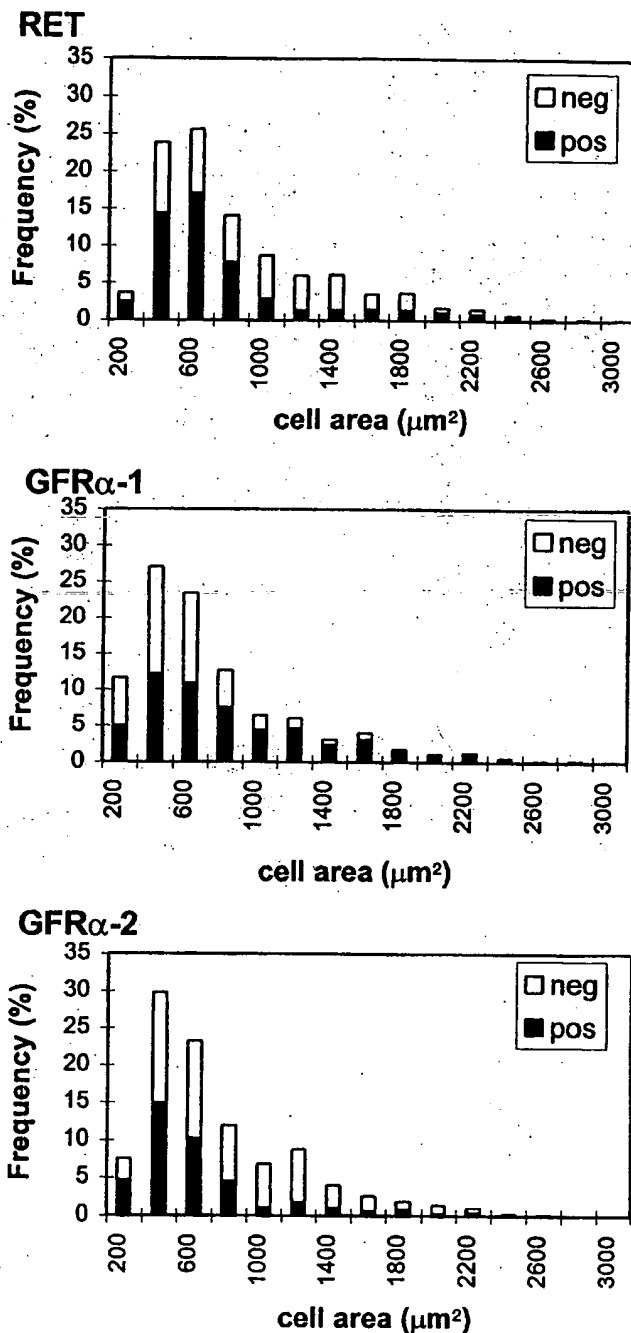


Figure 1. Cell size distribution of DRG cell profiles positively and negatively labeled for RET, GFR α -1, and GFR α -2 within L4/5 dorsal root ganglia. RET and GFR α -2 are present predominantly in small and intermediate diameter DRG cell profiles but are also present in some large diameter DRG cell profiles. GFR α -1 is more evenly distributed through the whole cell size spectrum.

lation of DRG cells, namely the trkA immunoreactive cells. GFR α -2 mRNA was observed in very few trkA immunoreactive cells (3%) (Table 1), and although RET mRNA was expressed by a significant number of trkA cells (28%) (Table 1), they belonged to a group that also showed IB4 labeling (Table 1). The majority of trkA cells do not show IB4 labeling (Averill et al., 1995; Michael et al., 1997) and did not express either RET or GFR α -2

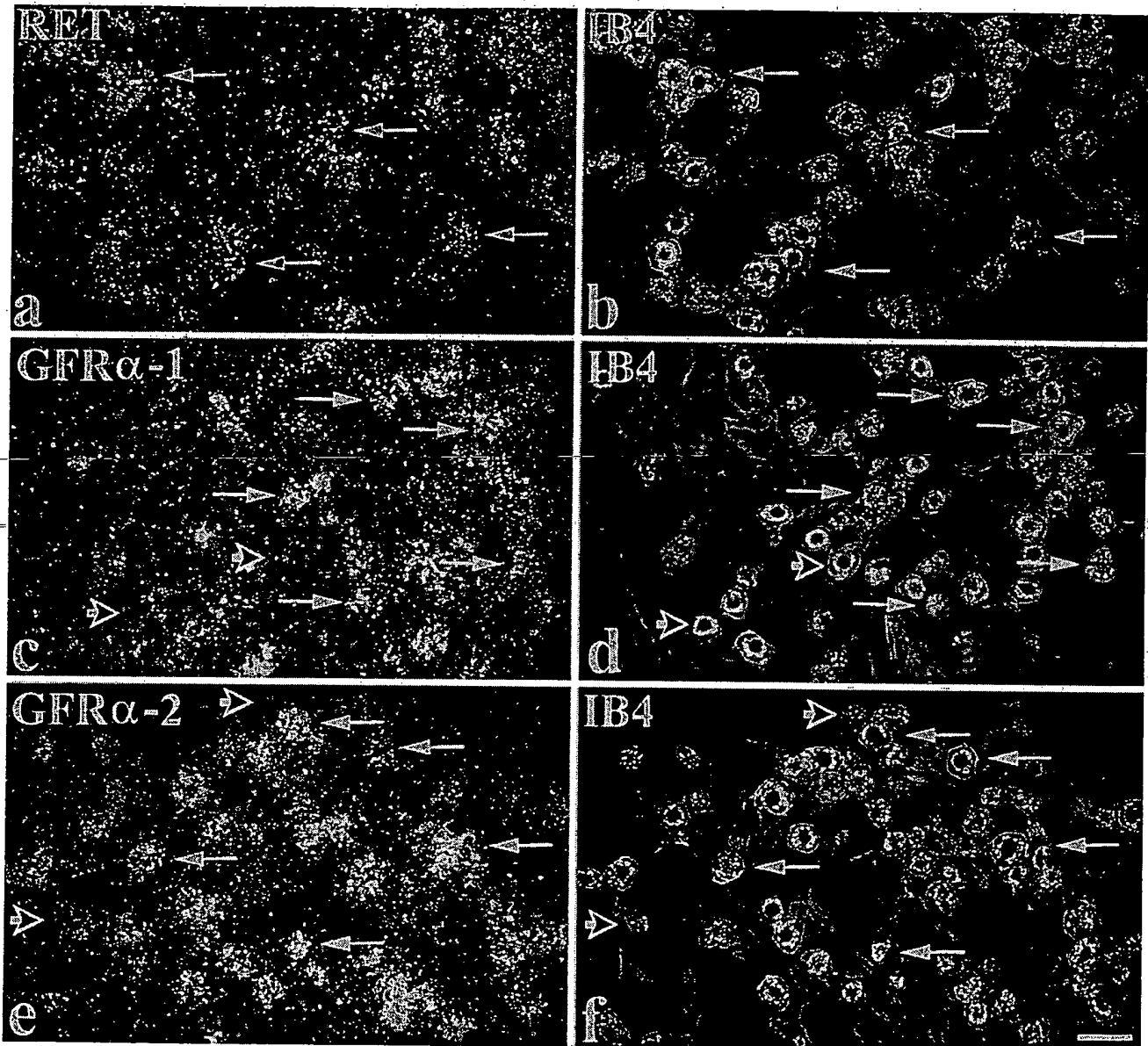


Figure 2. Expression of RET, GFR α -1, and GFR α -2 in IB4-labeled DRG cells. *In situ* hybridization for RET (a), GFR α -1 (c), or GFR α -2 (e) was combined with IB4 labeling (b, d, f). a and b show that many IB4 cells express RET (arrows indicate double-labeled cells). A similar pattern is seen in c and d and in e and f in relation to GFR α -1 and GFR α -2, except that the GFR α components are expressed in a smaller proportion of IB4 cells. Long arrows indicate IB4-labeled cells that express GFR α -1 or GFR α -2, whereas short open arrows indicate IB4 cells that do not express GFR α -1 or GFR α -2. Scale bar, 50 μ m.

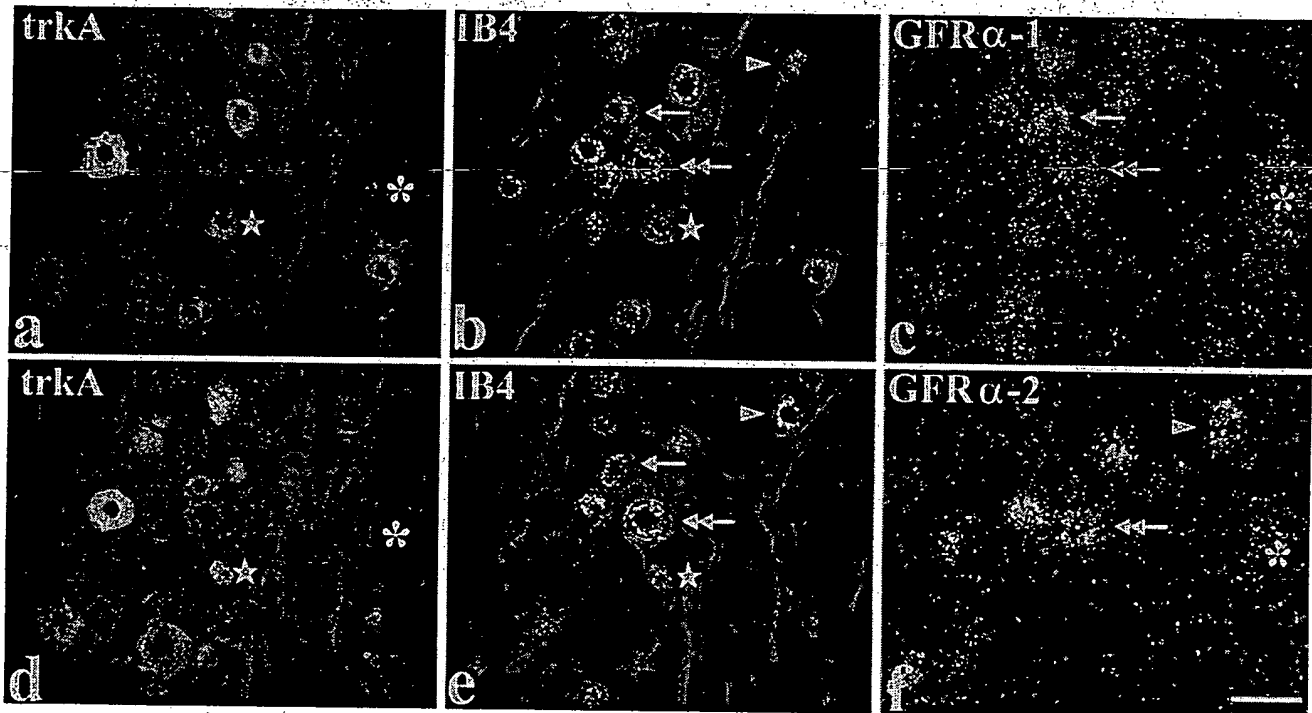
mRNAs (Table 1). However, a small number of these cells do express GFR α -1 mRNA (Table 1). The GDNF receptor components were also expressed in the third subpopulation of DRG cells, namely large neurons that can be identified by labeling with anti-neurofilament antisera such as N52. GFR α -1 and RET mRNAs are expressed by a significant number of N52 immunoreactive cells (40 and 33%, respectively) (Table 1), but GFR α -2 is virtually absent (only 5% of N52 cells).

To further study the pattern of RET expression, a polyclonal antiserum to RET was used (Molliver et al., 1997). Staining of L4/5 DRG sections (Fig. 4) revealed immunoreactivity in a population of DRG cells similar to that labeled by *in situ* hybridization. Thus 72% of L4/5 DRG cell profiles were RET

immunoreactive, and of these the majority were also IB4-labeled (96% of IB4 cells were RET immunoreactive) (Fig. 4). Only 27 and 30%, respectively, of RET immunoreactive cells showed immunoreactivity for trkA or for the neuropeptide CGRP (Fig. 4). The distribution of RET immunoreactivity in the lumbar enlargement of the spinal cord was also studied. RET immunoreactive terminals were present principally in lamina IIi (Fig. 4), the same region in which IB4 labeling is observed (Fig. 4). It was interesting, given that some large diameter DRG cells express RET (see above), that clear labeling for RET immunoreactive terminals was not observed in the regions of the spinal cord where these neurons terminate, i.e., the deep dorsal horn or the ventral horn.

Table 1. Percentage of DRG neurons co-expressing immunoreactivity for *trkA*, IB4, *trkA* + IB4, or NS2 and *in situ* hybridization signal for RET, GFR α -1, and GFR α -2 mRNAs

	RET mRNA		GFR α -1 mRNA		GFR α -2 mRNA	
	% RET expressing other	% other expressing RET	% GFR α -1 expressing other	% other expressing GFR α -1	% GFR α -2 expressing other	% other expressing GFR α -2
TrkA	15.0 \pm 0.8	27.7 \pm 2.2	17.9 \pm 1.2	18.0 \pm 1.0	2.8 \pm 0.4	2.9 \pm 0.4
IB4	78.7 \pm 1.1	95.3 \pm 0.3	49.5 \pm 1.0	46.0 \pm 3.6	78.3 \pm 1.8	54.5 \pm 0.6
TrkA + IB4	13.5 \pm 2.2	77.0 \pm 8.4	2.5 \pm 0.5	12.7 \pm 1.5	2.1 \pm 0.6	9.2 \pm 2.3
NS2	25.8 \pm 3.3	33.0 \pm 2.0	40.0 \pm 3.8	40.0 \pm 2.0	16.7 \pm 1.7	5.0 \pm 0.4

**Figure 3.** GFR α -1 and GFR α -2 expression in IB4 cells. GFR α -1 and GFR α -2 are coexpressed in one group of IB4 cells, expressed separately in other groups, and not expressed at all in a fourth group. Serial sections are shown triple-labeled for *trkA* (a, d), IB4 (b, e), and either GFR α -1 (c) or GFR α -2 (f) mRNAs. A IB4 cell expressing only GFR α -1 is identified by an arrow. An arrowhead indicates a IB4 cell that expresses only GFR α -2. The double arrow indicates a IB4 cell that expresses both GFR α -1 and GFR α -2. Note that none of these cells are *trkA* immunoreactive. The star indicates a IB4 cell that expresses neither GFR α -1 nor GFR α -2. This cell is also *trkA* immunoreactive. Also shown is a large cell (asterisk) that expresses both GFR α -1 and GFR α -2. It is not IB4-labeled or *trkA* immunoreactive. Scale bar, 50 μ m.

GDNF reverses axotomy-induced changes in the IB4-binding population of sensory neurons

To investigate the trophic effects of GDNF on sensory neurons, the ability of GDNF and NGF to reverse axotomy-related changes in different populations of sensory neurons was compared. Two different doses of these factors were used: a low dose of 1.2 μ g/d and a high dose of 12 μ g/d administered continuously over 14 d (these doses were based on our own and others previous findings) (Bennett et al., 1996b, Verge et al., 1995), and because these proteins are being administered *in vivo*, these doses are much higher than would be considered appropriate *in vitro*.

There were marked phenotypic changes in the IB4-binding population of small diameter DRG cells after 2 weeks of axotomy, including a reduction in the percentage of DRG cell profiles that bind IB4, from ~40% to <20% (Fig. 5, Table 2). Intrathecal application of low-dose GDNF significantly increased the number of DRG cell profiles binding IB4 after axotomy (p <

0.001; unpaired *t* test), and the high-dose GDNF treatment was even more effective (p < 0.001; unpaired *t* test) (Fig. 5, Table 2). In contrast, intrathecal application of NGF (at either dose) had no significant effect on this marker (Fig. 5, Table 2). TMP is an enzyme present principally in the IB4-binding "trk-less" population of DRG cells. A histochemical reaction was used to reveal TMP activity within DRG cells, and this produced a black reaction product within the cytoplasm of cells. Axotomy led to a large reduction in the proportion of DRG cell profiles that expressed TMP activity (Fig. 5, Table 2). Intrathecal administration of GDNF at a low dose produced a significant increase in the proportion of cell profiles expressing TMP activity compared with no treatment (p < 0.05; unpaired *t* test) (Table 2). Intrathecal administration of GDNF at a high dose after axotomy was even more effective (p < 0.001; unpaired *t* test) (Fig. 5, Table 2) and restored TMP activity to a level not significantly different from normal. Intrathecal administration of NGF (at either dose)

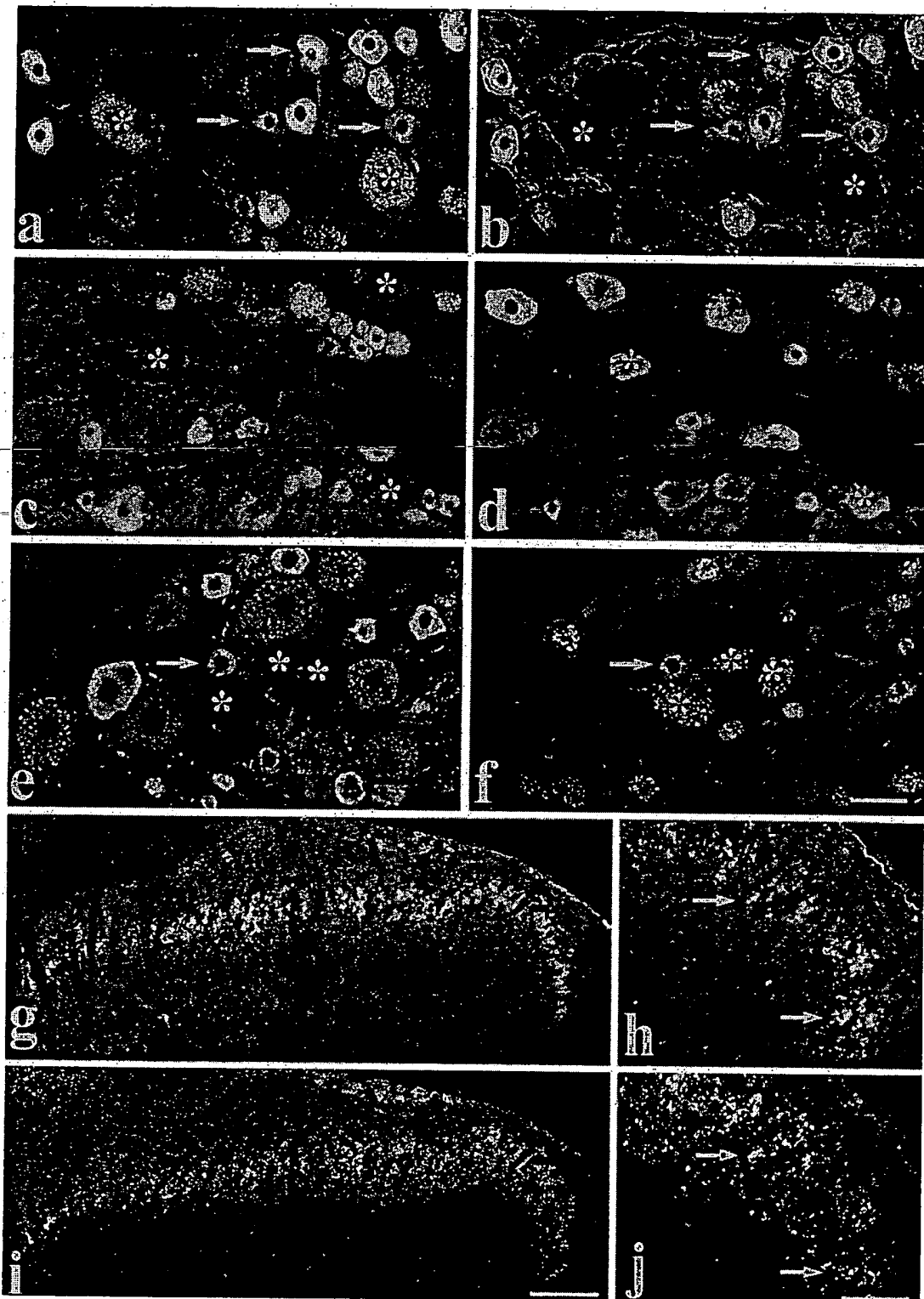


Figure 4. Colocalization of RET immunoreactivity with neurochemical markers in DRG cells and spinal cord. *a–f*, Dual labeling showing RET immunofluorescence (*a, c, e*) combined with IB4 labeling (*b*), trkA immunofluorescence (*d*), and CGRP immunofluorescence (*f*) in DRG cells. *Arrows* indicate extensive colocalization of RET and IB4 in small diameter cells (*a, b*). Note that all IB4 cells show RET immunoreactivity. However, several RET positive cells do not bind IB4 (*asterisks*). RET labeling is not evident in many trkA cells (*c, d*). *Asterisks* denote trkA cells that are not co-labeled for RET. Similarly, few CGRP-expressing DRG cells are RET immunoreactive (*e, f*). *Asterisks* indicate cells that do not express RET but are labeled for CGRP. The *arrow* indicates a cell that is dual-labeled. *g–j*, Low-magnification (*g, i*) and high-magnification (*h, j*) micrographs showing RET immunofluorescence (*g, h*) and IB4 (*i, j*) double labeling in the dorsal horn of the spinal cord. Labeling is most intense in inner lamina II. *Arrows* in *h* and *j* indicate individual double-labeled axons. Scale bars (shown in *f*): *a–f*, 50 μ m; (shown in *i*): *g, i*, 100 μ m; (shown in *j*): *h, j*, 30 μ m.

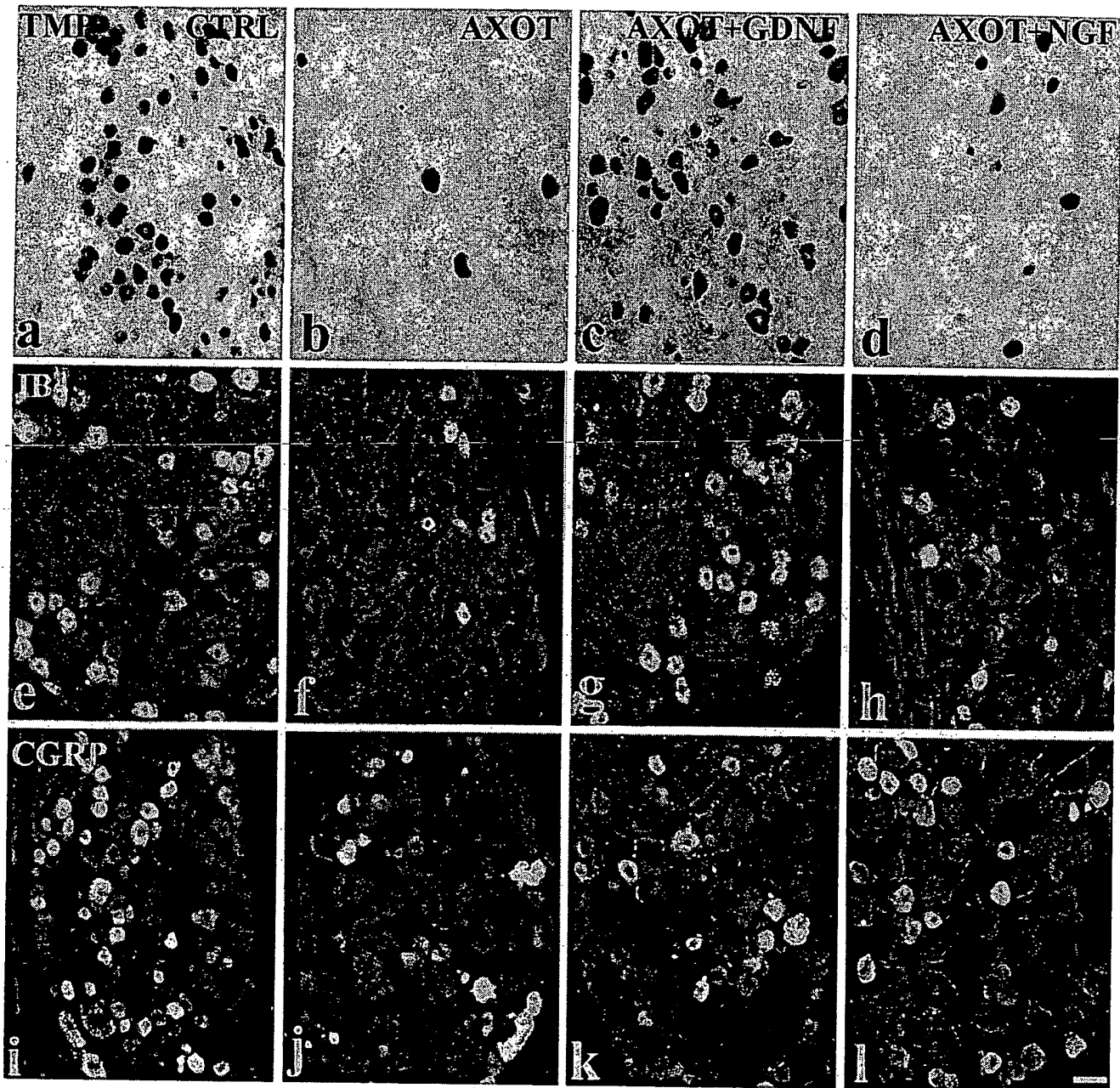


Figure 5. Histochemistry for TMP (*a–d*), IB4 labeling (*e–h*), and CGRP immunofluorescence (*i–l*) in dorsal root ganglia of control animals (*a, e, i*), animals with unilateral sciatic nerve section (*b, f, j*), animals with unilateral sciatic nerve section combined with intrathecal GDNF treatment (*c, g, k*), and animals with unilateral sciatic nerve section combined with intrathecal NGF treatment (*d, h, l*). Sciatic nerve section causes a loss of TMP (*b*) and IB4 (*f*) labeling, which is prevented by GDNF treatment (*c, g*) but not by NGF (*d, h*). In contrast, the loss of CGRP staining caused by sciatic nerve section (*j*) is prevented by NGF (*l*) but not by GDNF (*k*). Scale bar, 50 μ m. CTRL, Control; AXOT, axotomized.

was ineffective in restoring the proportion of DRG cell profiles expressing TMP activity after axotomy (Fig. 5, Table 2). Somatostatin is a neuropeptide expressed in a subgroup of *trk*-less DRG cells (Kashiba et al., 1996); its expression drops after axotomy (Table 2). Administration of GDNF at a low dose produced a small nonsignificant increase in the number of DRG cell profiles expressing somatostatin after axotomy. Intrathecal administration of GDNF at a high dose prevented this axotomy-induced change ($p < 0.05$; unpaired t test; compared with axo-

tomy alone) (Table 2). Intrathecal administration of NGF was ineffective in preventing this change (Table 2).

These effects are in contrast to those seen in the other population of small diameter DRG cells, those that express the *trkA* receptor and the neuropeptide CGRP. CGRP expression in DRG cell profiles fell markedly after axotomy, from ~40% of cell profiles to ~25%. Intrathecal application of NGF at a low dose could partially prevent this reduction (Table 2). Intrathecal application of NGF at a high dose prevented this reduction ($p <$

Table 2. The percentage of profiles stained for IB4, TMP, CGRP, or SOM in naive animals or after axotomy alone or axotomy in combination with treatment with GDNF (1.2 or 12 μ g/d) or NGF (1.2 or 12 μ g/d)

	Naive	Axotomized	Axotomized + GDNF 1.2	Axotomized + GDNF 12	Axotomized + NGF 1.2	Axotomized + NGF 12
IB4	41.1 \pm 0.7% (7498)	19.1 \pm 1.0% (8400)	33.7 \pm 0.9% (7664)	36.0 \pm 0.6% (5878)	20.7 \pm 1.7% (6626)	22.7 \pm 2.7% (5999)
TMP	36.6 \pm 0.7% (5446)	19.6 \pm 4.7% (8440)	28.7 \pm 2.4% (7653)	38.6 \pm 0.9% (7751)	20.4 \pm 0.5% (5979)	20.2 \pm 0.3% (5657)
CGRP	40.3 \pm 0.5% (8394)	24.5 \pm 4.3% (6243)	19.3 \pm 0.6% (8401)	26.8 \pm 1.3% (6732)	34.6 \pm 0.9% (6331)	38.8 \pm 0.9% (5380)
SOM	5.4 \pm 0.1% (6756)	2.6 \pm 0.26% (5560)	3.5 \pm 0.2% (7983)	4.8 \pm 0.41% (5569)	2.0 \pm 0.03% (6570)	2.3 \pm 0.1% (5177)

The numbers in parentheses represent the total number of profiles counted. SOM, Somatostatin.

0.05; unpaired *t* test) (Fig. 5, Table 2). Administration of GDNF (at a low dose or a high dose) had no significant effect on the proportion of DRG cell profiles expressing CGRP after axotomy (Fig. 5, Table 2).

A size analysis was performed to ensure that changes in DRG cell profile counts after different interventions did not occur as a consequence of alterations in cell size. The mean cell profile size in L4/5 ganglia in normal animals was $477 \pm 28 \mu\text{m}^2$ ($n = 4$), after 2 week sciatic axotomy it was $449 \pm 38 \mu\text{m}^2$ ($n = 4$), and after sciatic axotomy and GDNF treatment (12 μ g/d; $n = 3$) it was $494 \pm 33 \mu\text{m}^2$. There was no significant difference between these groups ($p > 0.2$; unpaired *t* test).

Thus, NGF and GDNF had complementary actions in their ability to rescue phenotypic changes in *trk*- and non-*trk*-expressing small DRG neurons, respectively. We did not find any significant effects of GDNF on the percentage of DRG cells expressing IB4 and TMP in the normal DRG (data not shown).

GDNF reverses a number of axotomy-induced changes within the dorsal horn of the spinal cord

The alterations seen in DRG cell bodies were also reflected in changes within the dorsal horn after axotomy. TMP activity and IB4 binding were normally present within lamina II of the dorsal horn, the same region in which RET immunoreactive terminals were present (Fig. 4). After 2 weeks of axotomy, TMP activity was virtually absent from the sciatic projection territory of the dorsal horn. IB4 binding was also markedly reduced (Figs. 6, 7a). Quantitative image analysis demonstrated that continuous intrathecal administration of GDNF at a low dose had a significant effect on TMP activity and IB4 binding after axotomy ($p < 0.05$; unpaired *t* test; compared with no treatment) (Figs. 6, 7a). Administration of GDNF at a high dose was more effective and could almost completely restore TMP activity and IB4 binding levels within the dorsal horn ($p < 0.001$, unpaired *t* test, comparing GDNF treatment with axotomy alone; $p > 0.2$, compared with intact) (Figs. 6, 7a). Administration of NGF at a low dose had no significant effect on IB4 binding after axotomy and produced only a slight increase in TMP activity after axotomy ($p < 0.05$; unpaired *t* test; comparing NGF treatment with axotomy alone) (Figs. 6, 7a). NGF administration at a high dose had a small but significant effect in restoring TMP activity and IB4 binding (by ~ 10 –15%, $p < 0.05$; unpaired *t* test comparing NGF treatment with axotomy alone) (Figs. 6, 7a). The effect of NGF on TMP activity within the dorsal horn was much less than that of GDNF ($p < 0.001$; comparing GDNF with NGF treatment at both high and low doses).

CGRP immunoreactive terminals are normally present within laminae I and II of the dorsal horn, the region in which *trkA*-expressing DRG cells terminate (Averill et al., 1995; Molliver et al., 1995). After axotomy there was $\sim 60\%$ reduction in CGRP immunoreactivity within the sciatic termination territory (Fig.

7a), as determined by image analysis. Intrathecal treatment with NGF at either a low or high dose largely prevented this change ($p < 0.001$; unpaired *t* test; comparing NGF treatment at either dose to no treatment) (Fig. 7a). GDNF treatment at a low dose had no significant effect on CGRP levels after axotomy ($p > 0.05$; unpaired *t* test). GDNF treatment at a high dose had a small ($\sim 10\%$) but significant rescue effect on CGRP levels ($p < 0.05$; unpaired *t* test; comparing GDNF treatment to no treatment).

The cholera toxin B subunit (CTB) binds to the GM1 receptor, which is selectively expressed by myelinated sensory afferents. CTB undergoes transganglionic transport by these afferents and so can be used to study A-fiber terminations within the dorsal horn of the spinal cord. In normal animals (Fig. 8), CTB-labeled terminals were present within lamina I and the deep laminae of the spinal cord (laminae III–IV). There were some terminals present in lamina II but very few labeled fibers were present in lamina I. Image analysis demonstrated that the ratio of labeling in lamina I to lamina III was extremely low (0.003 ± 0.0006) (Fig. 8b). Two weeks after axotomy, CTB was present throughout lamina II, including lamina I, and there was also more intense labeling within lamina I (Fig. 8). This change is accepted to indicate A-fiber sprouting into the superficial laminae (Woolf et al., 1992, 1995; Bennett et al., 1996b). There was a significant increase in the ratio of labeling within lamina I to lamina III (to 0.631 ± 0.07 after axotomy; $p < 0.01$; unpaired *t* test) (Fig. 7b). In animals that had received a 2 week intrathecal infusion of GDNF at a low dose, the A-fiber sprouting within lamina II was largely prevented (Fig. 8). Very few CTB-labeled terminals were present within lamina I. Quantitative image analysis demonstrated that the ratio of CTB staining between lamina I and lamina III after this treatment was 0.016 ± 0.002 ($p < 0.01$; unpaired *t* test compared with no treatment) (Fig. 7b). Treatment with GDNF at the higher dose was even more effective (the ratio of CTB staining between lamina I and lamina III was 0.007 ± 0.003 , which was not significantly different from that seen in normal intact animals). The difference between untreated and GDNF-treated axotomized animals was highly significant ($p < 0.001$; unpaired *t* test) (Fig. 7b). The profuse CTB labeling that normally occurs within lamina I after axotomy also appeared to be prevented by GDNF treatment.

Trophic factor effects on electrophysiological properties of axotomized C-fibers

Axotomy produces a conduction velocity slowing in C-fibers; we investigated the efficacy of GDNF and NGF in reversing this change. The conduction velocity (CV) distribution of C-fibers projecting through the normal tibial nerve was unimodal, with a mean of 0.86 ± 0.06 m/sec. After two weeks of axotomy, velocity was slowed to a mean of 0.68 ± 0.03 m/sec, and this was significant ($p < 0.01$; unpaired *t* test). This slowing was also apparent as a leftward shift in the cumulative sum plots of CV of units (Fig.

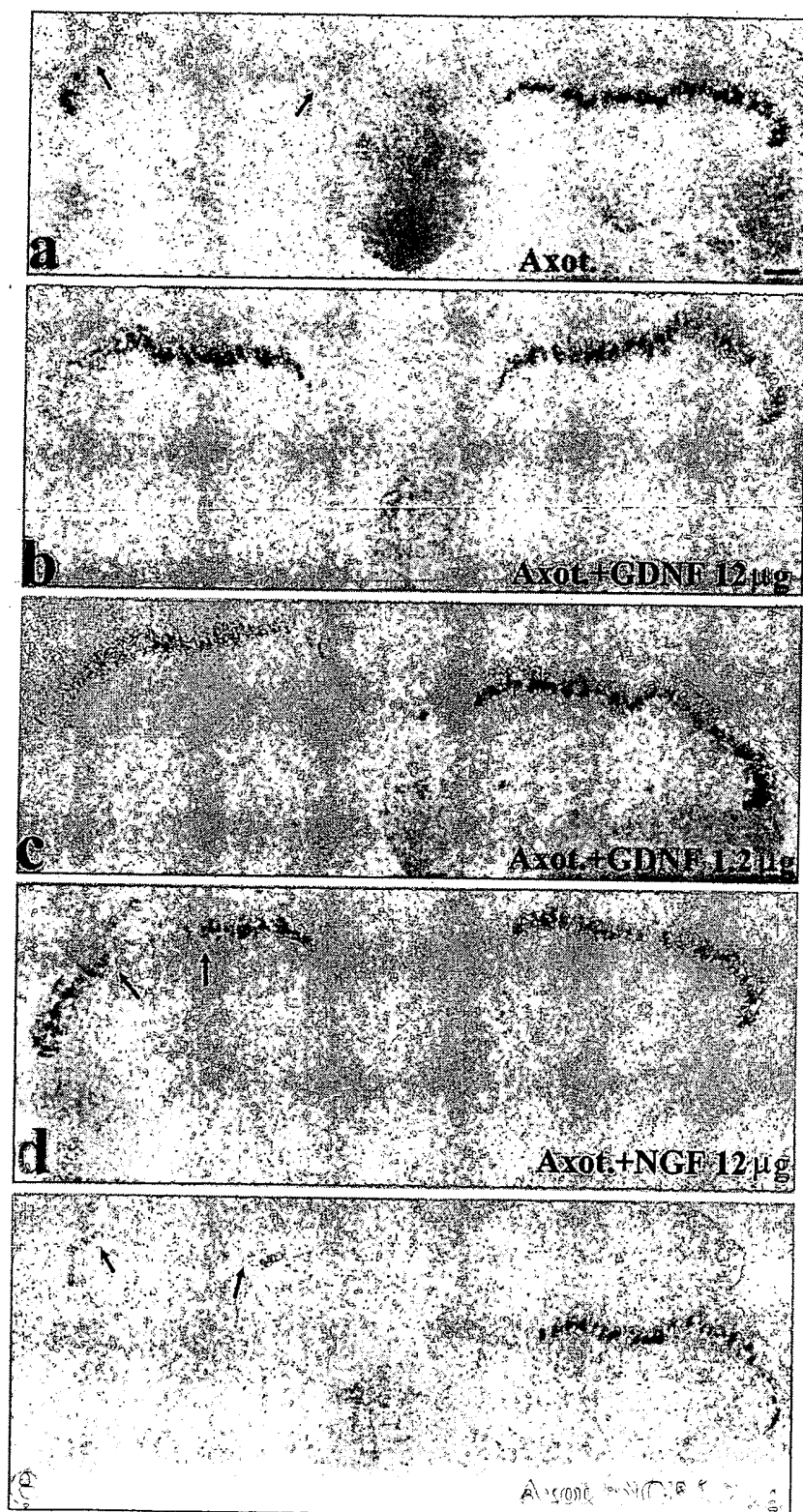


Figure 6. Histochemistry for TMP at the level of L4 in the dorsal horn of animals with unilateral sciatic nerve section (*a*), animals with unilateral sciatic nerve section combined with high (12 μ g/d) (*b*) and low (1.2 μ g/d) (*c*) dose intrathecal GDNF treatment, and animals with unilateral sciatic nerve section combined with high (12 μ g/d) (*d*) and low (1.2 μ g/d) (*e*) dose intrathecal NGF. Sciatic nerve section causes a loss of TMP in the sciatic termination territory within lamina III (demonstrated by arrows). GDNF treatment at either dose is effective at preventing this loss (*b*, *c*), whereas NGF is much less effective at either dose used (*d*, *e*). Scale bar, 100 μ m. *Axot.*, Axotomized.

9), and this shift was also statistically significant ($p < 0.01$; Kolmogorov–Smirnov). Intrathecal provision of GDNF, at 12 μ g/d, throughout the 2 week period of axotomy, partially and significantly prevented this slowing (Fig. 9) ($p < 0.05$; Kolmogorov–Smirnov). The slowest conducting C-fibers were especially

rescued by GDNF. NGF at 12 μ g/d also had a partial and significant effect in preventing axotomy-induced slowing (Fig. 9) ($p < 0.05$; Kolmogorov–Smirnov), although in this case C-fibers throughout the CV distribution were more equally affected, suggesting that GDNF and NGF do not affect the same population

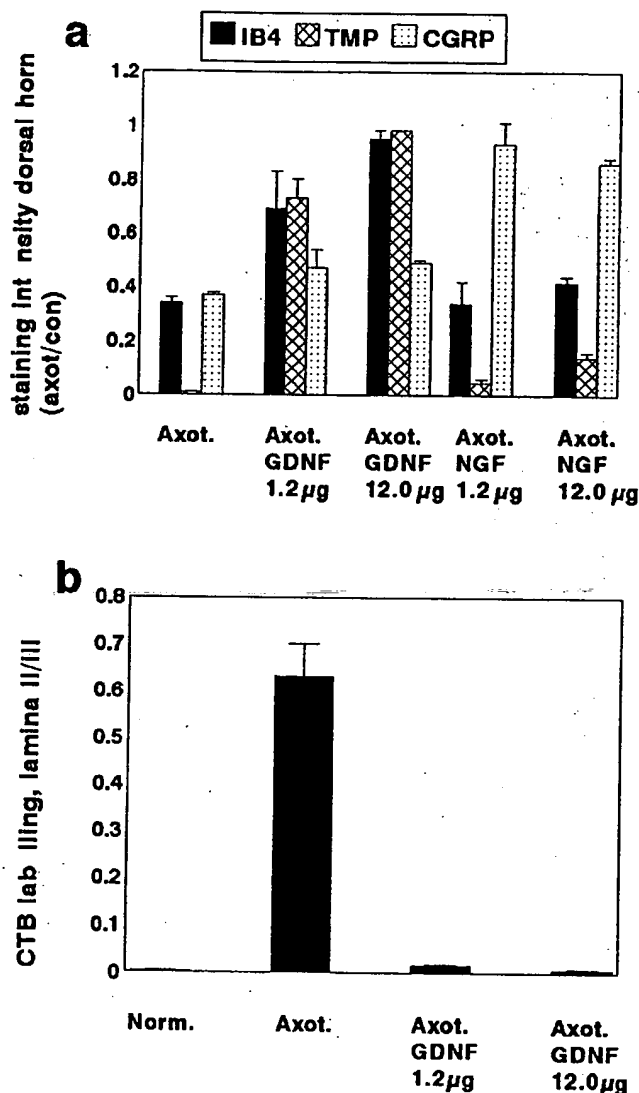


Figure 7. *a*, The ratio of the area occupied by IB4, TMP, or CGRP stained terminals within lamina II of the dorsal horn of the spinal cord on the axotomized side versus the normal side in animals that have undergone axotomy ($n = 4$) or axotomy in combination with an intrathecal infusion of GDNF at a dose of either 1.2 μ g/d ($n = 3$) or 12 μ g/d ($n = 4$) or NGF at a dose of either 1.2 μ g/d ($n = 3$) or 12 μ g/d ($n = 3$). GDNF at a dose of 12 μ g/d almost completely prevented the axotomy-induced reduction in staining intensity of IB4 and TMP ($p < 0.001$; unpaired t test; comparing GDNF with no treatment after axotomy). The lower dose of GDNF (1.2 μ g/d) also had a significant effect in preventing the axotomy-induced reduction in staining intensity of these markers but was less effective than the higher dose. The high dose GDNF had a small but significant effect in preventing the axotomy-induced reduction in CGRP staining ($p < 0.05$; unpaired t test). NGF could almost completely prevent the axotomy-induced reduction in CGRP staining ($p < 0.001$; unpaired t test; comparing NGF with no treatment after axotomy). NGF at 12 μ g/d had a small but significant effect on the axotomy-induced reduction in IB4 and TMP expression ($p < 0.05$; unpaired t test). *b*, The ratio of the area occupied by CTB-labeled terminals in lamina II compared with lamina III of the dorsal horn in normal ($n = 5$), axotomized ($n = 4$), and axotomy + GDNF (Axot. GDNF) 1.2 μ g/d ($n = 3$) and 12 μ g/d ($n = 4$) animals. Note that there is a significant increase in labeling in lamina II after axotomy ($p < 0.01$; unpaired t test), which is almost completely prevented by treatment with GDNF at the higher dose. GDNF treatment at the low dose also had a significant effect ($p < 0.01$ compared with no treatment; unpaired t test) but was less effective than the higher dose.

of afferents. Consistent with this suggestion, intrathecal provision of both NGF and GDNF, at 12 μ g/d each, produced the greatest rescue of C-fiber CV. In fact, in this case neither the CV distribution nor the mean CV (0.83 ± 0.03 m/sec) differed significantly from that seen in intact animals ($p > 0.05$; Kolmogorov-Smirnov and unpaired t test, respectively). Thus, these results provide an independent measure of the ability of GDNF and NGF, delivered by this route and at this dose, to produce a near-complete reversal of axotomy effects in C-fibers.

DISCUSSION

The principal conclusion of this work is that GDNF is a trophic factor for a substantial subgroup of adult primary sensory neurons that are neurotrophin independent. This conclusion is based on two lines of investigation: the localization of receptor components and the selective rescue effects of exogenous GDNF on axotomized sensory neurons, as discussed below.

GDNF receptor component expression within sensory neurons

The signal transducing domain of the GDNF receptor RET was found to be present in 60–70% of DRG cell profiles. GFR α -1 and GFR α -2, the ligand binding domains for GDNF and neurturin, had a more restricted distribution (they were expressed in 45 and 33% of DRG cell profiles, respectively). GDNF receptor components were strikingly expressed by the IB4 binding, *trk*-less population of DRG cells. Almost all IB4 cells express RET. Approximately 50% of IB4 cells also express GFR α -1. This implies that 50% of IB4 cells coexpress both receptor components and are therefore likely to be highly sensitive to GDNF. The other 50% of the IB4 cells express RET, apparently in the absence of GFR α -1. GDNF has been reported by some authors to be able to activate RET in the absence of GFR α -1 and also to be able to act via the related neurturin receptor component GFR α -2 (Baloh et al., 1997; Buj-Bello et al., 1997; Klein et al., 1997; Sanicola et al., 1997). We found that this receptor component was also highly localized within the IB4-binding population of DRG cells. In some cells it was coexpressed with GFR α -1 and in others it was expressed independently of GFR α -1. The majority (80%) of IB4-binding DRG cells expressed either one or both ligand binding components. Therefore GDNF may be able to act on a larger population of IB4 cells than just those that express GFR α -1. These findings also suggest that a proportion of the IB4-binding population of DRG cells are likely to be responsive to neurturin. RET immunoreactive terminals were found to project principally to lamina III of the dorsal horn of the spinal cord, the same lamina in which the IB4-binding DRG cells terminate. In contrast to the IB4 cells, the other population of small diameter DRG cells (those that express *trkA*) generally lack RET, GFR α -1, and GFR α -2. Any coexpression is largely accounted for by the known overlap between *trkA* and IB4 (18% of *trkA* cells also bind IB4) (Averill et al., 1995). A significant number of large diameter DRG cells (as revealed by staining with N52) express GFR α -1 or RET or both, suggesting that these cells may also be responsive to GDNF.

Neuroprotective effects of GDNF on sensory neurons

The receptor localization data discussed above shows that a large proportion of the "neurotrophin-independent" population of small diameter DRG cells express receptor components for GDNF. Markers that can be used to define this population include binding of the lectin IB4 and the enzyme TMP. A small subset of these cells also expresses the neuropeptide somatosta-

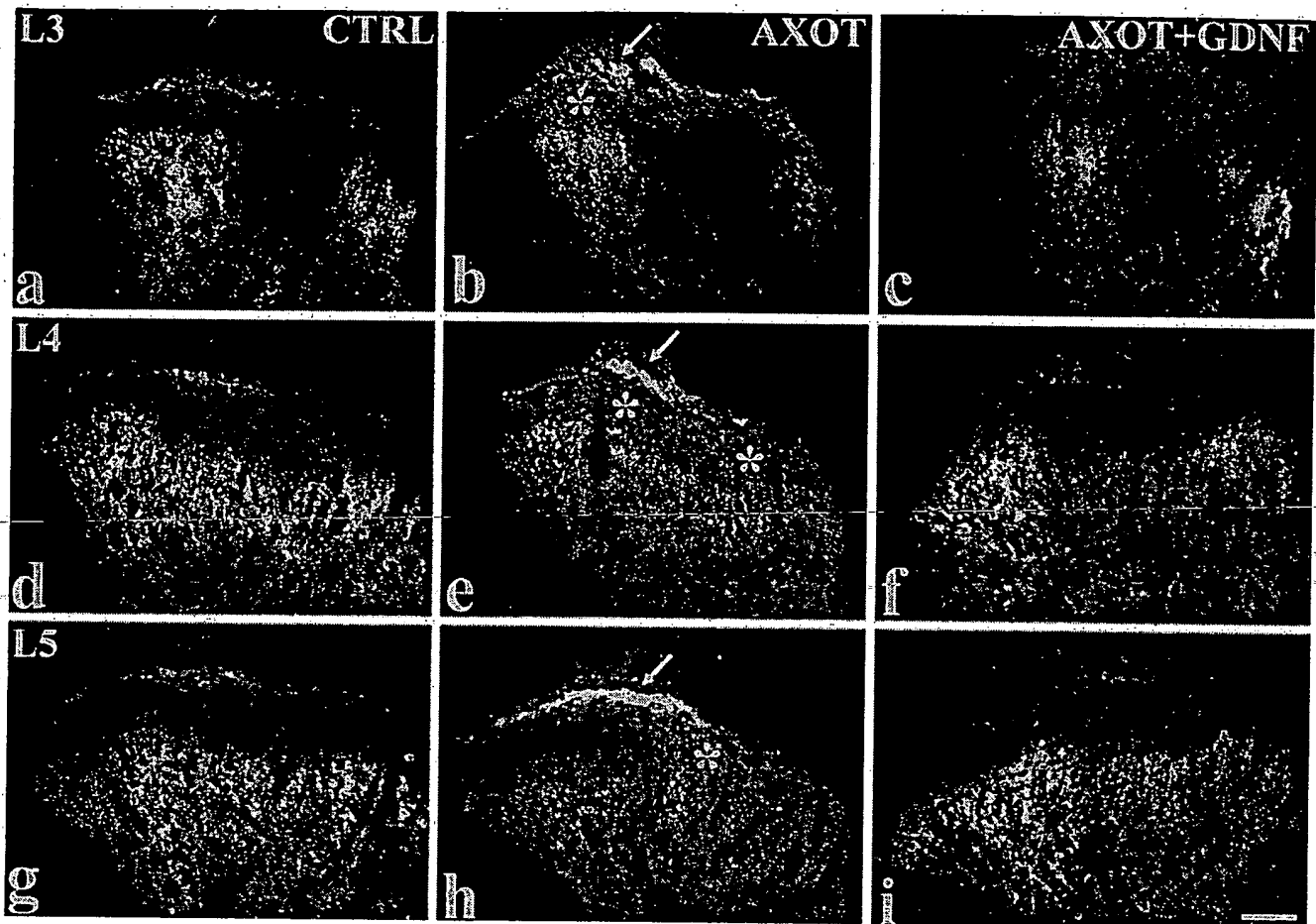


Figure 8. Transport of CTB to the dorsal horn of the spinal cord at the level of L3 (*a–c*), L4 (*d–f*), and L5 (*g–i*) after sciatic nerve label in control (CTRL) animals (*a, d, g*), animals that have undergone axotomy (AXOT) (*b, e, h*), and animals that have undergone axotomy combined with GDNF (AXOT+GDNF) treatment (12 μ g/d) (*c, f, i*). In the normal animal, CTB-labeled terminals are present in lamina I and the deeper laminae of the dorsal horn (III–IV) but are excluded from lamina II (*a, d, g*). After axotomy, CTB-labeled terminals appear in lamina II (denoted by asterisks), and there is also more dense labeling of axon bundles within lamina I (arrows in *b, e, h*). These axotomy-related changes are prevented by treatment with GDNF, where the CTB labeling pattern appears the same as control, and this is seen consistently throughout L3–L5 (*c, f, i*). Scale bar, 100 μ m.

tin. In this study we directly examined whether the IB4-binding population of sensory neurons would be responsive to GDNF (as compared with NGF) after axotomy. Intrathecal delivery was used, which we have previously demonstrated to be effective at delivering trophic factors to sensory neurons (Bennett et al., 1996b; Michael et al., 1997).

After axotomy we found that at both doses used, GDNF was much more effective than NGF at restoring IB4 binding, TMP staining, and somatostatin expression within both the DRG and the dorsal horn of the spinal cord. Conversely, NGF was much more effective than GDNF at restoring CGRP expression within the DRG and dorsal horn after axotomy. These findings complement those on receptor distribution. NGF has selective effects on the CGRP-expressing population of DRG cells, whereas conversely, GDNF has selective actions on the IB4-binding (i.e., neurotrophin-independent) population of cells. The known overlap between these markers (Averill et al., 1995) probably accounts for the limited nonspecific effects seen. Our electrophysiological results provide an independent means of assessing the trophic effects of GDNF and NGF on small diameter DRG cells (C-fibers). GDNF and NGF appeared to prevent conduction velocity slowing after axotomy in distinct populations of C-fibers, and

importantly, the actions of these factors when administered together were additive. We have shown previously that conduction velocity slowing in large sensory neurons, induced by axotomy, is only marginally affected by intrathecal GDNF treatment (Munson and McMahon, 1997).

We have also demonstrated that GDNF could prevent the axotomy-induced A-fiber sprouting into lamina II of the dorsal horn. This may represent a direct effect of GDNF on large DRG neurons or it may occur as a consequence of the rescue effect of GDNF on IB4-binding small diameter DRG cells. There is now a body of evidence suggesting that degenerative atrophy of C-fiber terminals within lamina II after axotomy (Knyihar-Csillik et al., 1987) is critically important for A-fibers sprouting into this region. This evidence derives from the fact that C-fibers in the sciatic nerve have a more restricted mediolateral and rostrocaudal distribution than sciatic A-fibers, and the sprouting of A-fibers occurs only in the termination region of axotomized C-fibers (Woolf et al., 1995). Furthermore, capsaicin, which selectively damages C-fibers, can induce A-fiber sprouting (Mannion et al., 1996). We have shown previously that NGF can prevent A-fiber sprouting (Bennett et al., 1996b), and the demonstration here that GDNF is also effective is likely to represent the “rescue” of the

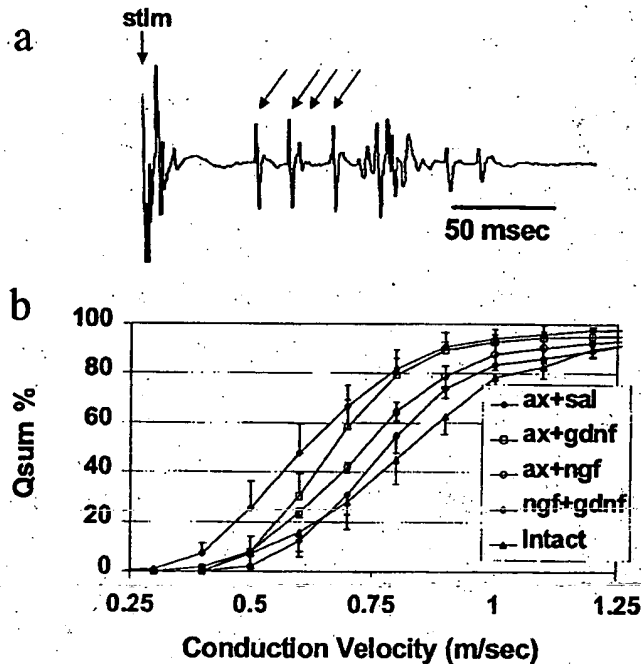


Figure 9. The conduction velocity (CV) of C-fibers projecting through the tibial nerve was measured by stimulation of that nerve electrically and recording and averaging activity in fine strands of the L5 dorsal root. *a*, shows a representative recording from an animal in which the tibial nerve had been cut and tied 2 weeks previously; the animal was treated continuously with intrathecal GDNF and NGF (each at 12 μ g/d). Arrows show examples of individual C-fiber potentials occurring in response to the stimulation. *b*, Cumulative sum plots showing the average CV distributions constructed from groups of animals receiving different treatment ($n = 3$ –5 animals per group). Error bars show SEM. Note that axotomy results in a significant slowing of C-fibers (seen as a leftward shift in the Qsum plots), and both NGF and GDNF partially prevent this slowing.

IB4-binding population of small diameter afferents after axotomy. These results are interesting in that, as we have demonstrated here, NGF and GDNF support largely separate populations of C-fibers and yet either can prevent the sprouting response after axotomy.

Functional implications of GDNF effects

Our data indicate that GDNF has a potent and selective effect on the IB4-binding population of DRG cells, and similar selectivity has recently been observed *in vitro* (Molliver et al., 1997; Leclerc et al., 1998). The IB4 population of primary afferents are primarily small in diameter. Given that 80–90% of C-fibers are nociceptors (Lynn and Carpenter, 1982; Kress et al., 1992), IB4-binding DRG cells must be principally nociceptive in function (Willis and Coggeshall, 1991). These neurons are capsaicin sensitive (Fitzgerald, 1983) and possess free nerve endings in various tissues, including skin, muscle, joint, and viscera. It has recently been shown that this group of sensory neurons selectively expresses the purinergic receptor P2X₃ (Vulchanova et al., 1996). This receptor is thought to be important in mediating the nociceptive actions of ATP (Cook et al., 1997). The sensitivity of this population to GDNF suggests that this factor may be important in the development and maintenance of pain-signaling systems.

One important question is whether GDNF is normally required for the phenotypic maintenance of the IB4 population of

DRG cells or whether the rescue effects on these cells reflect a purely pharmacological action. GDNF is produced by peripheral targets (Trupp et al., 1995) and may normally be available to these afferents. It is unknown, as yet, whether neurturin also has actions on the IB4-binding population of DRG cells.

It is interesting that the IB4-binding population of DRG cells develops such marked sensitivity to GDNF during postnatal development. During embryonic development these neurons are dependent for survival on NGF and are absent in animals that lack *trkA* (Silos-Santiago et al., 1995). The developmental regulation of RET has been studied by Molliver et al. (1997) in the mouse. RET was only clearly seen in DRG cells during the late embryonic and early postnatal period and reached the adult levels by approximately postnatal day 7. At the time RET is reaching its peak, the same neurons downregulate *trkA* and lose their NGF sensitivity (Bennett et al., 1996a; Molliver and Snider, 1997). Molliver et al. (1997) also reported a pattern of GFR α -1/RET distribution similar to what we report here.

Nerve injury may result in abnormalities of sensation and importantly the generation of a chronic pain state in both animals and man. One important mechanism for these changes is the impaired retrograde transport of trophic factors after nerve injury (McMahon and Bennett, 1997). As a consequence of nerve injury, there is a large upregulation of GDNF expression within the damaged nerve (Trupp et al., 1995), as has been shown previously for NGF (Lindholm et al., 1987). Expression of GFR α -1 has also been reported to increase in injured nerves (Baloh et al., 1997; Trupp et al., 1997), and this may act to present GDNF to regenerating neurons. Our results imply that the upregulation of GDNF expression in damaged nerves is not sufficient to prevent axotomy-induced changes.

The restitution of IB4 binding, TMP activity, and somatostatin expression by GDNF after axotomy may indicate a general beneficial action of GDNF in normalizing the properties of damaged sensory neurons. These anatomical findings were supported by the evidence that GDNF can partially prevent the conduction velocity slowing that occurs in a population of C-fibers after axotomy. The A-fiber sprouting that occurs after axotomy has previously been implicated in the generation of some aspects of neuropathic pain. The suggestion is that when the large diameter, low-threshold mechanoreceptive A-fibers form synapses in lamina II with presumed pain-signaling postsynaptic dorsal horn systems, this provides an explanation for the condition of allodynia, or touch-evoked pain, that is frequently seen in neuropathic pain patients (Woolf et al., 1992).

Behavioral data suggest that GDNF can exert trophic effects on IB4 binding nociceptive afferents without altering their responses to acute noxious thermal and mechanical stimuli (D. L. H. Bennett and S. B. McMahon, unpublished observations). This is in marked contrast to the actions of NGF, which acts on the other major group of nociceptors, those expressing *trkA*. NGF acutely or chronically administered to animals and man can produce pain and hyperalgesia (Lewin et al., 1993; Petty et al., 1994; Woolf et al., 1994; Andreev et al., 1995). Because many forms of neuropathy in man affect small diameter nociceptive afferents, our results suggest that GDNF may be of some use in the treatment of these conditions. In particular, we would predict that GDNF may add to, rather than simply substitute for, the effects of NGF in the treatment of neuropathies.

REFERENCES

- Andreev NY, Dimitrova N, Koltzenburg M, McMahon SB (1995) Peripheral administration of nerve growth factor in the adult rat produces a thermal hyperalgesia that requires the presence of sympathetic postganglionic neurones. *Pain* 63:109–115.
- Averill S, McMahon SB, Clary SB, Reichardt LF, Priestley JVP (1995) Immunocytochemical localization of trkA receptors in chemically identified subgroups of adult rat sensory neurons. *Eur J Neurosci* 7:1484–1494.
- Baloh RH, Tansey MG, Golden JP, Creedon DJ, Heukeroth RO, Keck CL, Zimonjic DB, Popescu NC, Johnson EM, Milbrandt J (1997) TrnR2, a novel receptor that mediates neurturin and GDNF signaling through Ret. *Neuron* 18:793–802.
- Beck KD, Valverde J, Alexi T (1995) Mesencephalic dopaminergic neurons protected by GDNF from axotomy-induced degeneration in the adult brain. *Nature* 373:339–341.
- Bennett DLH, Averill S, Clary DO, Priestley JV, McMahon SB (1996a) Postnatal changes in the expression of the trkA high affinity NGF receptor in primary sensory neurons. *Eur J Neurosci* 8:2204–2208.
- Bennett DLH, French J, Priestley JVP, McMahon SB (1996b) NGF but not NT-3 or BDNF prevents the A fiber sprouting into lamina II of the spinal cord that occurs following axotomy. *Mol Cell Neurosci* 8:211–220.
- Bowenkamp KE, Hoffman AF, Gerhardt GA, Henry MA, Biddle PT, Hoffer BJ, Granholm ACE (1995) Glial cell line-derived neurotrophic factor supports survival of injured midbrain dopaminergic neurons. *J Comp Neurol* 355:479–489.
- Buj-Bello A, Buchman VL, Horton A, Rosenthal A, Davies AM (1995) GDNF is an age-specific survival factor for sensory and autonomic neurons. *Neuron* 15:821–828.
- Buj-Bello A, Adu J, Pinon LGP, Horton A, Thompson J, Rosenthal A, Chinchetru M, Buchman V, Davies A (1997) Neurturin responsiveness requires a GPI-linked receptor and Ret receptor tyrosine kinase. *Nature* 387:721–724.
- Canzian F, Ushijima T, Nagao M, Matera I, Romeo G, Ceccherini I (1995) Genetic mapping of the RET protooncogene on rat chromosome 4. *Mamm Genome* 6:433–435.
- Cook SP, Vulchanova L, Hargreaves KM, Elde R, McCleskey EW (1997) Distinct ATP receptors on pain-sensing and stretch sensing neurons. *Nature* 387:505–508.
- Durbec P, Marcos-Gutierrez CV, Kilkenny C, Grigoriou M, Wartiovaara K, Suvanto P, Smioth D, Ponder B, Costantini F, Saarma M, Sariola H, Pachnis V (1996) GDNF signalling through the Ret receptor tyrosine kinase. *Nature* 381:789–793.
- Fitzgerald M (1983) Capsaicin and sensory neurons: a review. *Pain* 15:109–130.
- GFR α Nomenclature Committee (1997) Nomenclature of GPI linked receptors for the GDNF ligand family. *Neuron* 19:485.
- Henderson CE, Phillips HS, Pollock RA, Avies A, Lemeulle C, Armanini M, Simmons L, Moffet B, Vanden R (1994) GDNF: a potent survival factor for motoneurons present in peripheral nerve and muscle. *Science* 266:1062–1064.
- Jing S, Wen D, Yu Y, Holst PL, Luo Y, Fang M, Tamir R, Antonio L, Hu Z, Cupples R, Louis JC, Hu S, Altrock BW, Fox GM (1996) GDNF-induced activation of the ret protein tyrosine kinase is mediated by GDNFR- α , a novel receptor for GDNF. *Cell* 85:1113–1124.
- Kashiba H, Ueda Y, Senba E (1996) Coexpression of preprotachykinin-A, α -calcitonin gene-related peptide, somatostatin, and neurotrophin receptor family messenger RNAs in rat dorsal root ganglion neurons. *Neuroscience* 70:179–189.
- Klein RD, Sherman D, Ho WH, Stone D, Bennett G, Moffat B, Vanden R, Simmons L, Gu Q, Hongo J, Devaux B, Poulsen K, Armanini M, Nozaki C, Asai N, Goddard A, Phillips H, Henderson C, Takahashi M, Rosenthal A (1997) A GPI-linked protein that interacts with RET to form a candidate neurturin receptor. *Nature* 387:717–721.
- Knyihar-Csillik E, Rakic P, Csillik B (1987) Transganglionic degenerative atrophy in the substantia gelatinosa of the spinal cord after peripheral nerve transection in rhesus monkeys. *Cell Tissue Res* 247:599–604.
- Kotzbauer PT, Lampe PA, Heukeroth RO, Golden JP, Creedon DJ, Johnson EM, Milbrandt JD (1996) Neurturin a relative of glial-cell-line-derived neurotrophic factor. *Nature* 381:467–470.
- Kress M, Koltzenburg M, Reeh PW, Handwerker HO (1992) Responsiveness and functional attributes of electrically localized terminals of cutaneous C-fibers in vivo and in vitro. *J Neurophysiol* 68:581–595.
- Leclerc PG, Ekstrom P, Edstrom A, Priestley JV, Averill S, Tonge DA (1998) Effects of glial cell line-derived neurotrophic factor on axonal growth and apoptosis in adult mammalian sensory neurons in vitro. *Neuroscience* 82:545–558.
- Lewin GR, Ritter AM, Mendell LM (1993) Nerve growth factor-induced hyperalgesia in the neonatal and adult rat. *J Neurosci* 13:2136–2148.
- Lin LF, Doherty DH, Lile JD, Bektesh S, Collins F (1993) GDNF: a glial cell line-derived neurotrophic factor for midbrain dopaminergic neurons. *Science* 260:1130–1132.
- Lindholm D, Heumann R, Meyer M, Thoenen H (1987) Interleukin-1 regulates synthesis of nerve growth factor in non-neuronal cells rat sciatic nerve. *Nature* 330:658–659.
- Lynn B, Carpenter SE (1982) Primary afferent units from the hairy skin of the rat hind limb. *Brain Res* 238:29–43.
- Mannion RJ, Doubell TP, Coggeshall RE, Woolf CJ (1996) Collateral sprouting of uninjured primary afferent A-fibers into the superficial dorsal horn of the adult rat spinal cord after topical capsaicin treatment of the sciatic nerve. *J Neurosci* 16:5189–5195.
- Matheson CR, Garnahan J, Ulrich JL, Bocangel D, Zhang TJ, Yan Q (1997) Glial cell line-derived neurotrophic factor (GDNF) is a neurotrophic factor for sensory neurons: comparison with the effects of the neurotrophins. *J Neurobiol* 32:22–32.
- McMahon SB (1986) The localization of fluoride-resistant acid phosphatase (FRAP) in the pelvic nerves and sacral spinal cord of rats. *Neurosci Lett* 64:305–310.
- McMahon SB, Bennett DLH (1997) Growth factors and pain. In: *Handbook of pharmacol* 130 (Dickenson A, Besson J-M), pp 135–157. Berlin: Springer.
- McMahon SB, Armanini MP, Ling LH, Phillips HS (1994) Expression and coexpression of Trk receptors in subpopulations of adult primary sensory neurons projecting to identified peripheral targets. *Neuron* 12:1161–1171.
- Michael GJ, Priestley JV (1996a) Expression of trkA and p75 nerve growth factor receptors in the adrenal gland. *NeuroReport* 7:1617–1622.
- Michael GJ, Priestley JV (1996b) Combined immunocytochemistry and in situ hybridization. In: *In situ hybridization techniques for the brain* (Henderson Z, ed), pp 111–118. New York: Wiley.
- Michael GJ, Averill S, Nitkunan A, Rattray M, Bennett DLH, Yan Q, Priestley JV (1997) Nerve growth factor treatment increases brain-derived neurotrophic factor selectively in trkA-expressing dorsal root ganglion cells and in their central terminations within the spinal cord. *J Neurosci* 17:8476–8490.
- Molliver DC, Snider WD (1997) Nerve growth factor receptor trkA is down-regulated during postnatal development by a subset of dorsal root ganglion neurons. *J Comp Neurol* 381:428–438.
- Molliver DC, Radeke MJ, Feinstein SC, Snider WD (1995) Presence or absence of trkA protein distinguishes subsets of small sensory neurons with unique cytochemical characteristics and dorsal horn projections. *J Comp Neurol* 361:404–416.
- Molliver DC, Wright DE, Leitner ML, Parsadanian AS, Doster K, Wen D, Yan Q, Snider WD (1997) IB4-binding nociceptors switch from NGF to GDNF dependence in early postnatal life. *Neuron* 19:849–861.
- Moore MW, Klein RD, Farinas I, Sauer H, Armanini M, Phillips HS, Reichardt LF, Ryan AM, Carver-Moore K, Rosenthal A (1996) Renal and neuronal abnormalities in mice lacking GDNF. *Nature* 382:76–79.
- Munson JB, McMahon SB (1997) Effects of GDNF on axotomized sensory and motor neurons in adult rats. *Eur J Neurosci* 9:1126–1129.
- Oppenheim RW, Houenou LJ, Johnson JE, Lin L-FH, Li L, Lo AC, Newsome AL, Prevette DM, Wang S (1995) Developing motor neurons rescued from programmed and axotomy-induced cell death by GDNF. *Nature* 373:344–346.
- Petty BG, Cornblath DR, Adornato BT, Chaudhry V, Flexner C, Wachsmann M, Sinicropi D, Burton LE, Peroutka SJ (1994) The effect of systemically administered recombinant human nerve growth factor in healthy human subjects. *Ann Neurol* 36:244–246.
- Sanicola M, Hession C, Worley P, Carmillo P, Ehrenfels C, Walus L, Robinson S, Jaworski G, Wei H, Tizard R, Whitty A, Pepinsky R, Cate R (1997) Glial cell line-derived neurotrophic factor-dependent RET activation can be mediated by two different cell-surface accessory proteins. *Proc Natl Acad Sci USA* 94:6238–6243.
- Silos-Santiago I, Molliver DC, Ozaki S, Smeyne RJ, Fagan AM, Barbacid M, Snider WD (1995) Non-TrkA-expressing small DRG neurons are lost in TrkA deficient mice. *J Neurosci* 15:5929–5942.
- Silverman JD, Kruger L (1990) Selective neuronal glycoconjugate ex-

- pression in sensory and autonomic ganglia: relation of lectin reactivity to peptide and enzyme markers. *J Neurocytol* 19:789-801.
- Treanor JJ, Goodman L, de Sauvage F, Stone DM, Poulsen KT, Beck CD, Gray C, Armanini MP, Pollock RA, Hefti F, Phillips HS, Goddard A, Moore MW, Buj-Bello A, Davies AM, Asai N, Takahashi M, Vandlen R, Henderson CE, Rosenthal A (1996) Characterization of a multi-component receptor for GDNF. *Nature* 382:80-83.
- Trupp M, Ryden M, Jornvall H, Funakoshi H, Timmusk T, Arenas E, Ibanez CF (1995) Peripheral expression and biological activities of GDNF, a new neurotrophic factor for avian and mammalian peripheral neurons. *J Cell Biol* 130:137-148.
- Trupp M, Arenas E, Fainzilber M, Nilsson A-S, Sieber B-A, Grigoriou M, Kilkenny C, Salazar-Grueso E, Pachnis V, Arumae U, Sariola H, Saarma M, Ibanez CF (1996) Functional receptor for GDNF encoded by the c-ret proto-oncogene. *Nature* 381:785-788.
- Trupp M, Belluardo N, Funakoshi H, Ibanez CF (1997) Complementary and overlapping expression of glial cell line-derived neurotrophic factor (GDNF), c-ret proto-oncogene, and GDNF receptor- α indicates multiple mechanisms of trophic actions in the adult rat CNS. *J Neurosci* 17:3554-3567.
- Verge VM, Richardson PM, Wiesenfeld-Hallin Z, Hokfelt T (1995) Differential influence of nerve growth factor on neuropeptide expression *in vivo*: a novel role in peptide suppression in adult sensory neurons. *J Neurosci* 15:2081-2096.
- Verge VM, Gratto KA, Karchewski LA, Richardson PM (1996) Neurotrophins and nerve injury in the adult. *Philos Trans R Soc Lond B Biol Sci* 351:423-430.
- Vulchanova L, Riedl M, Shuster S, Wang J, Buell G, Surprenant A, North RA, Elde R, (1996) Immunohistochemical localization of the P2X3 receptor subunit in rat dorsal root ganglion (DRG) neurons. *Soc Neurosci Abstr* 22:1810.
- Willis WD, Coggeshall RE (1991) Sensory mechanisms of the spinal cord, Ed 2. New York: Plenum.
- Woolf CJ, Shortland P, Coggeshall RE (1992) Peripheral nerve injury triggers central sprouting of myelinated afferents. *Nature* 355:75-78.
- Woolf CJ, Safieh-Garabedian B, Ma QP, Crilly P, Winter J (1994) Nerve growth factor contributes to the generation of inflammatory sensory hypersensitivity. *Neuroscience* 62:327-331.
- Woolf CJ, Shortland P, Reynolds M, Ridings J, Doubell T, Coggeshall RE (1995) Reorganization of central terminals of myelinated primary afferents in the rat dorsal horn following peripheral axotomy. *J Comp Neurol* 360:121-134.
- Wright DE, Snider WD (1995) Neurotrophin receptor mRNA expression defines distinct populations of neurons in rat dorsal root ganglia. *J Comp Neurol* 351:329-338.
- Yan Q, Matheson C, Lopez OT (1995) *In vivo* neurotrophic effects of GDNF on neonatal and adult facial motor neurons. *Nature* 373:341-344.

with B set at regular intervals ($\Delta\theta \sim 10^\circ$) of the rotation angle θ , we obtain a full spatial profile of $|\Phi_{\text{QD}}(k_x, k_y)|^2$. This represents the projection in k space of the probability density of a given electronic state confined in the QD.

The model provides a simple explanation of the magnetic field dependence of the resonant current features e_1 to e_7 . In particular, the forbidden nature of the tunneling transition associated with e_4 and e_5 at $B = 0$ T is due to the odd parity of the final state wave function, which corresponds to the first excited state of a QD.

Figure 3A shows the spatial form of $G(B) \sim |\Phi_{\text{QD}}(k_x, k_y)|^2$, in the plane (k_x, k_y) for the three representative QD states corresponding to the peaks e_2 , e_4 , and e_7 . The measured values of $G(B)$ for two directions of B , parallel and antiparallel to the $[01\bar{1}]$ axis, are shown (Fig. 3B). The contour plots reveal the characteristic form of the probability density distribution of a ground state orbital and the characteristic lobes of the higher energy states of the QD. The electron wave function has a biaxial symmetry in the growth plane, with axes corresponding quite closely (within measurement error of 10°) to the main crystallographic directions $[01\bar{1}]$ and $[2\bar{3}3]$. In particular, detailed examination of the data reveals that the projected probability density of the ground state has an elliptical form, with the major axis along the $[01\bar{1}]$ direction.

Although our measurements reveal detailed information about the symmetry of the QD wave functions with respect to the in-plane coordinates, they give us no information about the z dependence. This is directly related to the morphology of the QDs. In general, the dot height is much smaller than the dimensions of the base (I). Therefore, the quantization energy of confinement along z is much higher than that for in-plane motion. Our discussion of the magnetotunneling data has made two important and reasonable assumptions. The first is that the motion along z is separable from the in-plane motion. This approximation allows us to label the QD state using the quantum numbers n_1 and n_2 for the in-plane motion and n_3 for motion along z . Our second assumption is that all of the observed peaks involve final (QD) states that share the same type of quantum confinement along z , i.e., have the same value of n_3 ($= 0$).

In recent years, several different approaches have been used to calculate the eigenstates of QDs. They include perturbation effective mass approaches (I), eight-band $k \cdot p$ theory ($10, 22, 23$), and empirical pseudopotential models (24). Calculations generally depict the form of the wave functions as plots of the probability density in real space, $|\Psi_{\text{QD}}(r)|^2$. A tunnel current measurement can provide no information about the phase of the wave function, but, in general, the phase of $\Psi_{\text{QD}}(r)$ is easily obtained from a model calculation. Once the phase factor is known, it is a straightforward task for theoreticians to Fourier transform the calculations of

the wave function into k space. A direct comparison could then be made with our spatial maps.

Our technique has allowed us to observe successive features in $I(V)$ corresponding to resonant tunneling through a limited number of discrete states whose wave functions display the symmetry of the ground state and first and second excited states of QDs. However, the simple device configuration does not permit us to determine whether an excited state peak and a ground state peak correspond to the same QD. This question could be resolved by experiments on structures with electrostatic gates (18).

Despite the large number of QDs in our sample (10^6 to 10^7 for a $100\text{-}\mu\text{m}$ -diameter mesa), we observed only a small number of resonant peaks over the bias range (~ 100 mV) close to the threshold for current flow. This behavior has been reported in earlier studies ($13\text{--}18$) and, although not fully understood, is probably related to the limited number of conducting channels in the emitter that can transmit electrons from the doping layer to the QDs at low bias. There is no reason to believe that the dots studied are atypical of the distribution as a whole.

Magnetotunneling spectroscopy provides us with a means of probing the spatial form of the wave functions of electrons confined in zero-dimensional QDs. The technique is both noninvasive and nondestructive and allows us to probe spatially quantum states that are buried hundreds of nanometers below the surface.

References and Notes

1. D. Bimberg, M. Grundmann, N. N. Ledentsov, *Quantum Dot Heterostructures* (Wiley, New York, 1999), and references therein.
2. J. Y. Marzin, J. M. Gerard, A. Izraël, D. Barier, G. Bastard, *Phys. Rev. Lett.* **73**, 716 (1994).
3. R. J. Nötzel, J. Temmyo, T. Tamamura, *Nature* **369**, 131 (1994).
4. L. Landin, M. S. Miller, M.-E. Pistol, C. E. Pryor, L. Samuelson, *Science* **280**, 262 (1998).
5. A. P. Alivisatos, *Science* **271**, 933 (1996).
6. S. A. Empedocles and M. G. Bawendi, *Science* **278**, 2114 (1997).
7. M. F. Crommie, C. P. Lutz, D. M. Eigler, *Science* **262**, 218 (1993).
8. S. H. Pan et al., *Nature* **403**, 746 (2000).
9. N. B. Zhitenov et al., *Nature* **404**, 473 (2000).
10. O. Stier, M. Grundmann, D. Bimberg, *Phys. Rev. B* **59**, 5688 (1999).
11. A. Patané et al., *Phys. Rev. B*, in press.
12. A. K. Geim et al., *Phys. Rev. Lett.* **72**, 2061 (1994).
13. P. C. Main et al., *Phys. Rev. Lett.* **84**, 729 (2000).
14. M. Narihiro, G. Yusa, Y. Nakamura, T. Noda, H. Sakaki, *Appl. Phys. Lett.* **70**, 105 (1997).
15. I. E. Itskevich et al., *Phys. Rev. B* **54**, 16401 (1996).
16. I. Hapke-Wurst et al., *Semicond. Sci. Technol.* **14**, L41 (1999).
17. T. Suzuki, K. Nomoto, K. Taira, I. Hase, *Jpn. J. Appl. Phys. Part 1* **36**, 1917 (1997).
18. D. G. Austing et al., *Appl. Phys. Lett.* **75**, 671 (1999).
19. R. K. Hayden et al., *Phys. Rev. Lett.* **66**, 1749 (1991).
20. P. H. Beton et al., *Phys. Rev. Lett.* **75**, 1996 (1995).
21. J. W. Sakai et al., *Phys. Rev. B* **48**, 5664 (1993).
22. C. Pryor, *Phys. Rev. B* **57**, 7190 (1998).
23. W. Yang, H. Lee, T. J. Johnson, P. C. Sercel, A. G. Norman, *Phys. Rev. B* **61**, 2784 (2000).
24. L.-W. Wang, J. Kim, A. Zunger, *Phys. Rev. B* **59**, 5678 (1999).
25. The work is supported by the Engineering and Physical Sciences Research Council (UK). A.L. gratefully acknowledges the support of the Fundação de Amparo à Pesquisa do Estado de São Paulo Foundation (Brazil). E.E.V. and Y.V.D. gratefully acknowledge support from the Royal Society.

21 June 2000; accepted 16 August 2000

Potent Analgesic Effects of GDNF in Neuropathic Pain States

Timothy J. Boucher,¹ Kenji Okuse,² David L. H. Bennett,^{1*} John B. Munson,¹ John N. Wood,² Stephen B. McMahon^{1†}

Neuropathic pain arises as a debilitating consequence of nerve injury. The etiology of such pain is poorly understood, and existing treatment is largely ineffective. We demonstrate here that glial cell line-derived neurotrophic factor (GDNF) both prevented and reversed sensory abnormalities that developed in neuropathic pain models, without affecting pain-related behavior in normal animals. GDNF reduces ectopic discharges within sensory neurons after nerve injury. This may arise as a consequence of the reversal by GDNF of the injury-induced plasticity of several sodium channel subunits. Together these findings provide a rational basis for the use of GDNF as a therapeutic treatment for neuropathic pain states.

The neurotrophic factor GDNF promotes survival of a subgroup of developing sensory neurons (1). In adult animals, approximately 60% of dorsal root ganglion neurons normally express receptor components for GDNF ($2, 3$), and this factor promotes neurite out-

growth in vitro and regeneration in vivo of both large- and small-caliber sensory neurons ($4, 5$). GDNF is known to have neuroprotective effects on damaged adult sensory neurons, including the reversal of axotomy-induced changes in gene expression ($2, 6, 7$).

REPORTS

One of the most important functional consequences of peripheral nerve damage is the emergence of neuropathic pain. Such pains are often intense, persistent, and refractory to existing analgesic therapy. Here, we have examined the ability of GDNF to reverse the sensory abnormalities found in animal models of neuropathic pain and have studied putative mechanisms of action.

Adult rats received a partial ligation of one sciatic nerve (8) and continuous concurrent intrathecal infusion of GDNF or vehicle (9). Ipsilateral paw sensitivity to mechanical and thermal stimuli was assessed. Vehicle-treated animals developed significant mechanical and thermal hyperalgesia (drop of flexion-withdrawal thresholds from 12.1 ± 1 to 2.2 ± 0.3 g, noxious heat-induced paw withdrawal latency from 11.9 ± 0.5 to 7.4 ± 0.5 s, $P < 0.01$; Fig. 1A). These changes were seen within 2 days, persisting throughout the 15-day observation period (8). With GDNF treatment, neither mechanical nor thermal hyperalgesia developed (no change in threshold from baseline values at any time after surgery, $P > 0.1$; Fig. 1A). In a second model, animals received a fifth lumbar (L5) spinal nerve ligation [modified from (10)] with intrathecal GDNF or vehicle as before (9). Vehicle-treated animals developed profound hyperalgesia ($P < 0.01$); infusion of GDNF prevented any significant changes from preoperative baselines (Fig. 1B). Identical treatment with biologically active doses of nerve growth factor (NGF) or the neurotrophin NT-3 (5, 11) had no effect on the emergence or degree of sensory abnormality (Fig. 1B).

We then started GDNF treatment 2 days after spinal nerve ligation. Mechanical and thermal hyperalgesia developed within 2 days (drop from 12.7 ± 1.5 to 3 ± 0.6 g, 11.4 ± 0.3 to 9.1 ± 0.5 s, $P < 0.01$; Fig. 1C). These persisted in vehicle-treated animals ($P < 0.01$) but were reversed by GDNF treatment, after which thresholds reverted to normal levels ($P > 0.1$). Hyperalgesia reemerged within 3 days of cessation of GDNF infusion ($P < 0.01$). Identical chronic administration of GDNF to normal animals led to no change in responses to noxious thermal or mechanical stimuli; withdrawal thresholds did not significantly vary from baseline values (13 ± 1 g, 13 ± 0.5 s; $P > 0.1$). Acute peripheral treatment with GDNF (plantar injections of 0.1, 1, and 10 μ g) did not affect pain-related behavior; thermal withdrawal thresholds did

not significantly differ from baseline values when tested 0, 2, 4, 6, and 24 hours after injection ($P > 0.5$).

A critical and necessary event for neuropathic pain is the development of spontaneous activity following nerve damage (12). This activity arises from damaged neurons themselves and from those whose axons are intact but come in peripheral nerves along with degenerating axons [(13), see (14)]. Therefore, we studied ectopic activity in both L5 and L4 DRG neurons after spinal nerve ligation of L5 alone and tested the effects of GDNF treatment (15). In the L5 dorsal root 3 and 7 days after this injury, 31 ± 3 and $19 \pm 2\%$ of damaged myelinated sensory fibers exhibited spontaneous activity, compared with essentially zero in the acutely cut nerve (1237 myelinated units sampled; Fig. 2A). Mean spontaneous activity was 23 ± 2 spikes per second. No spontaneous activity was seen in C fibers at these time points (0/197 units). With GDNF treatment, fewer fibers exhibited spontaneous discharges (18 ± 1 and $11 \pm 1\%$ at 3 and 7 days, respectively; $P < 0.01$, ANOVA), and these units discharged less

frequently (14 ± 2 spikes per second; $P < 0.05$, *t* test). Thus, the afferent barrage entering the cord was greatly reduced (from 6.7 ± 0.7 to 2.5 ± 0.4 impulses per second per myelinated fiber; $P < 0.01$, *t* test; Fig. 2B). Using spike-triggered averaging, we found that spontaneously active units were among the slower conducting A fibers (Fig. 3B). GDNF selectively prevented ectopic activity in the slowest of these ($P < 0.05$, Kolmogorov-Smirnov test).

Qualitatively similar changes were seen in the L4 dorsal root after L5 spinal nerve ligation, with $14 \pm 2\%$ of myelinated sensory fibers exhibiting spontaneous activity (270 units sampled), averaging 16 ± 2 spikes per second. With GDNF treatment, fewer L4 fibers exhibited ectopic discharges ($3 \pm 2\%$; $P < 0.01$, *t* test), and the afferent barrage was reduced from 2.5 ± 0.5 to 0.7 ± 0.5 impulses per second per myelinated fiber ($P < 0.03$, *t* test; Fig. 2B). The conduction velocity of spontaneously active units in L4 was not significantly different from that of silent units, suggesting that most were low-threshold mechanoreceptors ($P > 0.1$, *t* test; Fig.

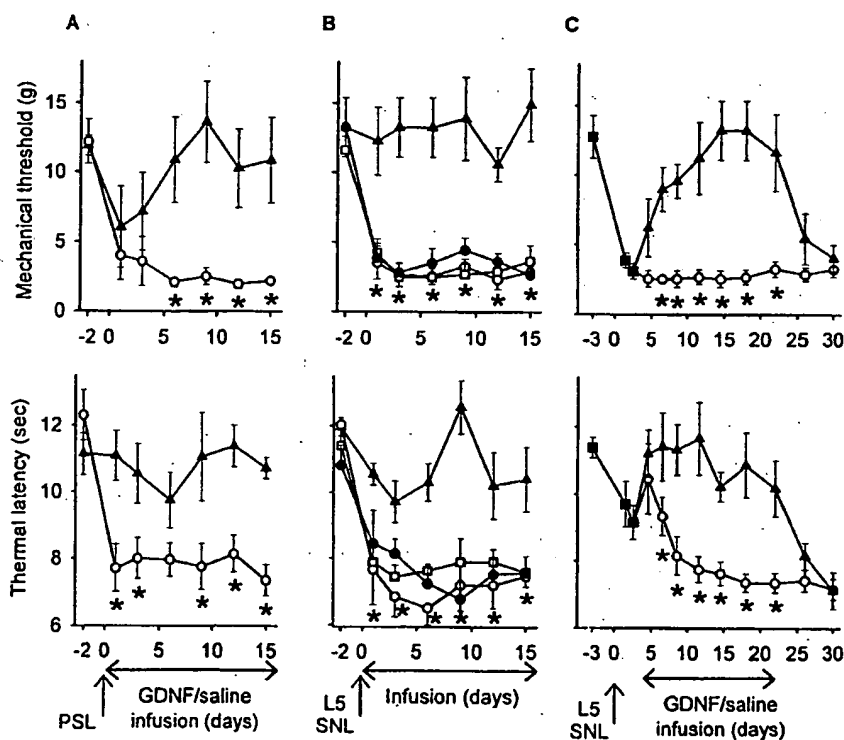


Fig. 1. Nociceptive responses of animals subjected to either partial sciatic ligation (PSL) or L5 spinal nerve ligation (SNL) combined with trophic factor treatment. Mechanical (upper) and thermal (lower) thresholds were tested. (A) PSL results in mechanical and thermal hyperalgesia in vehicle-treated animals (open circles). GDNF prevented the development of these sensory abnormalities (filled triangles). (B) L5 SNL also results in mechanical and thermal hyperalgesia. Intrathecal GDNF, but not NGF (open squares), NT-3 (filled circles), or vehicle prevented this. (C) Delayed infusion of GDNF but not saline reverses the sensory abnormalities established by a previous L5 SNL. The cessation of GDNF infusion results in the reemergence of hyperalgesia. Asterisks denote significant difference between vehicle- and GDNF-treated animals on each testing day (mean \pm SEM; see text for details). Filled squares denote pretreatment thresholds.

¹Centre for Neuroscience Research, King's College London, London SE1 7EH, UK. ²Department of Biology, University College London, London, WC1E 6BT UK.

*Present address: Department of Medicine, University College Hospital, London WC1E 6AU, UK.

†To whom correspondence should be addressed. E-mail: stephen.mcmahon@kcl.ac.uk

REPORTS

3A). GDNF prevented ectopic activity across this range of conduction velocities (distribution of saline and GDNF-treated units not significantly different, $P > 0.05$, Kolmogorov-Smirnov). No spontaneous activity was seen in C fibers in L4.

Ectopic activity in damaged nerves can be blocked with low concentrations of tetrodotoxin (TTX), suggesting a role for TTX-sensitive sodium channels in this event (16). Nerve damage induces novel, rapidly repriming sodium-channel activity (17). Concomitantly, transcripts encoding the type III embryonic sodium channel are up-regulated, and the two TTX-resistant channels in DRG neurons, SNS and NaN, are down-regulated (18). We examined the transcript levels of SNS, NaN, and the type III channel in the L4 and L5 DRG after L5 spinal nerve ligation using reverse transcriptase-polymerase chain reac-

tion (RT-PCR) (19). In L5, expression of the type III channel was increased, and SNS and NaN transcripts were decreased after this in-

jury (Fig. 4A). By using PCR conditions in the linear range (19), densitometric analysis of band intensity showed an increase in type III expression (26 ± 6 to 180 ± 21 , arbitrary units) and decreases in SNS and NaN expression (146 ± 12 to 58 ± 8 and 180 ± 8 to 100 ± 23 respectively; $P < 0.05$, ANOVA; Fig. 4B). The only significant change in the L4 DRG 7 days after L5 spinal nerve ligation was an increase in SNS expression (185 ± 5 to 307 ± 2 , arbitrary units; $P < 0.001$, ANOVA). GDNF treatment suppressed expression of the type III channel and partially restored SNS and NaN levels in L5 (mean band intensities 54 ± 12 , 117 ± 12 , 137 ± 33 respectively; not significantly different from naïve, $P > 0.1$, ANOVA), but had no effect on the subunits measured in L4. Changes in TTX-resistant channels are therefore poorly correlated with ectopic activity and neuropathic pain behavior. Plasticity of type III expression in damaged afferents is consistent with a significant role for it in the pathogenesis of neuropathic pain (20). The lack of significant changes in L4 may reflect the lower incidence

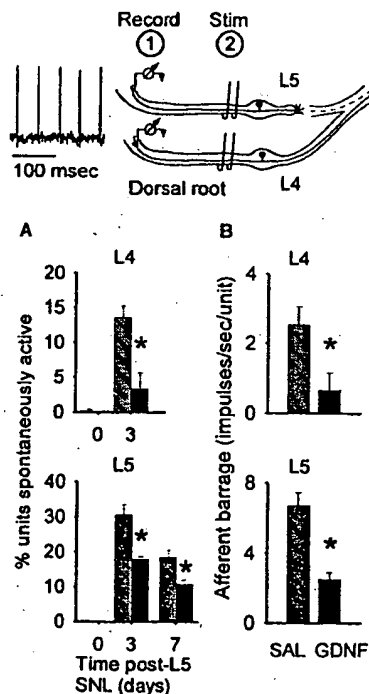


Fig. 2. GDNF reduces ectopic discharges in L4 and L5 sensory neurons following L5 spinal nerve ligation. (Top) Spontaneously active units were recorded from fine strands of the L4 or L5 dorsal root (circled 1) (example inset), and the total number of units in each strand was calculated by stimulating the whole root (circled 2). For L4 recordings the L4 spinal nerve was acutely cut 10 mm distal to the DRG. (A) L5 spinal nerve ligation induces spontaneous activity in many L4 and L5 myelinated afferents. This effect is markedly reduced by intrathecal GDNF treatment. (B) GDNF reduces the proportion and firing frequency of ectopically discharging units, thereby dramatically decreasing the total afferent barrage entering the spinal cord. Asterisks denote significant difference between vehicle- and GDNF-treated animals (mean \pm SEM; see text for details).

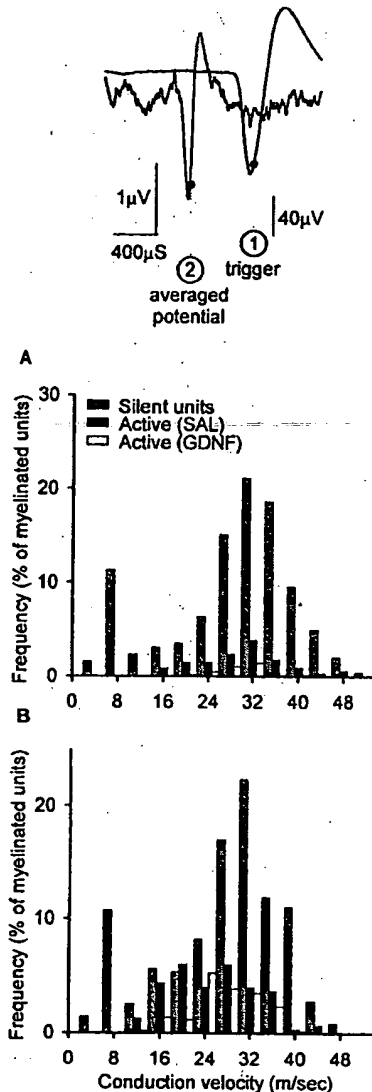


Fig. 3. The conduction velocity of spontaneously active sensory neurons after L5 spinal nerve ligation was estimated by spike-triggered averaging. (Top) A spontaneously active unit in the dorsal root (circled 1) triggered a retrospective averaged recording in the appropriate whole root (circled 2). The conduction velocity of silent afferents was calculated from the stimulation experiments shown in Fig. 2. For L4 sensory neurons (A), ectopic firing is seen in units with a wide range of conduction velocities, and the whole of this range appears to be affected by GDNF treatment. For L5 sensory neurons (B), spontaneously active units are a slower subset of myelinated fibers, and GDNF treatment selectively affects the slowest of these. These slower conducting afferents may have been erstwhile myelinated nociceptors, or fibers representative of the whole population of myelinated afferents but particularly slowed following axotomy.

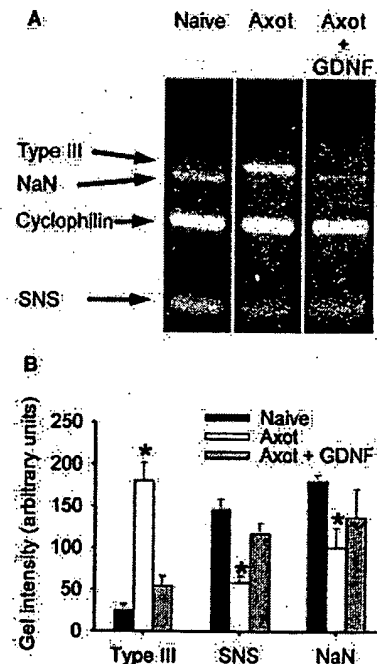


Fig. 4. Altered expression of sensory neuron sodium channel α subunits after L5 spinal nerve ligation: effects of GDNF treatment. RT-PCR analysis of L5 DRG RNA extracts from naïve and nerve-injured rats treated with GDNF or vehicle. RT-PCR reactions using primer pairs for type III, NaN, cyclophilin, and SNS were added to the reaction mixture (19). (A) Nerve injury up-regulates type III and down-regulates NaN and SNS; treatment with GDNF prevents the novel expression of the type III channel and partially restores SNS and NaN transcripts. (B) Densitometric analysis of band intensity across each experimental group. Asterisks denote significant difference from naïve; $P < 0.05$, ANOVA.

REPORTS

of ectopic activity in these neurons and/or other contributory mechanisms.

The nerve damage that precipitates neuropathic pain leads to many changes in sensory neurons, including alterations in putative neurotransmitters/modulators, receptors, ion channels, structural proteins, and anatomic terminations (21). The relative contributions of these reactive changes are currently unknown, especially the role of small-caliber nociceptive neurons or large-caliber mechanosensitive afferents (22). There is conflicting evidence regarding the role of nociceptors. Antisense treatment against SNS (normally expressed in nociceptors) reduces neuropathic pain behavior (23). However, few unmyelinated afferents discharge ectopically in neuropathic models (24), and mechanical hyperalgesia is unaffected by the C fiber toxin RTX (25). We have also found that the development of neuropathic pain behavior is unaffected in null mutant mice lacking the SNS channel (26). In contrast, the data here and in the literature support a pivotal role for myelinated afferents in the generation of neuropathic pain: animal models show that an essential drive for abnormal pain sensitivity is the generation of ectopic activity in damaged sensory neurons (12, 27), arising almost exclusively in myelinated neurons; in human neuropathic pain states, activation of large A β afferents is capable of inducing pain (28); selective lesions of large myelinated afferents reduce neuropathic pain behavior in animals (29).

The ectopic activity that arises in neuropathic conditions is TTX-sensitive. Only the expression of the TTX-sensitive type III α subunit is known to increase following nerve injury (20), and we show here that GDNF prevents this. It is unclear whether GDNF acts tonically to repress type III expression under normal circumstances. As GDNF treatment does not affect pain-related behavior in normal animals, the analgesic actions reported here are unlikely to represent general effects on pain signaling systems. However, as GDNF regulates the expression of a variety of genes in both large- and small-caliber sensory neurons, including some functionally relevant for nociceptive behavior [P2X3 and VR1 (6, 7)], effects other than those on the type III sodium channel may contribute to its analgesic actions. This question can only be definitively addressed with specific, type III channel blockers, which have yet to be developed. However, the data presented here provide a rational basis for, and demonstrate the efficacy of, GDNF in the treatment of neuropathic pain.

References and Notes

1. A. Buj-Bello, V. L. Buchman, A. Horton, A. Rosenthal, A. M. Davies, *Neuron* 15, 821 (1995).
2. D. L. H. Bennett et al., *J. Neurosci.* 18, 3059 (1998).
3. D. C. Molliver et al., *Neuron* 19, 849 (1997).
4. P. Ledere et al., *Neuroscience* 82, 545 (1998).
5. M. S. Ramer, J. V. Priestley, S. B. McMahon, *Nature* 403, 312 (2000).
6. E. J. Bradbury, G. Burnstock, S. B. McMahon, *Mol. Cell. Neurosci.* 12, 256 (1998).
7. P. Ogun-Muyiwa, R. Helliwell, P. McIntyre, J. Winter, *Neuroreport* 10, 2107 (1999).
8. Z. Seltzer, R. Dubner, Y. Shir, *Pain* 43, 205 (1990).
9. Experiments were carried out in accordance with the UK Animals (Scientific Procedures) Act 1986. Trophic factors were delivered at 12 μ g/day (2). See (30) for details of surgery as well as behavioral and statistical analyses.
10. S. H. Kim and J. M. Chung, *Pain* 50, 355 (1992).
11. E. J. Bradbury, S. Khemani, V. R. King, J. V. Priestley, S. B. McMahon, *Eur. J. Neurosci.* 11, 3873 (1999).
12. K. Sheen and J. M. Chung, *Brain Res.* 610, 62 (1993).
13. M. Michaelis, X. Liu, W. Janig, *J. Neurosci.* 20, 2742 (2000).
14. Y. Li, M. J. Dorsi, R. A. Meyer, A. J. Belzberg, *Pain* 85, 493 (2000).
15. See (30) for details of recording ectopic discharges in primary afferent neurons.
16. I. Omana-Zapata, M. A. Khabbaz, J. C. Hunter, D. E. Clarke, K. R. Bley, *Pain* 72, 41 (1997).
17. J. A. Black et al., *J. Neurophysiol.* 82, 2776 (1999).
18. J. Fjell et al., *Brain Res. Mol. Brain Res.* 67, 267 (1999).
19. See (30) for details of RT-PCR analysis of sodium channel expression in sensory neurons.
20. S. G. Waxman, *Pain* 56, S133 (1999).
21. T. J. Boucher, B. J. Kerr, M. S. Ramer, S. W. N. Thompson, S. B. McMahon, *Proc. 9th World Congr. Pain* 16, 175 (2000).
22. M. S. Gold, *Pain* 84, 117 (2000).
23. J. Lai, J. C. Hunter, M. H. Ossipov, F. Porreca, *Methods Enzymol.* 314, 201 (2000).
24. X. Liu, S. Eschenfelder, K.-H. Blenk, W. Janig, H.-J. Häbler, *Pain* 84, 309 (2000).
25. M. H. Ossipov, D. Bian, T. P. J. Malan, J. Lai, F. Porreca, *Pain* 79, 127 (1999).
26. B. J. Kerr, S. B. McMahon, J. N. Wood, unpublished observations.
27. Y. W. Yoon, H. S. Na, J. M. Chung, *Pain* 64, 27 (1996).
28. J. N. Campbell, S. N. Raja, R. A. Meyer, S. B. Mackinnon, *Pain* 32, 89 (1988).
29. D. Bian, M. H. Ossipov, C. Zhong, T. P. Malan, F. Porreca, *Neurosci. Lett.* 241, (1998).
30. Supplementary material is available at www.sciencemag.org/feature/data/1054233.shl.
31. We thank V. Cheah for expert technical assistance, Amgen for supplying rhGDNF, and Genentech for the gift of rhNGF and rhBDNF. This work was supported by the Medical Research Council (T.J.B., D.L.H.B., J.B.M., J.N.W., and S.B.M.) and the Wellcome Trust (J.N.W., K.O., and S.B.M.).

21 July 2000; accepted 22 August 2000

Long-Term Survival But Impaired Homeostatic Proliferation of Naïve T Cells in the Absence of p56^{lck}

Benedict Seddon,¹ Giuseppe Legname,² Peter Tomlinson,¹ Rose Zamoyska^{1*}

Interactions between the T cell receptor (TCR) and major histocompatibility complex antigens are essential for the survival and homeostasis of peripheral T lymphocytes. However, little is known about the TCR signaling events that result from these interactions. The peripheral T cell pool of p56^{lck} (lck)-deficient mice was reconstituted by the expression of an inducible lck transgene. Continued survival of peripheral naïve T cells was observed for long periods after switching off the transgene. Adoptive transfer of T cells from these mice into T lymphopoietic hosts confirmed that T cell survival was independent of lck but revealed its essential role in TCR-driven homeostatic proliferation of naïve T cells in response to the T cell-deficient host environment. These data suggest that survival and homeostatic expansion depend on different signals.

Despite environmental antigenic stimulation and thymic production, the size of the peripheral T cell pool is maintained at a remarkably constant level (1). In common with cells of other tissues, T cells require specific signals in order to survive. In contrast to memory T cells (2–4), naïve T cells require interactions of the TCR with self major histocompatibility complex (MHC) anti-

gens for their prolonged survival (5–10). Furthermore, T cells also have the capacity to proliferate under T lymphopoietic conditions, and for naïve T cells this too requires recognition of self MHC antigens (8, 11–13). However, less is known about the TCR signals that govern these processes. The src family protein tyrosine kinase p56^{lck} (lck) is involved in the most proximal phosphorylation events during TCR signaling and plays crucial roles at multiple points in T cell development (14, 15). It seemed likely, therefore, that lck would play a critical role in the transduction of survival and homeostatic signals through the TCR.

To evaluate the role of lck in T cell homeostasis, we produced mice that express lck in

¹Division of Molecular Immunology, National Institute for Medical Research, The Ridgeway, Mill Hill, London NW7 1AA, UK. ²Institute for Neurodegenerative Diseases, University of California–San Francisco, San Francisco, CA 94143, USA.

*To whom correspondence should be addressed. E-mail: rzamoys@nimr.mrc.ac.uk

Subclassified Acutely Dissociated Cells of Rat DRG: Histochemistry and Patterns of Capsaicin-, Proton-, and ATP-Activated Currents

JEFFREY C. PETRUSKA,⁴ JINTANA NAPAPORN,³ RICHARD D. JOHNSON,¹
JIANGUO G. GU,² AND BRIAN Y. COOPER²

¹Department of Physiological Sciences, College of Veterinary Medicine, University of Florida; ²Department of Oral Surgery and Diagnostic Sciences, Division of Neuroscience, University of Florida College of Dentistry;

³Department of Pharmaceutics, University of Florida College of Pharmacy; and ⁴Department of Neuroscience, McKnight Brain Institute, University of Florida College of Medicine, Gainesville, Florida 32610

Received 9 December 1999; accepted in final form 19 July 2000

Petruska, Jeffrey C., Jintana Napaporn, Richard D. Johnson, Jianguo G. Gu, and Brian Y. Cooper. Subclassified acutely dissociated cells of rat DRG: histochemistry and patterns of capsaicin-, proton-, and ATP-activated currents. *J Neurophysiol* 84: 2365–2379, 2000. We used a “current signature” method to subclassify acutely dissociated dorsal root ganglion (DRG) cells into nine subgroups. Cells subclassified by current signature had uniform properties. The type 1 cell had moderate capsaicin sensitivity (25.9 pA/pF), powerful, slowly desensitizing ($\tau = 2,300$ ms), ATP-activated current (13.3 pA/pF), and small nondesensitizing responses to acidic solutions (5.6 pA/pF). Type 1 cells expressed calcitonin gene-related peptide immunoreactivity (CGRP-IR), manifested a wide action potential (7.3 ms), long duration afterhyperpolarization (57.0 ms), and were IB4 positive. The type 2 cell exhibited large capsaicin activated currents (134.9 pA/pF) but weak nondesensitizing responses to protons (15.3 pA/pF). Currents activated by ATP and $\alpha\beta$ -m-ATP (51.7 and 44.6 pA/pF, respectively) had fast desensitization kinetics ($\tau = 214$ ms) that were distinct from all other cell types. Type 2 cells were IB4 positive but did not contain either substance P (SP) or CGRP-IR. Similar to capsaicin-sensitive nociceptors in vivo, the afterhyperpolarization of the type 2 cell was prolonged (54.7 ms). The type 3 cell expressed, amiloride-sensitive, rapidly desensitizing ($\tau = 683$ ms) proton-activated currents (127.0 pA/pF), and was insensitive to ATP or capsaicin. The type 3 cell was IB4 negative and contained neither CGRP nor SP-IR. The afterhyperpolarization (17.5 ms) suggested nonnociceptive function. The type 4 cell had powerful ATP-activated currents (17.4 pA/pF) with slow desensitization kinetics ($\tau = 2,813$ ms). The afterhyperpolarization was prolonged (46.5 ms), suggesting that this cell type might belong to a capsaicin-insensitive nociceptor population. The type 4 cell did not contain peptides. The type 7 cell manifested amiloride-sensitive, proton-activated currents (45.8 pA/pF) with very fast desensitization kinetics ($\tau = 255$ ms) and was further distinct from the type 3 cell by virtue of a nondesensitizing amiloride-insensitive component (6.0 pA/pF). Capsaicin and ATP sensitivity were relatively weak (4.3 and 2.9 pA/pF, respectively). Type 7 cells were IB4 positive and contained both SP and CGRP-IR. They exhibited an exceptionally long afterhyperpolarization (110 ms) that was suggestive of a silent (mechanically insensitive) nociceptor. We concluded that presorting of DRG cells by current signatures separated them into internally homogenous subpopulations that were distinct from other subclassified cell types.

INTRODUCTION

Acute and primary cultures of dorsal root ganglion (DRG) cells are commonly employed in investigations of sensory physiology. Interpretation of the data from such studies is confounded by the complexity of the DRG cell population. Cells harvested from the DRG could represent more than 25 functionally diverse afferent populations that are specialized to encode a variety of sensory events. Cultured cell bodies formerly gave rise to peripheral processes unique to muscle (annulospiral, flowerspray, golgi), joint (Ruffini, Pacinian), touch (Pacinian, Merkel, Meisner, Ruffini, guard hair, down hair, A δ and C itch), warmth (C warm), cooling (A δ and C cooling), and pain (noted below) sensations (Darian-Smith 1984a,b; Iggo 1985). While nociceptors are probably the afferents of greatest interest, they are composed of highly specialized subpopulations.

Classic sharp electrode and crushed end recordings have revealed a diverse and highly specialized nociceptive population, in vivo. A number of functional subtypes have been characterized in numerous preparations. Careful characterization of afferent properties have revealed a nociceptor population that includes representatives of A β , A δ , and C fiber, cutaneous, deep, muscle, and visceral nociceptive subgroups that express single and multiple transduction capacities in various combinations. This diverse nociceptor pool would include A β high-threshold mechanoreceptors (HTM), A δ HTM, A δ polymodal nociceptors (PMN), A δ mechanoheat (MH) nociceptors, A δ cold nociceptors, C HTM, C PMN, C MH nociceptors, C heat nociceptors, C chemonociceptors, and A δ and C “silent” nociceptors (Belmonte and Giraldez 1981; Campbell et al. 1990; Cervero 1994; Cooper and Sessle 1993; Mense 1993; Schaible and Grubb 1993; Tanelian and Beuerman 1984). The advantage of being able to study these subpopulations in vitro is manifest. However, identification of specific nociceptive subgroups in DRG culture with anything approaching the detail that is possible with classic in vivo methods has proven difficult.

To distinguish nociceptive from nonnociceptive groups in vitro, laboratories have relied on evidence that a number of

Address for reprint requests: B. Cooper, Dept. of Oral Surgery and Diagnostic Sciences, Division of Neuroscience, Box 100416, JHMH, University of Florida College of Dentistry, Gainesville, FL 32610. (E-mail: Bcooper@dental.ufl.edu).

The costs of publication of this article were defrayed in part by the payment of page charges. The article must therefore be hereby marked “advertisement” in accordance with 18 U.S.C. Section 1734 solely to indicate this fact.

anatomic and functional properties of nociceptors covary with cell size and/or action potential shape (e.g., presence of a "hump" or "shoulder"). These criteria have been shown to be correlates of thinly myelinated and unmyelinated fiber groups that include the majority of nociceptive subpopulations (Harper and Lawson 1985; Yoshida and Matsuda 1979). Cell size and action potential shape also correlate well with high-threshold mechanoreception (Djouhri et al. 1998; Koerber et al. 1988; Ritter and Mendel 1992; Rose et al. 1986), a property that is present in most nociceptive subgroups (see above). However, laboratories working in vitro have relied mainly on a binary, pharmacological classification scheme in which nociceptive cells are identified a posteriori, according to capsaicin sensitivity. These schemes, while useful, cannot hope to reveal the rich diversity of a nociceptive population that is comprised of 10 or more distinct phenotypes that include a number of important capsaicin *insensitive* subtypes.

It is likely that capsaicin sensitivity can identify perhaps four subsets of heat-reactive nociceptive cells, but it cannot distinguish between them. In vivo, capsaicin activates a large portion of the C heat nociceptive, C PMN, and at least half of the C MH nociceptive pool (Baumann et al. 1991; Belmonte et al. 1991; Chen et al. 1997; Szolcsányi et al. 1988). A portion of the A δ MH and A δ silent nociceptor group is also activated (Baumann et al. 1991; Meyer et al. 1991; Szolcsányi et al. 1988; Treede et al. 1998). Moreover, it is not generally acknowledged that warm fibers, as well as some A β low-threshold mechanoreceptors, are also capsaicin sensitive (Baumann et al. 1991; Szolcsányi et al. 1988). Therefore the identification of nociceptors based solely on capsaicin reactivity will result in inclusion of several functional cell types, many of which may be nociceptive, but belong to functionally distinct nociceptive subclasses, and still others cells that are not a part of the pain system. In addition, reliance on identification of nociceptive populations by capsaicin sensitivity alone will certainly leave an important portion of the nociceptive population (A δ and C high-threshold mechanoreceptors, A δ and C mechanocold, A δ and C silent, C chemosensitive) inaccessible to investigation in vitro.

To identify functional nociceptive DRG subpopulations in vitro, it is first necessary to develop criteria that can readily classify cells into distinct, but internally homogenous subpopulations whose properties can be determined and combined across a series of experiments. Additional criteria are then needed to determine which cells are nociceptive and the specific nociceptive subpopulations they represent.

The work of the Scroggs and Lawson laboratories represent two recent, and complementary approaches to cell classification and nociceptor specification (Cardenas et al. 1995; Djouhri et al. 1998; Lawson 1996; McCarthy and Lawson 1997). Although differing in detail, both of these methods are ultimately based on the notion that functionally uniform cell populations can be identified by their repertoire of voltage-activated currents. Due to the great diversity of voltage-activated currents in DRG (Dib-Hajj et al. 1998; Gold et al. 1996; Mayer and Westbrook 1983; Roy and Narahashi 1992; Tate et al. 1998), these techniques have the potential to provide criteria by which a large number of DRG subpopulations might be distinguished. Four subpopulations of cells (types 1, 2, 3, and 4) have been characterized by Scroggs and associates. These populations are

internally uniform with respect to reactivity to capsaicin and serotonin (Cardenas et al. 1995, 1997a,b).

Methods developed by the Lawson laboratory complement this approach by providing criteria to more completely identify nociceptive subgroups. Using sharp electrode recordings and traditional characterization methods, Lawson and colleagues (Djouhri et al. 1998; Lawson 1996; McCarthy and Lawson 1997) have shown that the duration of afterhyperpolarization distinguishes 1) nociceptive C and A δ subgroups from nonnociceptive A β fibers, 2) nociceptive from nonnociceptive groups from within the A δ and C fiber categories, and 3) mechanically sensitive from mechanically insensitive (silent) nociceptor populations. Importantly, these criteria do not rely on capsaicin sensitivity, thus permitting capsaicin-insensitive nociceptive populations to be revealed. While this technique has been shown to work well in vivo, it is not clear that it can be successfully applied in vitro.

In the experiments described below, we used cluster analysis to form nine subclasses of cells that were distinguished by voltage-activated current signatures. The current signature method is an extension of procedures that were first applied to DRG cell classification by Scroggs and Cardenas (Cardenas et al. 1995). To determine whether these nine subgroups (clusters) had predictive validity, we have examined whether each subtype was homogenous with respect to histochemical phenotype (binding of the B4 isolectin from *Griffonia simplicifolia* (IB4), immunoreactivity (IR) for substance P (SP) and calcitonin gene-related peptide (CGRP), algescic reactivity (capsaicin, protons, ATP), and action potential features (duration, afterhyperpolarization). In the present report, current signatures of the nine cell clusters and the properties of five of these subclassified cell groups are presented in detail. Some of these data have been published in abstract form (Cooper et al. 1999a,b).

METHODS

Subjects

Adult male Sprague-Dawley rats (90–110 g) were anesthetized with a combination of xylazine (4 mg/kg) and ketamine (40 mg/kg). Following decapitation, the spinal cord was rapidly removed, and the dorsal root ganglia were dissected free. All animals were housed in American Association for Accreditation of Laboratory Animal Care-approved quarters, and all procedures were reviewed and approved by the local Institutional Animal Care and Use Committee.

Preparation of cells

Dissected ganglia were placed in a tube containing dispase (neutral protease, 5 mg/ml; Boehringer Mannheim) and collagenase (2 mg/ml; Sigma type 1). The tube was shaken for 60 min in a heated (35°C) bath. Following wash and trituration, recovered cells were plated on 6–10 polylysine-coated Petri dishes. Dishes were mounted on a Nikon Diaphot inverted microscope or kept in an aerated holding bath for later use. All recordings were completed within 10 h of plating.

Whole cell patch recording

Glass pipettes (Scientific Products B4416-1) were prepared (2–4 M Ω) with a Brown and Flaming type horizontal puller (Sutter model P87). Whole cell recordings were made with an Axopatch 200B (Axon Instruments). Stimuli were controlled and digital records captured with pClamp 6.0 software and Digipack 1200b A/D converter

A Classification Protocols

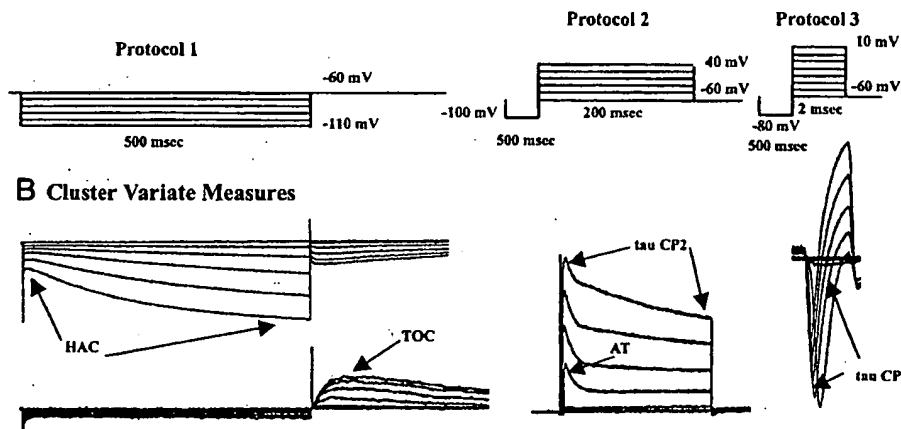


FIG. 1. Three protocols for cell classification. *A*: classification protocols 1, 2, and 3 produce current signatures exemplified in *B*. *B*: quantification of cluster variates from current signatures. Hyperpolarization-activated current (HAC) was measured as the difference, in pA, between the points indicated by the arrows on the last trace (-110 -mV step). Transient outward current (TOC), was measured as the peak current, in pA (relative to baseline) during the 500 ms that followed repolarization to -60 mV. The decay constant τ_{CP2} was derived from single or double exponential fits to the final outward current trace ($+40$ mV). The activation threshold of A-current peaks is indicated as well (AT). The decay constant τ_{CP3} was derived from single exponential fits to the inactivation phase of the 1st complete inward current trace. Fits were made between arrowheads. When double exponentials were required, the fastest component was used.

(Axon Instruments). Cells with a membrane potential more positive than -45 mV or more negative than -70 mV were not accepted. Series resistance (R_s) was compensated 40–60% with Axopatch 200B compensation circuitry. Leak current was assessed repeatedly throughout the protocol (average of 8 consecutive steps to -70 mV, $V_h = -60$, 10 ms duration). Leak currents were subtracted off-line. Cell size (in picofarads) was determined by integration of the averaged capacitive transient (10 mV step; $V_h = -60$).

Cell classification protocols

Cells were preselected according to diameter. Recordings were made exclusively from cells with diameters between 16 and 48 μ m. Cell diameter was estimated from the average of the longest and shortest axis as measured through an eyepiece micrometer scale. From among the smallest diameter cells (16–22 μ m), recordings were made only from cells with large nuclei (10–15 μ m). Cells were classified according to patterns of voltage-activated currents (current signatures) that were revealed by three classification protocols. 1) *Classification Protocol 1 (CP1)* was used to examine the pattern of hyperpolarization activated currents. With CP1, currents were evoked by a series of hyperpolarizing pulses presented from a V_h of -60 mV (10 mV per step to a final potential of -110 mV; 500-ms, 4-s interstimulus interval). 2) *Classification Protocol 2 (CP2)* was used to produce outward current patterns. From a V_h of -60 mV, a 500-ms conditioning pulse to -100 mV was followed by 200-ms depolarizing command steps (20 mV) to a final potential of $+40$ mV. 3) *Classification Protocol 3 (CP3)* was used to produce inward current patterns. With the cell held at -60 mV, a 500-ms conditioning pulse to -80 mV was followed by a series of depolarizing command steps (10-mV steps, 2.0 ms duration) to a final potential of $+10$ mV. The three protocols are illustrated in Fig. 1.

Cluster analysis

To determine whether cells could be subclassified according to their pattern of voltage-activated currents, cluster analysis was performed using up to five cluster variates that were derived from inward and outward current signatures. Two characteristics were quantified from the hyperpolarization test protocol. Hyperpolarization activated currents (HAC pA) were assessed as the total inward current measured during the last hyperpolarization step (-110 mV). Transient outward current (TOC pA) was measured as the peak current in a 500-ms window that followed repolarization (-60 mV) from the final hyperpolarization step (-110 mV). Two characteristics were assessed from the outward current protocol (CP2). Using the trace evoked by $+40$ mV, a curve of the form $A_1 \exp[-(t - k)/\tau_1] \dots + C$ (Clampfit 6.0)

was fit to the trace evoked at the strongest depolarization step. The tau of decay from single or double exponential fits was used as a clustering variable (τ_{CP2} ms). A second clustering variable from the CP2 protocol was the threshold (mV) of A-current peaks (AT; see Fig. 1). A-currents were confirmed by sensitivity to 4-aminopyridine (10 mM; $n = 5$). A fifth clustering variable was derived from the inward current protocol (CP3). A curve of the form noted above was fit to the declining phase of the first suprathreshold trace of the inward current. The tau of decay was used as a clustering variable (τ_{CP3} ms; see Fig. 1).

A nonhierarchical cluster analysis (K means analysis; FASTCLUS, Statistical Analysis System) was used to determine whether current signature variates could identify specific clusters of cells within populations of very small (<22 μ m), small (24–32 μ m), and medium (35–48 μ m)-sized neurons. Because FASTCLUS uses a sequential threshold procedure (Hair et al. 1998), clusters were seeded by representative data to avoid order effects. For a stopping rule, the maximum cubic cluster criterion (CCC) was determined from multiple cluster solutions (MAXCLUS) using from two to five cluster variates (HAC, TOC, τ_{CP2} , τ_{CP3} , AT). The predictive validity of the cluster solution was determined by the homogeneity of cell properties within a cluster. Cell properties included action potential features, currents evoked by alginate agents, the kinetics of these currents and histochemical profiles of the recorded cells. Because of the large number of cell clusters identified (9), it was necessary to limit this report to validation of five of the nine clusters.

Action potential

A 1-ms, 1,500-pA current step was used to determine afterhyperpolarization (AHP) and action potential duration at the base (APDb). To quantify AHP, we used a criterion of 80% recovery to baseline (AHP80) (Lawson et al. 1997). Measurements are detailed in Fig. 2.

Drugs and solutions

Plated cells were superfused in rat Tyrode's solution containing (in mM) 140 NaCl, 4 KCl, 2 MgCl₂, 2 CaCl₂, 10 glucose, and 10 HEPES, adjusted to pH 7.4 with NaOH. Recordings were made 3–10 h after plating at room temperature. Test solutions were applied via gravity-fed pipette positioned approximately 1 mm from the cell (sewer pipe). The recording electrodes were filled with (in mM) 120 KCl, 5 Na₂-ATP, 0.4 Na₂-GTP, 5 EGTA, 2.25 CaCl₂, 5 MgCl₂, and 20 HEPES, adjusted to pH 7.4 with KOH; osmolarity was approximately 315–325 mOsm. Capsaicin was prepared from a 10-mM stock solution (in 100% ethanol) to a final concentration of 500 to 5,000 nM. The final concentration of ethanol was $<0.1\%$. ATP and $\alpha\beta$ -m-ATP were

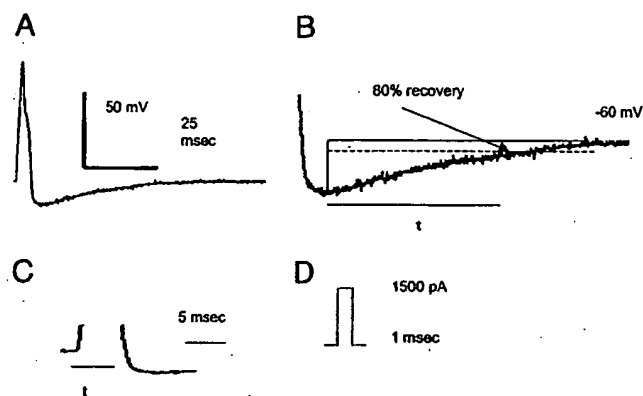


FIG. 2. Measurement of AHP80. Afterhyperpolarizations (AHPs) were measured as defined by Lawson and colleagues (Djourhi et al. 1998). *A*: representative action potential. Baseline corrected to -60 mV. *B*: the AHP80 was the time (t) required for the AHP (measured in mV) to decay to 80% of its peak value (arrow). *C*: the action potential duration (APDb) was measured as the time (t) from the 1st upward deflection of the AP waveform to its return to baseline (-60 mV). *D*: stimulus waveform. The amplitude of the current pulse was adjusted to threshold (1,500–3,500 pA, 500-pA steps). The duration was always 1 ms.

prepared from stock solutions of 10 mM (in water) to a final concentration of 10 μ M. Amiloride solution (100 μ M) was prepared fresh on the day of the experiment. All drugs were purchased from Sigma Chemical.

Immunohistochemistry

Most cells that were exposed to capsaicin, protons, and ATP were subsequently processed for the presence of substance P, CGRP and binding of isolectin GS-I-B4 (IB4). After a recording was completed, a photograph of the cell was taken. The bath solution was replaced with 4% paraformaldehyde (PFA) in phosphate-buffered saline (PBS) for 20–30 min and then replaced with a similar solution containing 0.4% Triton X-100. The cells were subsequently rinsed with PBS, and then incubated in 1:30 normal goat serum in PBS with Triton X-100 for 1 h. Cells were incubated over sequential evenings in solutions of polyclonal anti-substance P (SP; 1:3,000, Peninsula Labs) and then monoclonal anti-CGRP (1:2,000, RBI) antisera. The primary antisera were detected by incubation with the appropriate species-specific secondary antibodies conjugated with either AlexaFluor 594 (red) or AlexaFluor 488 (green; Molecular Probes). The cells were then incubated overnight in a 10- μ g/ml solution of HRP-conjugated GS-I-B4 isolectin. Lectin binding was visualized using the a tyramide-coumarin amplification solution (NEN). The cells were viewed with a Zeiss Axiophot microscope equipped with the appropriate fluorescence filters (Omega Optical). The expression of each of the three markers was determined by an experimenter (JP) blinded to the classification of each cell.

Statistics

Peak currents were normalized for cell size (pA/pF). Rise times were computed as the time difference between the first deviation from the baseline to 90% of the peak current observed. The exponential decay constants (τ) were derived from the expression $A_1 \exp[-(t - k)/\tau_1] + C$ (Clampfit 6.0). Fits were made at points between 10% of the peak current and 90% of the return to baseline using Clampfit software (Axon Instruments). The Mann-Whitney U test was applied to independent sample comparisons. The alpha level was set at 0.05.

RESULTS

Cluster analysis

Cells were classified based on currents evoked by a series of three classification protocols (Fig. 1). Classification protocols 1, 2, and 3 produced distinct patterns of hyperpolarization and depolarization activated inward and outward currents (Fig. 3). Five measures of current amplitude and inactivation were used to form variables that were suitable for cluster analysis (HAC, TOC, τ_{CP2} , τ_{CP3} , AT).

Using a K means procedure, we identified nine clusters of cells from very small (<22 μ m; $n = 38$), small (24–32 μ m; $n = 56$), and medium (32–48 μ m; $n = 59$)-sized neurons. Within the small cell population, two major subpopulations were formed by clustering on two current signature variables (TOC, τ_{CP2}). These were labeled types 1 and 2. Among very small-sized cells, cluster analysis identified two major subpopulations based on two cluster variables (HAC, τ_{CP3}). These cells were labeled types 3 and 7. Large CCC scores were obtained with both solutions (see Table 1). The greatest variety of cells was observed in the medium cell range. Here, using five cluster variables (HAC, TOC, τ_{CP2} , τ_{CP3} , AT), we identified five cell subpopulations. These were given labels types 4, 5, 6, 8, and 9. Current signatures that were representative of the cell clusters are illustrated in Fig. 3. Predictive validity of the clusters was determined by examining the physiological, pharmacological, and histochemical properties of the cells within each cluster ($n = 170$). If the cell properties of each cluster are uniform, a good cluster solution has been found.

Type 1 cell

CELL IDENTIFICATION AND ACTION POTENTIAL. Cells clustering in the type 1 group ($n = 32$) exhibited little hyperpolarization or transient outward current (Fig. 3; Table 1). All type 1 cells had small cell body diameters (24–30 μ m; 31.4 ± 1.1 pF, mean \pm SE), and broad action potentials with a pronounced deflection on the falling phase. A substantial AHP was observed (Fig. 4; Table 2).

ALGESIC PROFILE. Type 1 cells exhibited uniform algescic response profiles. Capsaicin sensitivity was present in most cases (22 of 28 cases). Capsaicin-induced currents (1 μ M) were typically slow in onset with a relatively modest peak amplitude (Fig. 4). Some current was present within 15 s, but peak currents required 30 or more seconds to fully develop. Regardless of capsaicin sensitivity, all type 1 cells manifested weak inward current in the presence of acidic solutions. These currents developed simultaneously with proton application, but onset kinetics were slow and current was maintained for the duration of proton application (Fig. 4). Nondesensitizing currents were observed at both pH 6.1 ($n = 17$) as well as pH 5.0 ($n = 24$); however, those at pH 6.1 were barely suprathreshold (2.62 ± 1.3 pA/pF). In contrast, powerful, rapidly activating, slowly desensitizing currents were evoked by ATP in all cases tested (10 μ M; $n = 6$; Fig. 4, Table 2). The kinetics of these currents were internally consistent (Table 3). As shown below, this form of ATP-activated current was markedly different from those in other capsaicin-sensitive cell types (types 2 and 7).

Cells clustering in this category exhibited uniform histochemistry. Six type 1 cells were prepared for immunocytochemistry following recordings. Five of the six cases contained CGRP-IR,

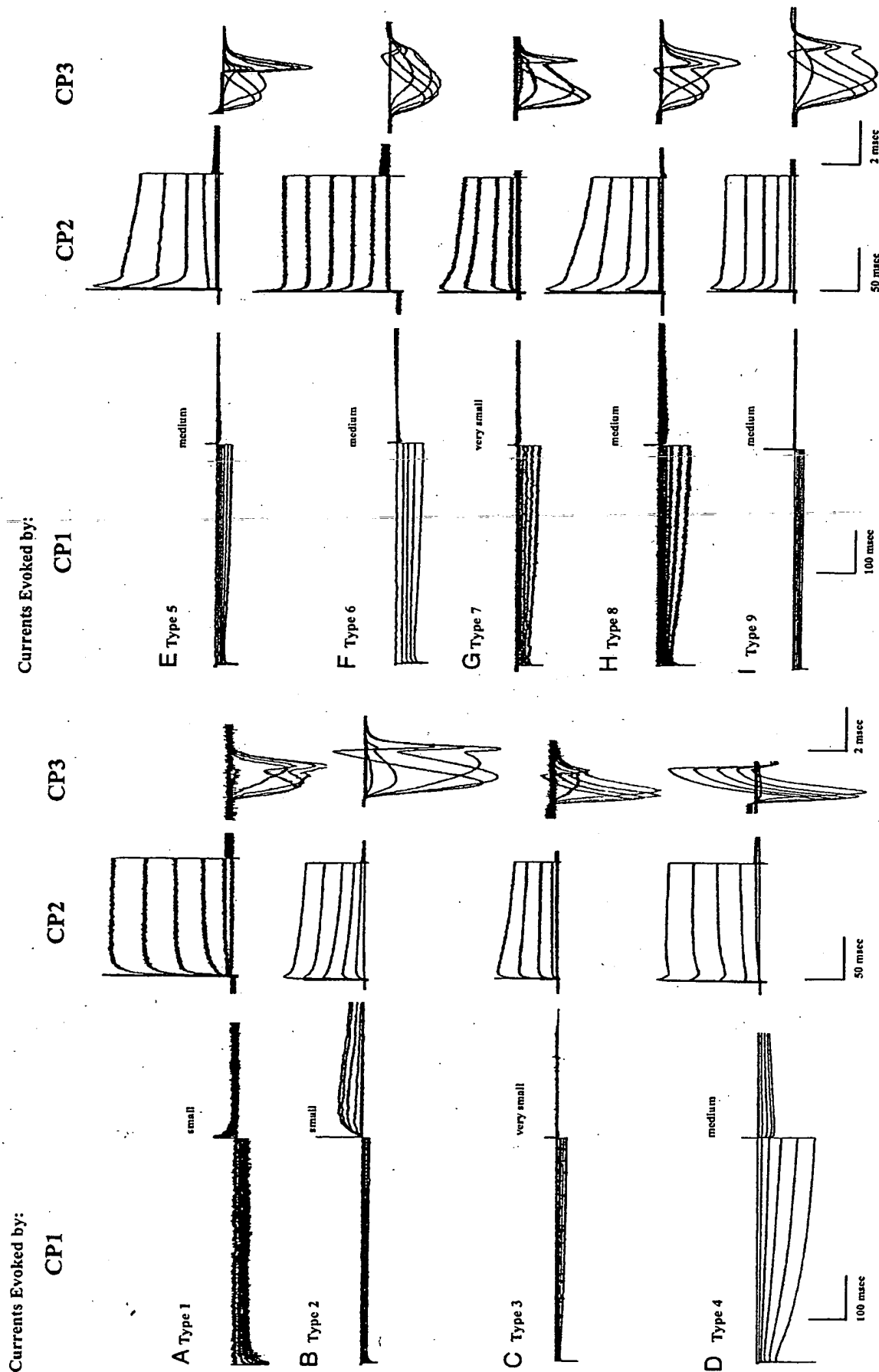


Fig. 3. Current signatures from cells of acutely dissociated adult rat dorsal root ganglion (DRG). Nine distinct signatures were identified by cluster analysis from very small (<22 μm), small (24–32 μm), and medium cell (35–48 μm) populations. Current signature patterns evoked by classification protocols CP1, CP2, and CP3 are shown for each cluster. Visually, CP1 and/or CP2 are usually sufficient to distinguish types 1, 2, 4, 5, 6, 8, and 9. CP3 is particularly important to distinguish types 3 and 7. Note the fast inactivation of inward current traces in type 3 relative to type 7. Vertical scale bars: for CP1: 100 pA (A); 500 pA (B); 500 pA (C); 500 pA (D); for CP2: 2,000 pA (A); 15,000 pA (B); 8,000 pA (C); 15,000 pA (D); for CP3: 2,000 pA (A); 5,000 pA (B); 5,000 pA (C); 10,000 pA (D); for CP1: 200 pA (E); 500 pA (F); 100 pA (G); 300 pA (H); 1,000 pA (I); for CP2: 10,000 pA (F); 4,000 pA (G); 2,000 pA (H); 10,000 pA (I); for CP3: 15,000 pA (E); 20,000 pA (F); 1,000 pA (G); 15,000 pA (H); 20,000 pA (I). Waveforms for CP1, CP2, and CP3 are presented in Fig. 1.

TABLE 1. Cluster analysis

Cluster	HAC, pA	TOC, pA	Tau CP2	Tau CP3	AT, mV	n	Cell Size
1	-3.2	19.7	22.3	-3.3	n/a	32	Small
2	-1.9	530.3	100.6	-1.3	n/a	24	Small
3	-35.7	-37.7	72.0	0.9	n/a	31	Very small
4	-590.4	-310.9	3.8	0.9	-20.0	24	Medium
5	-102.7	-33.9	9.0	-2.0	0.0	13	Medium
6	-126.9	-22.7	3.5	-2.1	-37.1	7	Medium
7	-36.0	-9.8	115.1	-1.8	n/a	10	Very small
8	-75.1	-20.7	7.8	-2.2	-20.0	7	Medium
9	2.6	8.7	4.5	2.7	-20.0	5	Medium

Cluster means for 5 cluster variates. The mean values for the 5 cluster variates are shown for each cell cluster. Separate cluster solutions were obtained for very small-, small-, and medium-sized cells. For clusters 1 and 2, only TOC and tau CP2 were needed; for clusters 3 and 7, only HAC and tau CP3 were required; for clusters 4, 5, 6, 8, and 9, all 5 variates were used to achieve a good cluster solution. Derivation of HAC, TOC, tau CP2, tau CP3, and AT are presented in Fig. 1. Cubic cluster criterion scores above 2 are considered good solutions (Hair et al. 1998). Cubic Clustering Criterion: very small, 3.45; small, 6.63; medium 21.30. HAC, hyperpolarization-activated current; TOC, transient outward current; CP2 and CP3, classification protocols 2 and 3; AT, activation threshold.

and five of six bound IB4 (see Fig. 5). One IB4 binding, CGRP-positive case was weakly SP-IR positive, while all others lacked SP-IR. Cell properties are summarized in Table 2.

Type 2 cell

CELL IDENTIFICATION AND ACTION POTENTIAL. All cells that clustered in this subgroup exhibited large transient outward current (Fig. 3; $n = 24$); no hyperpolarization-activated currents were observed. Transient outward currents were totally blocked by local perfusion with external solution containing 4-aminopyridine (4-AP, 10 mM; $n = 7$) or 80 μ M cadmium ($n = 6$). The type 2 cell cluster was made up of small diameter neurons (25–32 μ m; 33.0 pF) with long duration action potentials and prolonged AHP (Fig. 4; Table 2). A relatively small hump appeared on the falling phase of the action potential (see Fig. 3). The AHP80 of the type 2 cell differed significantly from that of types 3 ($U = 0$, $P < 0.002$) and 7 ($U = 0$, $P < 0.01$), but did not differ from other cell classes. The AP duration was significantly shorter than types 1 ($U = 5$, $P < 0.002$), but significantly longer than types 3 ($U = 0$, $P < 0.002$) and type 4 ($U = 0$, $P < 0.002$).

ALGESIC PROFILE. The pattern of algesic responses was consistent in all cases tested ($n = 22$). Profound inward currents were observed following presentation of capsaicin (500 nM; $n = 22$; Table 2). The onset and form of these currents were similar to type 1 cells. Capsaicin-induced currents were significantly larger than those observed in either the type 1 ($U = 13$, $P < 0.002$) or type 7 cells ($U = 9$, $P < 0.002$). There was weak proton activation of a nondesensitizing current at pH 6.1. Small currents of < 2 pA/pF were observed (1.5 ± 0.1 pA/pF; $n = 6$). Substantial inward currents were invariably present at pH 5.0 (Fig. 4; Table 2). These currents were similar to those of type 1 in form: immediate onset, slow onset kinetics, nondesensitizing; however, the amplitude of these currents were significantly larger ($U = 32$, $P < 0.002$). The proton-gated currents of the type 2 cell were insensitive to amiloride (100 μ M; $n = 5$). Reductions of current following a 2-min presentation of amiloride were no greater than expected from tachyphylaxis

(64.4 ± 8.0 and $72.1 \pm 7.4\%$ residual current for amiloride and control tests, respectively; $n = 7$ control cases).

Large inward currents were observed in all type 2 cells following presentation of 10 μ M ATP (Table 2; $n = 21$). Currents activated by ATP exhibited very fast kinetics (Fig. 4; Table 3). Both rise time and decay constants were significantly different from those of the type 4 cell ($U = 44$ and $U = 0$, $P < 0.002$, rise time and decay, respectively). Only decay constants differed between types 2 and 1 ($U = 0$, $P < 0.002$). Repeated application of ATP revealed a profound tachyphylaxis ($13.0 \pm 0.04\%$ residual current in a 2-min retest; $n = 7$). Currents of similar size and kinetics were observed following application of $\alpha\beta$ -m-ATP (44.6 ± 10.6 pA/pF; 10 μ M, $n = 8$).

Immunocytochemistry was performed on 20 of these same type 2 cells. None of the cases exhibited SP-IR or CGRP-IR. However, all cells bound IB4 (Fig. 5).

Type 3 cell

CELL IDENTIFICATION AND ACTION POTENTIAL. Cluster analysis placed 21 cells into the type 3 category. These were all very small diameter neurons (18–22 μ m; 21.2 ± 1.3 pF) that lacked transient outward current but expressed small hyperpolarization-activated currents (Fig. 3; Table 1). Decay constants fit to inward current traces (τ_{CP3}) indicated rapid inactivation (Table 1; see Fig. 3). The action potential durations (APDb) of type 3 cells were significantly shorter than all other cells with the exception of type 4 ($U = 0$, $P < 0.002$, all comparisons); the afterhyperpolarization differed from all subclassified cells ($U = 0$, $P < 0.002$, all comparisons). Unlike the type 1 and type 2 cells, there was no hump on the falling phase (Fig. 4).

ALGESIC PROFILE. Responses to ATP, capsaicin, and protons were examined in 21 type 3 cells. All 21 cells were capsaicin and ATP insensitive (500–1,000 nM capsaicin; 10 μ M ATP). In contrast to capsaicin-sensitive cells, type 3 cells exhibited powerful, rapidly activating, and desensitizing currents in acidic solutions (see Fig. 4; Table 3). A small but significant nondesensitizing component (3.6 ± 1.4 pA/pF) followed the rapidly desensitizing phase.

In addition to differences in form and amplitude, the type 3 cell was substantially more sensitive to protons than capsaicin-sensitive subtypes. Solutions at pH 6.1 produced large currents in all type 3 cells tested (95.6 ± 12.5 pA/pF; $n = 7$). While no current could be evoked at pH 7.0, rapidly desensitizing current was present at pH 6.8 (12.3 pA/pF; $n = 1$).

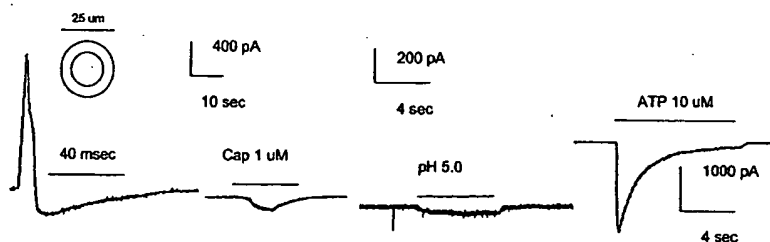
The rapidly desensitizing proton activated currents of type 3 cells were susceptible to block by amiloride (100 μ M; $n = 4$). Block was rapid (within 2 min), relatively complete ($12 \pm 8.0\%$ residual current), and was significantly greater than that expected from tachyphylaxis ($58.5 \pm 4.1\%$ residual desensitizing current; $n = 4$).

Immunocytochemistry was performed on all 21 type 3 cells exposed to multiple algesics. Twenty-one cases were IB4 negative; 20 of 21 cases lacked CGRP-IR; none of the cases contained SP-IR (Fig. 5).

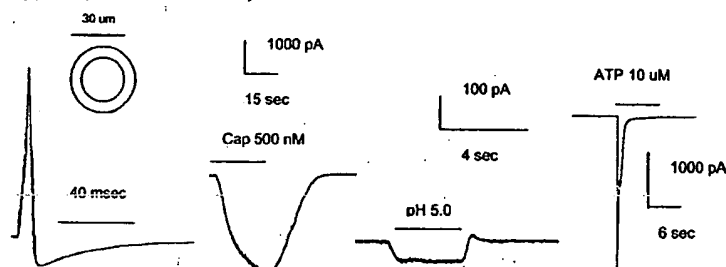
Type 4 cell

CELL IDENTIFICATION AND ACTION POTENTIAL. From among medium-sized neurons (35–48 μ m; 56.8 ± 1.9 pF), a cluster of

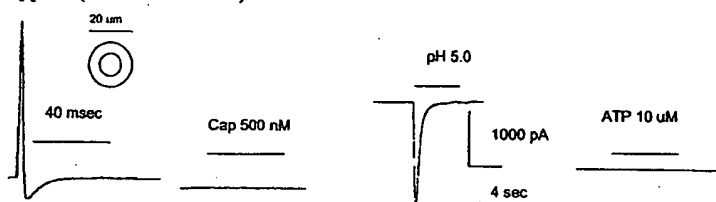
Type 1 (IB4+ SP- CGRP+)



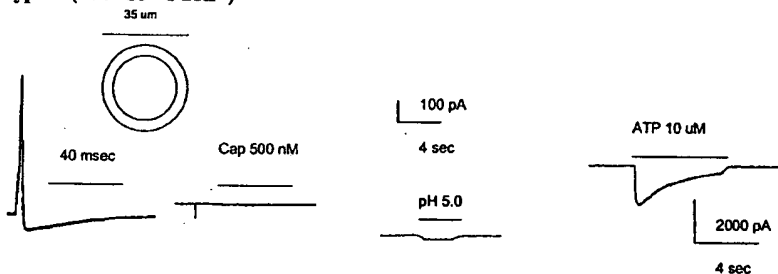
Type 2 (IB4+ SP- CGRP-)



Type 3 (IB4- SP- CGRP-)



Type 4 (IB4- SP- CGRP-)



Type 7 (IB4+ SP+ CGRP+)

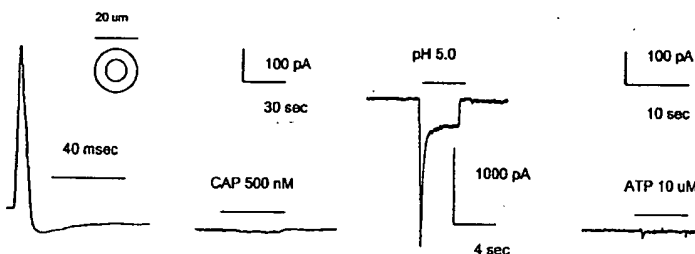


FIG. 4. Algesic response profiles in subclassified cell types. For each cell type, the action potential, response to capsaicin, pH 5.0 and ATP are presented from *left to right*. Doses and scales are indicated in each panel. All agents were presented by sewer pipe. The order of presentation was counterbalanced. Those cells that received all 3 treatments are presented in Table 2. The *inset* over the action potential illustrates the relative size of the cell body and nucleus for each subclassified cell. More complete information about size is presented in Table 2.

27 cells was subclassified as type 4. The principle distinguishing signature for these cells was the appearance of very large hyperpolarization-activated currents (Fig. 3; Table 1). The action potential duration of the type 4 cell was significantly less

than types 1, 2, and 7 ($U = 0$, $P < 0.002$ in all comparisons; Table 2 and Fig. 4) but did not differ from type 3. Cells of the type 4 cluster exhibited a substantial AHP80 that was comparable to capsaicin-sensitive cells. While the AHP did not differ

TABLE 2. Properties of subclassified cells

	Cell Type				
	1	2	3	4	7
<i>n</i>	28	22	21	24	8
Cell properties					
Diameter, μm	24–30	25–32	18–22	33–40	16–22
Size, pF	31.4 \pm 1.1	31.5 \pm 0.8	21.2 \pm 1.3	56.8 \pm 1.9	18.2 \pm 1.3
Input Resistance, M Ω	604.5 \pm 57.6	726.7 \pm 49.2	544.9 \pm 66.9	297.1 \pm 23.6	811.7 \pm 127.4
Membrane potential, mV	-56.0 \pm 0.4	-57.2 \pm 0.7	-51.7 \pm 1.3	-58.0 \pm 1.0	-48.4 \pm 1.9
Peak current					
Capsaicin, pA/pF	25.9 \pm 6.6	134.9 \pm 16.3 ^a	0.0	0.4 \pm 0.1	4.25 \pm 0.9
Protons, pA/pF	5.6 \pm 2.4	15.3 \pm 2.7 ^b	127.0 \pm 16.0	3.48 \pm 0.4	45.8 \pm 18.1 ⁱ
ATP, pA/pF	13.3 \pm 3.8 ^{c*}	51.7 \pm 10.1	0.0	17.4 \pm 3.5	2.9 \pm 0.4
$\alpha\beta$ -methylene-ATP, pA/pF	No test	44.6 \pm 10.3	0.0	1.6 \pm 0.5	No test
Action potential					
Duration, ms	7.35 \pm 0.5 ^d	5.9 \pm 0.1 ^e	3.5 \pm 0.2 ^f	3.1 \pm 0.1 ^g	6.5 \pm 0.2 ^h
Afterhyperpolarization, ms	57.0 \pm 8.1 ^k	54.7 \pm 7.6 ^k	17.5 \pm 1.7 ⁱ	46.5 \pm 5.5 ^k	110.2 \pm 9.8 ^j

Values are means \pm SE. Cell body properties, peak currents, and action potential features of subclassified cells are presented. The cases represent only those in which ATP, capsaicin, and protons were presented to the same cell. The order of presentation was counterbalanced. $\alpha\beta$ -methylene-ATP was presented in a limited number of additional cases (type 2, $n = 8$; type 4, $n = 5$). ^a Significantly greater than all other cells. ^b Significantly greater than type 1. ^c Significantly greater than type 4. ^d Significantly greater than all other cells. ^e Significantly greater than types 3 and 4. ^f Significantly less than types 1, 2, and 7. ^g Significantly less than types 1, 2, and 7. ^h Significantly greater than types 3 and 4. ⁱ Significantly less than all other cells. ^j Significantly greater than all other cells. ^k Significantly greater than type 3 and significantly less than type 7. ^l Approached significance vs. type 3, $P < 0.10$. Statistics and probabilities are presented in the text. For protons and ATP-activated currents, statistical comparisons were only made between currents of similar form (i.e., desensitizing or non-desensitizing). ^{*} $n = 6$.

significantly from that of capsaicin-sensitive types 1 and 2, it was significantly shorter than AHP80 of the type 7 cell, and significantly longer than the capsaicin-insensitive type 3 cell ($U = 0$, $P < 0.002$ in both comparisons).

ALGESIC PROFILE. Cells clustering as type 4 manifested homogenous properties. Capsaicin (500 nM) was presented by rapid perfusion to 15 type 4 cells. In some cases ($n = 7$) very weak currents of < 1 pA/pF were observed (0.40 ± 0.13 pA/pF; 500 nM). In an additional nine cells, 5 μM capsaicin was presented, but no current was detected. Despite the lack of significant capsaicin currents, weak nondesensitizing proton-activated currents were present in all type 4 cells (16 of 16 cases). These currents resembled those in capsaicin-sensitive cells (types 1 and 2) but were smaller in amplitude.

In the presence of ATP, all type 4 cells exhibited powerful inward currents that resembled those of type 1 cells ($n = 18$; Table 2; Fig. 4), but were significantly smaller in amplitude ($U = 22$, $P < 0.05$). Onset was simultaneous with application, but the kinetics of activation and desensitization were relatively slow. The rise time of ATP-activated currents were significantly slower in type 4 than in type 1 cells ($U = 14$, $P < 0.05$). There was no difference in decay time constants. In contrast to the type 2 cell, reactivity to $\alpha\beta$ -m-ATP was

weak (1.6 ± 0.5 pA/pF vs. 44.6 ± 10.3 pA/pF for type 2; $n = 5$ and 8).

Immunocytochemistry was performed on 16 cells that had been exposed to capsaicin, ATP, and protons. Cells classified as type 4 were very weakly IB4 positive using the biotinylated tyramide amplification procedure (Fig. 5; 6 of 10 cases). However, in six cells with tyramide-coumarin amplification, all cases were negative. None of the 16 cells could be shown to contain CGRP-IR or SP-IR.

Type 7 cell

CELL IDENTIFICATION AND ACTION POTENTIAL. Recordings were obtained from 10 very small diameter cells ($16\text{--}22 \mu\text{m}$; 18.2 ± 1.3 pF) that clustered together based on small hyperpolarization-activated currents and a slowly inactivating inward current signature (HAC, τ_{CP23}). Like other capsaicin-sensitive cells (types 1 and 2), the type 7 cell manifested a broad action potential and a substantial shoulder on the falling phase (Fig. 4). The duration of the AP differed significantly from types 1, 3, and 4 (see above). The AHP80 of the type 7 cluster was exceptionally long (110.2 ± 9.8 ms) and differed significantly from all other cell types.

TABLE 3. Kinetics of desensitizing currents evoked by ATP and protons

Cluster	Rise Time	Cases	Decay	Rise Time	Cases	Decay
Type 1	239.2 \pm 33.6 [*]	6	2,300.8 \pm 493.1	n/a		n/a
Type 2	173.8 \pm 41.2	22	214.3 \pm 48.8	n/a		n/a
Type 3	n/a		n/a	505.3 \pm 83.8 [†]	21	683.3 \pm 53.4 [†]
Type 4	354.9 \pm 44.4	24	2,813.4 \pm 404.6	n/a		n/a
Type 7	196.0 \pm 36.0	8	386.0 \pm 135.1	189.3 \pm 36.6	8	254.9 \pm 45.0

Values are means \pm SE. Rise time and decay constants for desensitizing currents evoked by ATP (left) or protons (right). Rise time was determined as the time (ms) between the 1st inward deflection to 90% of the peak current. All decay constants were derived from single exponential fits. ^{*} $P < 0.05$ vs. type 4. [†] $P < 0.02$ and $P < 0.002$ vs. type 7 for rise time and decay, respectively. Doses: ATP, 10 μM ; protons, pH 5.0.

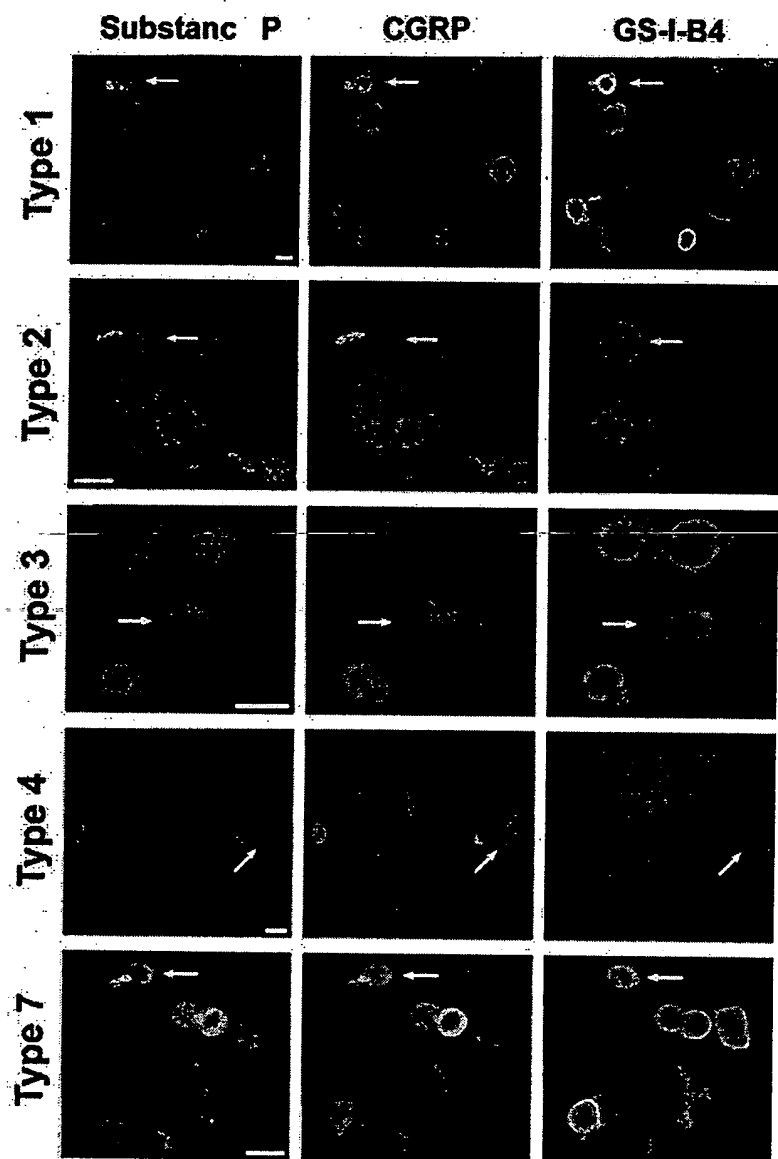


FIG. 5. Visualization of GS-I-B₄-binding and expression of the neuropeptides substance P (SP) and calcitonin gene-related peptide (CGRP) in recorded neurons reveals distinct patterns of distribution. Cell types determined by current signatures are indicated to the left of each row. The histochemical marker visualized in each panel is indicated above each column. Arrows indicate the individual cell in each field that was recorded. Expression patterns of SP/CGRP/GS-I-B₄ were as follows: type 1, -/+/-; type 2, -/-/+; type 3, -/-/-; type 4, -/-/-; type 7, +/+/-+. Scale bars indicate 25 μ m.

ALGESIC PROFILE. The type 7 cell class was uniform with respect to capsaicin, ATP, and proton sensitivity ($n = 8$). Following application of ATP, a transient peak was followed by a weak, nondesensitizing inward current (Table 2). Capsaicin-activated currents were similar to those of the type 1 cell, but significantly less in amplitude than the type 2 cells ($U = 7$, $P < 0.002$; Table 2). However, unlike capsaicin-sensitive cells that expressed only nondesensitizing proton-activated currents, protons evoked large amplitude currents with fast kinetics in type 7 cells. The form and amplitude of these currents were similar to type 3 cells. Despite this general similarity, the kinetics of proton-activated currents of type 7 cells differed significantly from those of type 3. Both rise time and decay constants were significantly shorter than proton-activated currents in type 3 cells ($U = 21$, $P < 0.02$ and $U = 3$, $P < 0.002$ for rise time and decay, respectively; Table 3). The transient portion of pH 5.0 activated currents could be blocked by brief application (2 min, local superfusion) of 100 μ M amiloride ($28.2 \pm 15.4\%$ residual current; $n = 4$). A substantial amilo-

ride-insensitive, nondesensitizing component was also present (6.0 ± 1.6 pA/pF; see Fig. 4).

Like the type 3 capsaicin-insensitive cell, there were very substantial proton-activated currents at pH 6.1 (45.8 ± 18.6 pA/pF; $n = 6$). It was noteworthy that the nondesensitizing component that was prominent at pH 5.0 was negligible at pH 6.1 (0.96 ± 0.42 pA/pF). Possibly, VR1 makes contributes to the nondesensitizing portion of the proton response at pH 5.0. No current could be evoked at pH 7.0, but significant transient and nondesensitizing current were present at pH 6.8 (28.3 pA/pF and 2.9 pA/pF, respectively; $n = 1$).

Eight type 7 cells were prepared for immunocytochemistry. All were IB4 positive and contained both SP-IR and CGRP-IR (Fig. 5).

DISCUSSION

We have used a current signature classification scheme to subclassify acutely dissociated DRG cells harvested from adult

rats. Cluster analysis formed nine subgroups based on variables derived from three classification test protocols. After examining the algescic profile (capsaicin, protons, ATP), action potential properties (APDb, AHP80), and histochemical phenotypes of five subclassified cell types, it was apparent that the current signature method could reliably identify distinct subsets of cells whose properties were internally homogenous. With minor exceptions, all clusters had uniform properties with respect to the algescics presented, the presence/absence of neuropeptides SP and CGRP, and the binding of IB4. Because cell subtypes were uniform with respect to afterhyperpolarization, AHP is likely to be useful, in vitro, to discern classic nociceptive subclasses with greater specificity than previously possible.

Current signatures, AHP, and nociceptive function

Action potential AHP appears to be a promising means of identifying cell bodies of nociceptors of all classes (Djourhi et al. 1998; Lawson et al. 1997; see also Koerber et al. 1988; Ritter and Mendell 1992; Villiere and McLachlan 1996). Using sharp electrode recordings, in vivo, Lawson and colleagues were able to distinguish nociceptive from nonnociceptive subgroups within the A δ and C fiber populations. Although specific subtypes within nociceptive populations could not be distinguished by AHP80 in vivo (e.g., A δ MH vs. A δ HTM; C MH vs. C PMN vs. C HTM vs. CH, etc.), all nociceptive classes (both capsaicin sensitive and insensitive) were clearly set apart from other groups (including silent type nociceptors). Because we were able to report that subclassified cells bodies also have uniform AHP80 in vitro, it is possible that this feature will be an aid to detailed nociceptor identification. Moreover, by combining algescic reactivity and AHP80, the ability to identify specific linkages between classic nociceptive subpopulations and subclassified cells is enhanced.

Although the afterhyperpolarization and action potential duration of cell clusters were internally consistent, they diverged from previous reports (Cardenas et al. 1995; see also Villiere and McLachlan 1996). In the studies by McLachlan, the full AHP was measured (complete return to baseline). This resulted in substantially longer and more variable records. In the studies of Cardenas, little or no AHPs were observed. Using a technique common in most patch-clamp studies, action potentials were evoked using a 30-ms, threshold current injection step (typically 200–400 pA). This technique precludes accurate measurement of AHP. The long current step (30 ms) is coincident with the AHP phase, thereby causing much of the AHP to be obscured. Therefore we adopted an alternative method (1-ms, 1,500- to 3,000-pA step) that permitted the AHP to be fully visualized. While we could not expect the AHP of patch-clamped cells to be identical with those recorded with sharp electrodes (Djourhi et al. 1998; Villiere and McLachlan 1996), it was likely that a similar ordering of AHPs would be observed. As we recorded only from small- and medium-sized cells, we were more likely to encounter nociceptive subtypes (Harper and Lawson 1985; Yoshida and Matsuda 1979). Accordingly, the AHP80 of type 1 (57 ms), type 2 (55 ms), type 4 (47 ms), and type 7 (110 ms) cells were clearly consistent with nociceptive function. The AHP80 of the type 3 cells (18 ms) was more likely to be associated with nonnociceptive function.

Current signatures and histochemical phenotype

Current signature identified cells were histochemically uniform. Types 1 and 7 contained peptides SP and/or CGRP, while types 2, 3, and 4 did not. It is well recognized that SP and CGRP are present in some nociceptor subpopulations; however, it has not been clear whether these peptides are associated with specific subclasses or distributed throughout the nociceptor family (Lawson et al. 1997; Leah et al. 1985; McCarthy and Lawson 1990, 1997). In either case, the presence of these peptides suggests a functionally distinct role for the subpopulations in which they are contained. Peptides CGRP and SP have been implicated in important peripheral and central components of the inflammatory response including vasodilation (Bharali and Lisney 1992; Holzer 1988; Lembeck and Holzer 1979), central sensitization (Dougherty et al. 1994; Honore et al. 1999; Neugebauer et al. 1995; Neumann et al. 1996), and posttraumatic sprouting (Belyantseva and Lewin 1999). Therefore cells expressing these peptides are of unique importance. If peptide-containing cells can be reliably identified by current signature alone, the study of these important subpopulations would be greatly simplified.

Cells classified by current signature also fell into uniform classes of IB4-positive and -negative populations. The binding of IB4 has been associated with unmyelinated afferent populations (Kitchener et al. 1993; Streit et al. 1985, 1986; Wang et al. 1998) and with important functional specializations (Stucky and Lewin 1999). Accordingly, cells classified as types 1, 2, and 7 are predicted to be unmyelinated afferents, while cells classified as types 3 and 4 are presumably myelinated. Further, as it has been shown that the IB4-binding population innervates cutaneous structures almost exclusively (Kitchener et al. 1993; Petruska et al. 1997; Plenderleith and Snow 1993; Wang et al. 1998), most, if not all, type 1, 2, and 7 neurons were likely to be cell bodies of cutaneous sensory afferents. Of course, the absence of IB4 binding in types 3 and 4 would not exclude these from the cutaneous afferent pool.

Taken together, the pattern of peptide expression and IB4 binding has a number of implications for subclassified cells. Type 1 neurons contained CGRP-IR and had IB4 binding but lacked SP-IR. While many DRG neurons that express CGRP also express SP (Lee et al. 1985a,b), the singular overlap of CGRP-IR with IB4-binding neurons was not unexpected. Based on this profile, type 1 and type 2 cells are likely to correspond to an IB4 binding, glial cell line derived neurotrophic factor (GDNF)-dependent, DRG population (Bennett et al. 1998; Molliver et al. 1997). Because they express CGRP, but not SP, yet bind IB4, type 1 cells are likely to belong to a subgroup of the GDNF-responsive population that innervates cutaneous tissue and expresses somatostatin (SOM) (Gibbins et al. 1987; Hokfelt et al. 1976; Perry and Lawson 1998; Wang et al. 1994). In a recent report, we have confirmed that 78% of type 1 cells express SOM-IR (Petruska et al. 2000b). In contrast, neurons positive for all three markers (type 7) were likely to be part of the nerve growth factor-dependent, small-diameter DRG population expressing tyrosine kinase (e.g., Molliver et al. 1995; Verge et al. 1989).

Current signatures, algescic response, and cell classification

Our current signature classification scheme is based on methods first used in DRG by Cardenas and Scroggs (Cardenas

TABLE 4. Classification decision table

Cell Type	CP1		CP2	CP3	Size Range, μm
	TOC	HAC	AT	τ_{decay}	
1	No	No	No	NR	24–30
2	Yes	No	NR	NR	25–32
3	No	< 100 pA	NR	Fast inactivation	18–22
4	No	> 300 pA	NR	NR	33–40
5	No	< 100 pA	0 mV	NR	35–45
6	No	< 100 pA	–40 mV	NR	35–45
7	No	< 100 pA	NR	Slow inactivation	16–22
8	No	< 100 pA	–20 mV	NR	35–45
9	No	No	–20 mV	NR	35–45

A classification decision table for 9 DRG cell types. Application of classification protocols 1, 2, and 3 (CP1, CP2, CP3), provides enough information, by simple inspection, to classify 9 cell types without application of any statistical procedures. Using the presence and absence of transient outward current (TOC) and the amplitude of hyperpolarization-activated currents (HAC) in combination with the threshold of A-current peaks (AT), it is possible to classify 7 cell types. CP3 is only required to separate types 3 and 7. The actual τ_{decay} need not be computed, as the apparent inactivation rates are distinct by inspection (see Fig. 2, C and G). The necessary and sufficient conditions for each cell type are shown in bold print. Note that size range simplifies the classification, but is not required. NR, test is not required.

et al. 1995). Their procedure specifies both capsaicin testing and Ca^{2+} current identification in addition to hyperpolarization-activated currents to identify four cell subtypes. We have demonstrated that simplified procedures, which include hyperpolarization and depolarization tests, can subclassify a larger number of DRG cells without the presentation of capsaicin or dissection of voltage-activated Ca^{2+} currents (Table 4). We have retained the original nomenclature for the four subtypes identified by Scroggs. Because we did not rely on capsaicin sensitivity or Ca^{2+} currents to subclassify cells, some variation in cell assignment might occur.

The type 1 cluster was a small (31.4 pF), capsaicin-sensitive cell, with weak nondesensitizing proton-activated currents and slow desensitizing response to ATP. The size of the cells and the amplitude and form of capsaicin-activated currents were consistent with those reported by Scroggs for their type 1 cell (26 pF) (Cardenas et al. 1995). The type 1 cell of Scroggs was identified as a subtype that lacked both hyperpolarization-activated or transient outward currents, and also by capsaicin sensitivity and by the presence of L, N, and T type Ca^{2+} currents. Although we did not examine the Ca^{2+} currents in these cells, our type 1 cluster matches the type 1 cell of Scroggs in other respects but may include, as well, a small group of capsaicin-insensitive cells. Whether they were sensitive to capsaicin or not, all cells clustering as type 1 had relatively uniform histochemistry (83% IB4 and CGRP positive), and all responded in the same respect to ATP and protons.

We have recently reported that type 1 cells co-expressed P2X₁, P2X₂, and P2X₃ subunits (Petruska et al. 2000b). Assembly of P2X₂ and P2X₃ subunits in expression systems have been associated with large amplitude slowly desensitizing ATP-activated currents that are consistent with those of type 1 cells (Lewis et al. 1995). It is not entirely clear whether P2X₁, P2X₂, and P2X₃ subunits can combine to form functional receptors that are distinct from heteromers of P2X₂ and P2X₃; however, differences in amplitude and kinetics of the responses of type 1 cells from those of type 4 suggest that a distinct combination is present and functional. It remains to be determined whether other properties associated with the type 1 cell of Scroggs (projection into superficial lamina of the spinal cord, sensitivity

to 5-HT, TTX-insensitive Na^{+} current) can be attributed to the type 1 cluster (Cardenas et al. 1995, 1997a,b; Del Mar and Scroggs 1996), but it is clear that this CGRP and somatostatin-expressing, capsaicin-sensitive cell population could contribute in an important fashion to posttraumatic pain. We suggest that it may be the cell body of a CMH or C polymodal nociceptor.

The premier capsaicin-sensitive DRG cell cluster was the type 2 cell. The Scroggs group identified a type 2 cell as a small (29 pF), capsaicin-sensitive cell that expressed L and N type Ca^{2+} currents, and A-type, transient outward current. We believe this cell can be identified reliably by the presence of transient outward current alone. Transient outward current is characteristic of cells expressing A-currents. We confirmed that the TOC of the type 2 cluster was sensitive to 4-AP and cadmium. Inhibition by 4-AP or divalent cations is a common property of A-currents (Conner and Stevens 1971; Gold et al. 1996; Talukder and Harrison 1995). Cells that clustered as type 2 were similar in size (31 pF) and had large amplitude (135 pA/pF) capsaicin-activated currents that were consistent with the type 2 cell of Scroggs (117 pA/pF) (Cardenas et al. 1995). The presence of a minor shoulder on the falling phase of the action potential was further evidence that cells clustering as type 2 are identical to those identified by Scroggs and colleagues using more invasive methods.

We found that the capsaicin sensitivity of type 2 cells was unsurpassed by other capsaicin-sensitive subtypes. Comparisons between capsaicin reactivity of the type 2 cell cluster and that of the other capsaicin-sensitive clusters (types 1 and 7) show virtually no overlap. It is somewhat surprising that the premier capsaicin-sensitive cell of the DRG contained no SP or CGRP. However, other cell clusters with powerful capsaicin-induced currents (types 5, 8, and 9) contain peptides SP and/or CGRP (Cooper et al. 2000). The algic response profiles of these cells are distinct from those of type 2 cells. We will contrast the properties of these cells with type 2 cells in a subsequent report on the remaining cell clusters. With respect to pharmacology, form, sensitivity, and kinetics, the proton-activated currents of type 2 cells were typical of cells expressing VR1 homomers (Caterina et al. 1997; Tominaga et al. 1998). Therefore proton-activated currents of the type 2 cell

cluster were likely to reflect proton sensitivity of the capsaicin receptor.

The pharmacology and kinetics of currents activated by ATP were consistent with the "mixed fast current" described recently by Burgard and others (Burgard et al. 1999; Petruska et al. 2000a). We found that, in contrast to other forms of ATP-activated currents, these exceptionally fast, large amplitude currents are exclusively expressed in the type 2 cell. The functional significance of this unique specialization is unclear, but certainly, the large amplitude and fast kinetics of these currents would provide a secure detection of any ATP that might be liberated in the periphery by tissue damage. The kinetics of these currents are consistent with those shown by co-expression of P2X₁ and P2X₃ receptor subunits in expression systems (Chen et al. 1995; Lewis et al. 1995; Ueno et al. 1999). We have recently found that all cells (10 cases) classified as type 2 co-express P2X₁ and P2X₃-IR (Petruska et al. 2000b).

The type 3 cell cluster was composed of very small (21 pF) ATP- and capsaicin-insensitive cells with minor hyperpolarization-activated currents and rapidly inactivating inward current signatures (CP3). Scroggs identified the type 3 cell as a small cell (15-pF), with weak hyperpolarization-activated currents, that expressed L, N, and T type Ca²⁺ currents and was insensitive to capsaicin. Using only current signatures, we identified a homogenous capsaicin-insensitive population that was a good match for the type 3 cell of Scroggs. While we are confident that we have thoroughly sampled cells in the small and medium size range, we are also confident that we have not thoroughly sampled cells in the very small range (<22 μ m). Because sampling was confined to cells with large diameter nuclei, a number of interesting cell clusters may yet be identified among this population. Moreover, as we have not replicated other characteristics associated with the type 3 cell of Scroggs (Ca²⁺ currents and TTX-sensitive Na⁺ currents) (Cardenas et al. 1997a), we cannot be certain that these two groups are identical. Whether these cells were identical or not, their properties offered an interesting contrast to other cell populations.

Cells clustering as type 3 were uniquely capsaicin- and ATP-insensitive cells and exhibited powerful, rapidly desensitizing, amiloride-sensitive proton-activated currents (Cooper et al. 1999a). The form and pharmacology of the latter was consistent with the expression of acid-sensing ion channels (ASIC/DRASIC) (Chen et al. 1998; Lingueglia et al. 1997; Waldmann et al. 1997a,b, 1999). The exceptionally short AHP80 of the type 3 cluster further suggested that it was an important cell group whose properties should contrast markedly with capsaicin-sensitive and -insensitive cells with much longer AHP80s. A better understanding of the relationship between AHP and functional sub-specialization of DRG neurons requires such contrasts.

The type 4 cell cluster was a medium-sized (57 pF), capsaicin-insensitive cell with weak proton reactivity and narrow action potential. Slowly desensitizing currents were always evoked by ATP. The response profile for capsaicin, protons, and ATP were consistent in all cases. Scroggs and Cardenas identified the type 4 cell as a medium-sized (54 pF) capsaicin-insensitive cell with very large hyperpolarization-activated currents (>800 pA), narrow action potential, and large N and T type calcium currents (Cardenas et al. 1995). Our type 4 cluster was composed exclusively of cells with exceptionally large

hyperpolarization-activated current (590 pA). While these currents were present in other medium-sized cells (types 5, 6, and 8), they were far smaller and could readily be distinguished by visual inspection alone. As cell clusters 5 and 8 are capsaicin-sensitive cells and type 6 has very weak hyperpolarization-activated current, we are confident that the type 4 cluster can be identified by this signature and is identical to that presented by the Tennessee group.

The type 4 cell cluster was particularly interesting due to properties implicating it as a capsaicin-insensitive, myelinated nociceptor. Regarding the latter, we have confirmed in a separate report that type 4 cells do not bind IB4 (10 of 11 cases) but do express NF-M-IR (9 of 9 cases). This pattern is strongly associated with myelinated afferents (see Petruska et al. 2000b). Despite the absence of a significant capsaicin response, this cell type consistently expressed properties associated with nociceptive cells. Similar to type 1, the type 4 cell manifested powerful, ATP-activated currents that represented co-expression of P2X₂ and P2X₃ subunits (Petruska et al. 2000b). Moreover, while there was a relatively narrow APDb (3.1 ms, no shoulder), the AHP80 (47 ms) was similar to those of capsaicin-sensitive subtypes (55 and 57 ms) and significantly longer than capsaicin-insensitive, ATP-insensitive cells (type 3). Given its long AHP80, and previous demonstrations that the type 4 cell of Scroggs was sensitive to PGE₂ and 5-HT (Cardenas et al. 1997a, 1999), it is likely that this cell belongs to a subgroup of capsaicin-insensitive nociceptors. The most likely candidates include the A δ HTM or A δ cold nociceptor.

We identified a fifth cell cluster that was not previously classified by the Scroggs group. The type 7 cell was a very small neuron (18 pF) with weak, but significant, capsaicin and ATP sensitivity. It was distinct from other capsaicin-sensitive cells due to the expression of fast desensitizing, amiloride-sensitive, proton-activated currents with a strong nondesensitizing component and the presence of peptides SP and CGRP. The long duration AHP80 (110 ms) and broad action potential (6.5 \pm 0.2 ms) contrasted greatly with the type 3 cell (18 and 3 ms, respectively) and were consistent with a nociceptive function. Lawson has shown that the longest AHP80s were observed in the silent nociceptive classes (Djourhi et al. 1998; Lawson et al. 1997). The exceptional length of the AHP in the type 7 cell easily set it apart from other characterized cell groups and suggested that it might represent a portion of the silent (or mechanically insensitive) nociceptor class in vitro (Cooper et al. 1991a,b; Meyer et al. 1991; Perl 1968; Schaible and Schmidt 1983; Weidner et al. 1999).

Cluster analysis confirmed that nine distinct cell populations could be found in DRG cells with diameters ranging from 16 and 45 μ m. However, we have not found it necessary to assign cells statistically. Rather, a simple decision table (Table 4) can be used to place cells in one of nine subgroups based on visual inspection of currents produced mainly by two classification protocols (CP1 and CP2). In most instances the assignment is simplified by cell diameter measurement. Because we have found that certain cell types are confined to distinct, nonoverlapping size ranges, the number of possible assignments will be reduced by taking cell size into account. Because this method was derived in acutely dissociated, adult DRG, some caution should be taken with other DRG preparations.

Profile construction in classified cell types

Classification of cells by current signature has important advantages over schemes that simply divide all cells into two mutually exclusive subtypes (e.g., IB4 positive/negative or capsaicin sensitive/insensitive), and rely on post hoc cell identification. While binary schemes have utility, they cannot capture the rich functional diversity of the nociceptive afferent pool. Using the current signature method, we have been able to identify nine distinct clusters of cells. We have shown that at least five of these subclasses have uniform properties with respect to analgesics and histochemistry. Four of the five exhibited action potential properties consistent with those of nociceptors, *in vivo*.

The classification of cells by this method has the substantial advantage of being able to predict algesic response profiles and histochemical phenotype by current signature alone. This has several applications in patch clamp experiments. If experiments require targeting of substance P expressing cells, current signature identification permits this determination without immunocytochemistry. Alternately, if ASIC expressing cells are targeted, current signatures offer the advantage of identifying such cells at the beginning rather than at the end of the experiment. More importantly, due to the uniform properties exhibited by subclassified cells, identification of a neuron by its unique signature allows its prior history to be transferred from experiment to experiment.

If current signatures reliably predict properties from experiment to experiment, an extensive profile of properties can be developed for each cell type. This building of profiles is best exemplified by the properties that have been attributed to the type 2 cell. A series of studies from this and the Scroggs laboratory have demonstrated that the type 2 cell 1) is the premier capsaicin-sensitive DRG cell (Cardenas et al. 1995 and above); 2) possesses weak, amiloride-insensitive, proton-activated currents that are characteristic of the vanilloid receptor; 3) is highly sensitive to ATP and expresses currents consistent in form, pharmacology, and histochemistry with the expression of P2X₁ and P2X₃ subunits (above and Petruska et al. 2000b); 4) projects into lamina I and II of the dorsal horn (Del Mar and Scroggs 1996); 5) uniquely expresses TTX-insensitive currents consistent with unmyelinated afferent pools (Cardenas et al. 1997a); 6) is sensitive to 5-HT via coupling of TTX-insensitive currents to a 5HT₄ receptor (Cardenas et al. 1997a); 7) possesses TTX-insensitive currents that are amplified by PGE₂ (Cardenas et al. 1997a); 8) has a long duration AHP80 consistent with nociceptors; and 9) belongs to a group of IB4-positive, neurofilament-negative cells that do not express either substance P or CGRP (above and Petruska et al. 2000b). It is possible to build a profile of cells if classification predicts properties with great accuracy and reliability. It is clear from previous reports that this was possible with respect to capsaicin, 5-HT, and PGE₂ reactivity. In the present report, we have shown that this uniformity includes histochemical phenotype as well as sensitivity to protons, ATP, and afterhyperpolarization.

The authors thank M. Oberdorfer for technical assistance.

This work was supported in part by the University of Florida Research Foundation.

REFERENCES

- BAUMANN TK, SIMONE DA, SHAIN CN, AND LAMOTTE RH. Neurogenic hyperalgesia: the search for the primary cutaneous afferent fibers that contribute to capsaicin-induced pain and hyperalgesia. *J Neurophysiol* 66: 212–227, 1991.

- BELMONTE C, GALLAR J, POZO MA, AND REBOLLO I. Excitation by irritant chemical substances of sensory afferent units in the cat's cornea. *J Physiol (Lond)* 437: 709–725, 1991.
- BELMONTE C AND GIRALDEZ F. Responses of cat corneal sensory receptors to mechanical and thermal stimulation. *J Physiol (Lond)* 321: 355–368, 1981.
- BELYANTSEVA IA AND LEWIN GR. Stability and plasticity of primary afferent projections following nerve regeneration and central degeneration. *Eur J Neurosci* 11: 457–468, 1999.
- BENNETT DL, MICHAEL GJ, RAMACHANDRAN N, MUNSON JB, AVERILL S, YAN Q, MCMAHON SB, AND PRIESTLEY JV. A distinct subgroup of small DRG cells express GDNF receptor components and GDNF is protective for these neurons after nerve injury. *J Neurosci* 18: 3059–3072, 1998.
- BHARALI LA AND LISNEY SJ. The relationship between unmyelinated afferent type and neurogenic plasma extravasation in normal and reinnervated rat skin. *Neuroscience* 47: 703–712, 1992.
- BURGARD EC, NIFORATOS W, VAN BIESEN T, LYNCH KJ, TOUMA E, METZGER RE, KOWALUK EA, AND JARVIS MF. P2X₂ receptor-mediated ionic currents in dorsal root ganglion neurons. *J Neurophysiol* 82: 1590–1598, 1999.
- CAMPBELL JN, RAJA SN, COHEN RH, MANNING DC, KAHN AA, AND MEYER RA. Peripheral neural mechanisms of nociception. In: *Textbook of Pain*, edited by Wall PD and Melzack R. New York: Churchill Livingstone, 1990, p. 22–45.
- CARDENAS CG, DEL MAR LP, COOPER BY, AND SCROGGS RS. 5HT₄ receptors couple positively to tetrodotoxin-insensitive sodium channels in a subpopulation of capsaicin-sensitive rat sensory neurons. *J Neurosci* 17: 7181–7189, 1997a.
- CARDENAS CG, DEL MAR LP, AND SCROGGS RS. Variation in serotonergic inhibition of calcium channel currents in four types of rat sensory neurons differentiated by membrane properties. *J Neurophysiol* 74: 1870–1879, 1995.
- CARDENAS CG, DEL MAR LP, AND SCROGGS RS. Two parallel signaling pathways couple 5HT_{1A} receptors to N- and L-type calcium channels in C-like rat dorsal root ganglion cells. *J Neurophysiol* 77: 3284–3296, 1997b.
- CARDENAS CG, MAR LP, VYSOKANOV AV, ARNOLD PB, CARDENAS LM, SURMEIER DJ, AND SCROGGS RS. Serotonergic modulation of hyperpolarization-activated current in acutely isolated rat dorsal root ganglion neurons. *J Physiol (Lond)* 518: 507–523, 1999.
- CATERINA MJ, SCHUMACHER HR, TOMINAGA M, ROSEN TA, LEVINE JD, AND JULIUS D. The capsaicin receptor: a heat-activated ion channel in the pain pathway. *Nature* 389: 816–824, 1997.
- CERVERO F. Sensory innervation of the viscera: peripheral basis of visceral pain. *Physiol Rev* 74: 95–137, 1994.
- CHEN C-C, AKOPIAN AN, SIVLOTTI L, COLQUHOUN D, BURNSTOCK G, AND WOOD JN. A P_{2X} purinoceptor expressed by a subset of sensory neurons. *Nature* 377: 428–431, 1995.
- CHEN C-C, ENGLAND S, AKOPIAN AN, AND WOOD JN. A sensory neuron-specific, proton-gated ion channel. *Proc Natl Acad Sci USA* 95: 10240–10245, 1998.
- CHEN X, BELMONTE C, AND RANG HP. Capsaicin and carbon dioxide act by distinct mechanisms on sensory nerve terminals in the cat cornea. *Pain* 70: 23–29, 1997.
- CONNER JA AND STEVENS CF. Voltage clamp studies of a transient outward membrane current in gastropod neural somata. *J Physiol (Lond)* 213: 21–30, 1971.
- COOPER BY, AHLQUIST ML, FRIEDMAN RM, AND LABANC JP. Properties of high-threshold mechanoreceptors in the goat oral mucosa. II. Dynamic and static reactivity in carrageenan-inflamed mucosa. *J Neurophysiol* 66: 1280–1290, 1991a.
- COOPER BY, AHLQUIST ML, FRIEDMAN RM, LOUGHNER BA, AND HEFT MW. Properties of high-threshold mechanoreceptors in the gingival mucosa. I. Responses to dynamic and static pressure. *J Neurophysiol* 66: 1272–1279, 1991b.
- COOPER BY, GU JG, PETRUSKA JC, AND JOHNSON RD. Subclassified small diameter afferent cell bodies manifest consistent patterns of ATP, proton and capsaicin-induced currents. *Abstr IASP* 9: 22, 1999a.
- COOPER BY, PETRUSKA JC, AND JOHNSON RD. Action potential features of immunocytochemically identified DRG cells sensitive to capsaicin, protons, or ATP. *Soc Neurosci Abstr* 25: 409, 1999b.
- COOPER BY, PETRUSKA JC, AND JOHNSON RD. ASIC-like currents in peptide containing subclassified cells of the adult rat DRG. *Soc Neurosci Abstr*. In press.

- COOPER BY AND SESSLE BJ. Anatomy and physiology of the trigeminal system. In: *The Headaches*, edited by Oleson J, Tfelt-Hansen P, and Welch KMA. New York: Raven, 1993, p. 87-93.
- DARIAN-SMITH I. The sense of touch: performance and peripheral neural processes. In: *Handbook of Physiology. The Nervous System. Sensory Processes*. Washington, DC: Am. Physiol. Soc., 1984a, sect. 1, vol. III, p. 739-788.
- DARIAN-SMITH I. Thermal sensibility. In: *Handbook of Physiology. The Nervous System. Sensory Processes*. Washington, DC: Am. Physiol. Soc., 1984b, sect. 1, vol. III, p. 879-913.
- DEL MAR LP AND SCROGGS RS. Lactoseries carbohydrate antigen, Gal1-4GlcNAc-R, is expressed by a subpopulation of capsaicin-sensitive rat sensory neurons. *J Neurophysiol* 76: 2192-2199, 1996.
- DIB-HAJI S, TYRRELL L, BLACK JA, AND WAXMAN SG. Na_v1, a novel voltage-gated Na channel, is expressed preferentially in peripheral sensory neurons and down regulated after axotomy. *Proc Natl Acad Sci USA* 95: 8963-8968, 1998.
- DIOUHRI L, BLEAZARD L, AND LAWSON SN. Association of somatic action potential shape with sensory receptive properties in guinea-pig dorsal root ganglion neurones. *J Physiol (Lond)* 513: 857-872, 1998.
- DOUGHERTY PM, PALECEK J, PALECKOVA V, AND WILLIS WD. Neurokinin-1 and neurokinin-2 antagonists attenuate the responses and NK-1 antagonists prevent the sensitization of primate spinothalamic tract neurons after intradermal capsaicin. *J Neurophysiol* 72: 1464-1475, 1994.
- GIBBINS IL, WATTCROW D, AND COVENTRY B. Two immunohistochemically identified populations of calcitonin gene-related peptide (CGRP)-immunoreactive axons in human skin. *Brain Res* 414: 143-148, 1987.
- GOLD MS, SHUSTER MJ, AND LEVINE JD. Characterization of six voltage-gated K⁺ currents in adult rat sensory neurons. *J Neurophysiol* 75: 2629-2646, 1996.
- HAIR JE, ANDERSON RE, TATHAM RL, AND CLARK WC. *Multivariate Data Analysis*. Englewood Cliffs, NJ: Prentice Hall, 1998, p. 467-515.
- HARPER AA AND LAWSON SN. Electrical properties of rat dorsal root ganglion neurones with different peripheral nerve conduction velocities. *J Physiol (Lond)* 359: 47-63, 1985.
- HOKFELT T, ELDE R, JOHANSSON O, LUFT R, NILSSON G, AND ARIMURA A. Immunohistochemical evidence for separate populations of somatostatin-containing and substance P-containing primary afferent neurons in the rat. *Neuroscience* 1: 131-136, 1976.
- HOLZER P. Local effector functions of capsaicin-sensitive sensory nerve endings: involvement of tachykinins, calcitonin gene-related peptide and other neuropeptides. *Neuroscience* 24: 739-768, 1988.
- HONORE P, MENNING PM, ROGERS SD, NICHOLS ML, BASBAUM AI, BESSON JM, AND MANTYH PW. Spinal substance P receptor expression and internalization in acute, short-term, and long-term inflammatory pain states. *J Neurosci* 19: 7670-7678, 1999.
- IGGO A. Sensory receptors in the skin of mammals and their sensory functions. *Rev Neurol* 141: 599-613, 1985.
- KITCHENER PD, WILSON P, AND SNOW PJ. Selective labelling of primary sensory afferent terminals in lamina II of the dorsal horn by injection of *Bandeiraea simplicifolia* isolectin B4 into peripheral nerves. *Neuroscience* 54: 545-551, 1993.
- KOERBER HR, DRUZINSKY RE, AND MENDELL LM. Properties of somata of spinal dorsal root ganglion cells differ according to peripheral receptor innervated. *J Neurophysiol* 60: 1584-1596, 1988.
- LAWSON SN. Peptides and cutaneous polymodal nociceptor neurones. In: *Progress in Brain Research. Peptides and Cutaneous Polymodal Nociceptor Neurones*, edited by Kumazawa T, Kruger L, and Mizumura K. New York: Elsevier Science, 1996, vol. 113, p. 369-385.
- LAWSON SN, CREPPS BA, AND PERL ER. Relationship of substance P to afferent characteristics of dorsal root ganglion neurones in guinea-pig. *J Physiol (Lond)* 505: 177-191, 1997.
- LEAH JD, CAMERON AA, AND SNOW PJ. Neuropeptides in physiologically identified mammalian sensory neurones. *Neurosci Lett* 56: 257-263, 1985.
- LEE Y, KAWAI Y, SHIOSAKA S, TAKAMI K, KUYAMA H, HILLYARD CJ, GIRGIS S, MACINTYRE I, EMSON PC, AND TOHYAMA M. Coexistence of calcitonin gene-related peptide and substance P-like peptide in single cells of the trigeminal ganglion of the rat: immunohistochemical analysis. *Brain Res* 330: 194-196, 1985a.
- LEE Y, TAKAMI K, KAWAI Y, GIRGIS S, HILLYARD CJ, MACINTYRE I, EMSON PC, AND TOHYAMA M. Distribution of calcitonin gene-related peptide in the rat peripheral nervous system with reference to its coexistence with substance P. *Neuroscience* 15: 1227-1237, 1985b.
- LENBECK P AND HOLZER P. Substance P as a neurogenic mediator of antidromic asodilation and neurogenic plasma extravasation. *Naunyn-Schmiedeberg's Arch Pharmacol* 310: 175-183, 1979.
- LEWIS C, NEIDHART S, HOLY C, NORTH RA, BUELL G, AND SURPRENANT A. Coexpression of P2X2 and P2X3 receptor subunits can account for ATP-gated currents in sensory neurons. *Nature* 377: 432-435, 1995.
- LINGUEGLIA E, DE WELLE JR, BASSILANA F, HEURTEAUX C, SAKAI H, WALDMANN R, AND LAZDUNSKI M. A modulatory subunit of acid-sensing ion channels in brain and dorsal root ganglion cells. *J Biol Chem* 272: 29778-29783, 1997.
- MAYER ML AND WESTBROOK GL. A voltage-clamp analysis of inward (anomalous) rectification in mouse spinal sensory ganglion neurones. *J Physiol (Lond)* 340: 19-45, 1983.
- MCCARTHY PW AND LAWSON SN. Cell type and conduction velocity of rat primary sensory neurons with calcitonin gene-related peptide-like immunoreactivity. *Neuroscience* 34: 623-632, 1990.
- MCCARTHY PW AND LAWSON SN. Differing action potential shapes in rat dorsal root ganglion neurones related to their substance P and calcitonin gene-related peptide immunoreactivity. *J Comp Neurol* 388: 547-549, 1997.
- MENSE S. Nociception from skeletal muscle in relation to clinical muscle pain. *Pain* 54: 241-289, 1993.
- MEYER RA, DAVIS KD, COHEN RH, TREEDE R-D, AND CAMPBELL JN. Mechanically insensitive afferents (MIAs) in cutaneous nerves of monkey. *Brain Res* 561: 252-261, 1991.
- MOLLIVER DC, WRIGHT DE, LEITNER ML, PARSADANIAN AS, DOSTER K, WEN D, YAN Q, AND SNIDER WD. IB4-binding DRG neurons switch from NGF to GDNF dependence in early postnatal life. *Neuron* 19: 849-861, 1997.
- NEUGERBAUER V, WEIRETTER F, AND SCHABLE H-G. The involvement of substance P and neurokinin-1 receptors in the hyperexcitability of dorsal horn neurons during development of acute arthritis in rat's knee joint. *J Neurophysiol* 73: 1574-1583, 1995.
- NEUMANN S, DOUBELL TP, LESLIE T, AND WOOLF CJ. Inflammatory pain hypersensitivity mediated by phenotypic switch in myelinated primary sensory neurons. *Nature* 384: 360-364, 1996.
- PERL ER. Myelinated afferent fibers innervating the primate skin and their response to noxious stimuli. *J Physiol (Lond)* 197: 593-615, 1968.
- PERRY MJ AND LAWSON SN. Differences in expression of oligosaccharides, neuropeptides, carbonic anhydrase and neurofilament in rat primary afferent neurons retrogradely labelled via skin, muscle or visceral nerves. *Neuroscience* 85: 293-310, 1998.
- PETRUSKA JC, COOPER BY, JOHNSON RD, AND GU JG. Co-expression of distinct functional P_{2X} receptors in primary afferents with the predominance of fast kinetics in a subpopulation of nociceptors. *Exp Brain Res*. In press, 2000a.
- PETRUSKA JC, COOPER BY, GU JG, RAU KK, AND JOHNSON RD. Distribution of P2X₁, P2X₂, and P2X₃ receptor subunits in rat primary afferents: relation to population markers and specific cell types. *J Chem Neuroanatomy*. In press, 2000b.
- PETRUSKA JC, STREIT WJ, AND JOHNSON RD. Localization of unmyelinated axons in rat skin and mucocutaneous tissue utilizing the isolectin GS-IB4. *Somatosens Mot Res* 14: 17-26, 1997.
- PLENDERLEITH MB AND SNOW PJ. The plant lectin *Bandeiraea simplicifolia* I-B4 identifies a subpopulation of small diameter primary sensory neurones which innervate the skin in the rat. *Neurosci Lett* 159: 17-20, 1993.
- RITTER AM AND MENDELL LM. Somal membrane properties of physiologically identified sensory neurons in the rat: effects of nerve growth factor. *J Neurophysiol* 68: 2033-2041, 1992.
- ROSE RD, KOERBER HR, SEDIVEC MJ, AND MENDELL LM. Somal action potential duration differs in identified primary afferents. *Neurosci Lett* 63: 259-264, 1986.
- ROY MR AND NARAHASHI T. Differential properties of tetrodotoxin-sensitive and tetrodotoxin-resistant sodium channels in rat dorsal root ganglion neurons. *J Neurosci* 12: 2104-2111, 1992.
- SCHABLE HG AND GRUBB BD. Afferent and spinal mechanisms of joint pain. *Pain* 55: 5-54, 1993.
- SCHABLE H-G AND SCHMIDT RF. Activation of groups III and IV sensory units in medial articular nerve by local mechanical stimulation of knee joint. *J Neurophysiol* 49: 35-44, 1983.
- STREIT WJ, SCHULTE BA, BALENTINE DJ, AND SPICER SS. Histochemical localization of galactose-containing glycoconjugates in sensory neurons and their processes in the central and peripheral nervous system of the rat. *J Histochem Cytochem* 33: 1042-1052, 1985.

- STREIT WJ, SCHULTE BA, BALENTINE JD, AND SPICER SS. Evidence for glycoconjugate in nociceptive primary sensory neurons and its origin from the Golgi complex. *Brain Res* 377: 1-17, 1986.
- STUCKY CL AND LEWIN GR. Isolectin B₄-positive and -negative nociceptors are functionally distinct. *J Neurosci* 19: 6497-6505, 1999.
- SZOLCSÁNYI J, ANTON F, REEH PW, AND HANDWERKER HO. Selective excitation by capsaicin of mechano-heat sensitive nociceptors in rat skin. *Brain Res* 446: 262-268, 1988.
- TALUKDER G AND HARRISON NL. On the mechanism of modulation of transient outward current in cultured rat hippocampal neurons by di- and trivalent cations. *J Neurophysiol* 73: 73-79, 1995.
- TANELIAN DL AND BEURMAN RW. Responses of rabbit corneal nociceptors to mechanical and thermal stimulation. *Exp Neurol* 84: 165-178, 1984.
- TATE S, BENN S, HICK C, TREZISE D, JOHN V, MANNION RJ, COSTIGAN M, PLUMPTON C, GROSE D, GLADWELL Z, KENDALL G, DALE K, BOUNTRA S, AND WOLF CJ. Two sodium channels contribute to the TTX-R sodium current in primary sensory neurons. *Nature Neurosci* 1: 653-655, 1998.
- TOMINAGA M, CATERINA MJ, MALMBERG AB, ROSEN TA, GILBERT H, SKINNER K, RAUMANN BE, BASBAUM AI, AND JULIUS D. The cloned capsaicin receptor integrates multiple pain-producing stimuli. *Neuron* 21: 531-543, 1998.
- TREDE R-D, MEYER RA, AND CAMPBELL JN. Myelinated mechanically insensitive afferents from monkey hairy skin: heat-response properties. *J Neurophysiol* 80: 1082-1093, 1998.
- UENO S, TSUDA M, IWANAGA T, AND INOUE K. Cell type-specific ATP-activated responses in rat dorsal root ganglion neurons. *Br J Pharmacol* 126: 429-436, 1999.
- VERGE VM, RICHARDSON PM, BENOIT R, AND RIOPELLE RJ. Histochemical characterization of sensory neurons with high-affinity receptors for nerve growth factor. *J Neurocytol* 18: 583-591, 1989.
- VILLIÈRE V AND MCLACHLAN EM. Electrophysiological properties of neurons in intact rat dorsal root ganglia classified by conduction velocity and action potential duration. *J Neurophysiol* 76: 1924-1941, 1996.
- WADDELL PJ AND LAWSON SN. Electrophysiological properties of subpopulations of rat dorsal root ganglion neurons in vitro. *Neuroscience* 36: 811-822, 1990.
- WALDMANN R, BASSILANA F, DE WELLES JR, CHAMPIGNY G, HEURTEAUX C, AND LAZDUNSKI M. Molecular cloning of a non-inactivating proton-gated Na⁺ channel specific for sensory neurons. *J Biol Chem* 272: 20975-20978, 1997a.
- WALDMANN R, CHAMPIGNY G, BASSILANA F, HEURTEAUX C, AND LAZDUNSKI M. A proton-gated cation channel involved in acid-sensing. *Nature* 386: 173-177, 1997b.
- WALDMANN R, CHAMPIGNY G, LINGUEGLIA E, DE WELLES JR, HEURTEAUX C, AND LAZDUNSKI M. H(+)-gated cation channels. *Ann NY Acad Sci* 868: 67-76, 1999.
- WANG H, RIVERO-MELIAN C, ROBERTSON B, AND GRANT G. Transganglionic transport and binding of the isolectin B₄ from *Griffonia simplicifolia* I in rat primary sensory neurons. *Neuroscience* 62: 539-551, 1994.
- WANG HF, ROBERTSON B, AND GRANT G. Anterograde transport of horseradish-peroxidase conjugated isolectin B₄ from *Griffonia simplicifolia* I in spinal primary sensory neurons of the rat. *Brain Res* 811: 34-39, 1998.
- WEIDNER C, SCHMELZ M, SCHMIDT R, HANSSON B, HANDWERKER HO, AND TOREBJÖRK HE. Functional attributes discriminating mechano-insensitive and mechano-responsive C nociceptors in human skin. *J Neurosci* 19: 10184-10190, 1999.
- YOSHIDA SH AND MATSUDA Y. Studies on sensory neurons of the mouse with intracellular recording and horseradish peroxidase injection techniques. *J Neurophysiol* 42: 1134-1145, 1979.

Sense and specificity: a molecular identity for nociceptors

Michael J Caterina* and David Julius†

Recent cloning efforts have identified families of ligand- or voltage-gated ion channels that are expressed by pain-sensing primary afferent neurons. Pharmacological, electrophysiological and genetic studies are beginning to reveal how these signaling molecules specify roles for subsets of sensory neurons in the pain pathway.

Addresses

Department of Cellular and Molecular Pharmacology, University of California – San Francisco, 513 Parnassus Avenue, San Francisco, California 94143-0450, USA

*e-mail: mcateri@itsa.ucsf.edu

†e-mail: julius@socrates.ucsf.edu

Current Opinion in Neurobiology 1999, 9:525–530

0959-4388/99/\$ – see front matter © 1999 Elsevier Science Ltd. All rights reserved.

Abbreviations

ASIC	acid-sensing ion channel
ATP	adenosine triphosphate
CGRP	calcitonin-gene-related peptide
DRASIC	acid-sensing ion-channel subtype
ENaC	amiloride-sensitive epithelial sodium channel
IB4	<i>Griffonia simplicifolia</i> isolectin B4
MDEG2	acid-sensing ion-channel subtype
P2X	ATP-gated ion channel
P2Y	G-protein-coupled ATP receptor
PN1	sodium channel subtype, TTX-S
SNS/PN3	sodium channel subtype, TTX-R
SNS2/NaN	sodium channel subtype, TTX-R
TTX-R	tetrodotoxin-resistant sodium channel
TTX-S	tetrodotoxin-sensitive sodium channel
VGSC	voltage-gated sodium channel
VR	vanilloid receptor
VRL-1	VR-like protein 1

Introduction

In mammals, the detection of potentially injurious stimuli is carried out by neurons in the pain pathway. Specialized cells within the peripheral nervous system are selectively equipped to detect noxious thermal, chemical or mechanical stimuli and to report the presence of these stimuli to the central nervous system [1]. These so-called nociceptive neurons are anatomically and functionally distinct from the neurons that detect innocuous stimuli, such as a light touch or gentle warming. Nociceptive neurons, such as primary sensory cells of the visual, olfactory and gustatory systems [2–6], express proteins that are believed to convey upon them their discrete sensory properties. Among these are a number of ion channels, identified within the past three years, that appear to be expressed exclusively or preferentially within selected subsets of primary afferent neurons (Figure 1). Ongoing studies of these molecules promise to provide insights into the basic mechanisms of nociception, the heterogeneity of nociceptor subtypes, and the changes undergone by these cells during chronic pain states of neuropathic or inflammatory origin.








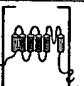






Using the tools of molecular biology, it is now possible to identify specific receptors and ion channels whose pharmacological and electrophysiological properties determine the functional characteristics of primary sensory neurons. Below, we highlight several areas in which significant progress has been made over the past couple of years.

How many types of nociceptor exist? What do they express and why?

Nociceptors can be broadly divided into two classes [1]: one group has small-diameter cell bodies and slowly conducting, unmyelinated axons (known as C fibers), whereas the other has medium-diameter cell bodies and faster conducting, lightly myelinated axons (known as Aδ fibers). These populations, however, are neither functionally nor anatomically homogeneous. C fibers, for example, can be further subdivided according to the noxious sensory modalities to which they respond. Many are polymodal, in that they respond to mechanical, thermal and chemical stimuli, whereas others are activated by only a subset of these modalities. Alternatively, C fiber nociceptors can be subdivided on the basis of histological markers [7–9]. One major group expresses pro-inflammatory peptides, such as substance P and calcitonin-gene-related peptide (CGRP), and project to the most superficial layers of the spinal cord dorsal horn (i.e. lamina I and the outer zone of lamina II). A second group does not express substance P or CGRP, but can be identified by the presence of specific enzymes (e.g. fluoride-resistant acid phosphatase) or binding sites for the lectin IB4. In comparison with substance-P-positive cells, these non-peptidergic C fibers project to the slightly deeper inner lamina II of the spinal cord dorsal horn. Molliver *et al.* [8] found that these two classes of neurons also differ in their expression of neurotrophin receptors and, consequently, in their responsiveness to these neurotrophins.

Are there functional correlates of these histological distinctions? Both neuronal classes are believed to respond to noxious thermal, chemical and mechanical stimuli, but recent studies suggest that these nociceptor cell types may contribute differentially to the initiation and maintenance of pain. For instance, peptidergic neurons appear to be the major effectors of neurogenic inflammation, releasing pro-inflammatory peptides such as substance P from their peripheral terminals in response to activation [10,11]. It also seems that these neurons are involved in the chronic pain that results from tissue inflammation [12]. In contrast, Malmberg *et al.*'s [13] analysis of protein kinase C gamma (PKCγ) knockout mice suggests that the IB4-positive, non-peptidergic neuronal population is more involved in chronic pain resulting from nerve injury. Further support for functional differences between these two cell types comes from a recent electrophysiological study by Stucky and Lewin [14], who found that IB4-positive and

Figure 1

Ion-channel subtype	Subunit topology	Stimuli and modulators	Expression in sensory neurons			Expressed outside sensory ganglia?
			Small-diameter	Medium-diameter	Large-diameter	
P2X3 P2X2		ATP H ⁺				No Yes
ASIC α ASIC β DRASIC MDEG2		H ⁺ Mechanical stimulus				Yes No Yes Yes
SNS/PN3 SNS2/NaN PN1		Voltage				No No Yes
VR1 VRL-1		Vanilloids Heat H ⁺				No Yes

Current Opinion in Neurobiology

Summary of selected ion-channel subtypes expressed in primary afferent neurons of the pain pathway. VGSCs (such as SNS/PN3, SNS2/NaN and PN1) are composed from polypeptides that contain four tandem repeats of the subunit structure shown. All other channels depicted here are formed from multimers of the indicated subunits. Filled ovals in the VR topological structure indicate ankyrin repeat domains. Horizontal filled bars indicate the neuronal size range in which each ion-channel subtype has been found. For P2X3 and VR1, expression is confined mostly to small-diameter neurons, but some medium-diameter neurons also appear to express these proteins. P2X3 is expressed predominantly in IB4-positive neurons. ASIC α is expressed predominantly in IB4-negative neurons. VR1 is expressed in both IB4-positive and IB4-negative neurons.

IB4-negative cells exhibit differences in the magnitudes of voltage-gated sodium currents and of heat-evoked currents.

Like C fiber nociceptors, A δ nociceptors can respond to noxious thermal, mechanical and/or chemical stimuli. Although some histological heterogeneity has been reported among these cells, nociceptive A δ neurons have more classically been subdivided on functional grounds [1,15]. Type II A δ nociceptors, for instance, exhibit a very short response latency to thermal stimuli and are activated at a moderate threshold temperature of 43°C. These neurons are thought to be responsible for our initial sensation of a burning stimulus. Type I A δ nociceptors, on the other hand, exhibit a much longer response latency and are activated only at much higher stimulus temperatures (> 50°C). These neurons, along with nociceptive C fibers, contribute to more persistent painful sensations.

Undoubtedly, the above classification scheme is oversimplified. Moreover, much remains to be learned regarding the functional importance of histological specializations among nociceptors. Nevertheless, the existing data provide a framework within which to characterize the expression patterns of functionally relevant markers, such as the ion channels discussed below. Similarly, the study of these molecules should facilitate a more complete understanding of how nociceptor heterogeneity contributes to the discriminative properties of the pain pathway.

ATP-gated ion channels

Even though adenosine triphosphate (ATP) is best known for its intracellular roles, it has been recognized for several decades that this molecule also functions as a diffusible extracellular signal [16]. ATP released from secretory vesicles or lysed cells can bind to and activate purinergic G-protein-coupled (P2Y) or ionotropic (P2X) receptors. ATP evokes currents in cultured nociceptors [17] and

causes pain when applied to a blister base [18]. In addition, Gu and MacDermott [19] found that ATP can act presynaptically to increase glutamate release from primary afferent neuron terminals in the spinal cord. These and other observations support a role for ATP in the pain pathway. Of the seven P2X receptor subtypes cloned so far, at least six are expressed in sensory neurons [20]. Greatest attention has focused on the P2X3 subtype because it is expressed selectively in small-to-medium diameter sensory neurons, primarily in the IB4-positive subset of C fibers [21^{*}]. P2X3 receptors contribute to kinetically and pharmacologically distinct currents in these cells as homomeric channels or heteromeric complexes formed in conjunction with a second subtype, P2X2 [22–24]. The significance of this finding has yet to be established, but it nevertheless provides evidence that these neurons exhibit a sensory apparatus distinct from that of peptidergic nociceptors.

Acid-gated ion channels

It has been known for some time that tissue acidification, as occurs in the context of inflammation or ischemia, can trigger a sensation of pain [25,26], and that protons (H⁺) can evoke multiphasic cationic currents in voltage-clamped, cultured sensory neurons [27,28]. Waldmann *et al.* [29,30] have recently identified a family of cation channels that are gated by reductions in pH. These proteins, named ASICs (for acid-sensing ion channels) are related to amiloride-sensitive epithelial sodium channels (ENaCs) and the degenerin/mec family of ion channels from *Caenorhabditis elegans*. Worms bearing mutations in the latter proteins show defects in mechanosensation [31] or constitutive channel activation, resulting in neurodegeneration [32]. ENaCs and ASICs are thought to have the same overall topology as P2X ATP receptors (i.e. two transmembrane domains with cytoplasmic amino and carboxyl termini), but the two protein families share little, if any, primary sequence similarity [16]. Five ASIC subtypes have been described thus far, and each

exhibits a distinct pattern of activation kinetics, pH dependence, and tissue specificity [29,30,33,34*]. Four of these subtypes are expressed in small-diameter sensory neurons, making them candidate mediators of proton-evoked nociception. ASIC α is expressed in many tissues, but in sensory ganglia, it appears to be expressed selectively by some IB4-negative small-diameter neurons, in a pattern that is complementary to that of P2X3 [29,34*]. In contrast, ASIC β , an amino-terminal splice variant of ASIC α , is expressed only in sensory ganglia, where it can be found on subsets of large- and small-diameter neurons [34*]. ASIC α and ASIC β exhibit monophasic current responses in heterologous expression systems. Interestingly, however, heterologous co-expression of the other two ASIC subtypes found in sensory neurons, DRASIC and MDEG2, more closely recapitulates the multiphasic proton-evoked current responses observed in cultured sensory neurons [33]. Thus, different combinations of subunits *in vivo* may confer diverse proton-response properties on nociceptor subtypes.

Given the structural similarities between ASICs and the putative mechanosensitive channels of *C. elegans*, Chen *et al.* [34*] have suggested that members of this family may also be involved in the detection of noxious or innocuous mechanical stimuli. Support for this model comes from a recent study demonstrating a role for ENaC channels in aortic baroreceptor function [35]. A more definitive assessment of the role of this channel family in noxious and innocuous mechanosensation may come from analysis of mice in which genes encoding ASICs or ENaCs have been disrupted.

Vanilloid receptors

Capsaicin, the ingredient that makes 'hot' peppers burn, specifically activates cation channels on small- and medium-diameter nociceptors [36]. Because the action of capsaicin depends upon a vanilloid moiety within its chemical structure, the target of capsaicin action has been referred to as the vanilloid receptor (VR) [37]. Recently, our group [38] used an expression cloning strategy to isolate a cDNA from sensory ganglia that encodes a nonselective cation channel (called VR1) that is gated by capsaicin and other vanilloid-containing compounds. VR1 is also activated by acidification and by an increase in ambient temperature to levels ($> 43^{\circ}\text{C}$) that produce pain in humans and pain-related behaviors in animals [38,39**]. VR1 is selectively expressed by both the substance-P-positive and the IB4-positive C fiber subclasses described above [39**,40*,41]. In addition, multiple-labeling experiments have revealed that other, less prevalent subsets of VR1-positive cells exist, including one that may represent capsaicin-responsive A δ neurons [40*].

The proton sensitivity and electrophysiological properties of VR1 raise the possibility that this channel mediates the delayed phase of the nociceptive response to tissue acidification, as previously suggested for native vanilloid receptors [42]. In addition, the temperature threshold exhibited by heterologously expressed VR1 is similar to the

$\sim 43^{\circ}\text{C}$ threshold of C fibers and type II A δ fibers [1], various chemical populations. So interpretation of the role of vanilloid co-receptors in heat-evoked nociception in a rat preparation, while some in agreement, while some in disagreement between capsaicin and heat-evoked nociception in sensory neurons. A recent study of heat-evoked nociception, are capsaicin and heat-evoked nociception, are capsaicin release of calcium. A multiple explanation for the multiple mechanisms of noxious thermal stimuli involve VR1.

Recent evidence comes from the identification of VR1 [43] protein 1 (VRL) but can be active exceeding 52°C strikingly similar *in vivo* [49] and f. saicin-insensitive [46*]. VRL-1 is ganglia it is more medium-to-large diameter profile and neurons [48*]. thermal response knockout expectation of the potential and chemical n

Voltage-gated channels

Voltage-gated sodium channels (VGSCs) are critical determinants of excitability. A remarkable property of sensory neurons is that they express VGSCs that are sensitive to inhibition (TTX-S), but also with atypical VGSCs that are resistant to this compound (TTX-R). Responses have been observed in neurons, and the inactivation kinetics on the occurrence of action potential

Recent molecular studies have identified a variety of VGSC isoforms. Among the TTX-R subtypes, PN1 and brain TTX-R subtyp

for C fibers and type II A δ fibers [1], various chemical populations. So interpretation of the role of vanilloid co-receptors in heat-evoked nociception in a rat preparation, while some in agreement, while some in disagreement between capsaicin and heat-evoked nociception in sensory neurons. A recent study of heat-evoked nociception, are capsaicin and heat-evoked nociception, are capsaicin release of calcium. A multiple explanation for the multiple mechanisms of noxious thermal stimuli involve VR1.

Recent evidence comes from the identification of VR1 [43] protein 1 (VRL) but can be active exceeding 52°C strikingly similar *in vivo* [49] and f. saicin-insensitive [46*]. VRL-1 is ganglia it is more medium-to-large diameter profile and neurons [48*]. thermal response knockout expectation of the potential and chemical n

Channels

Voltage-gated sodium channels (VGSCs) are critical determinants of excitability. A remarkable property of sensory neurons is that they express VGSCs that are sensitive to inhibition (TTX-S), but also with atypical VGSCs that are resistant to this compound (TTX-R). Responses have been observed in neurons, and the inactivation kinetics on the occurrence of action potential

Recent molecular studies have identified a variety of VGSC isoforms. Among the TTX-R subtypes, PN1 and brain TTX-R subtyp

identified, and they are e ganglia. SNS/PN3 is a T only within small- and m. The other TTX-R subty small-diameter neurons [5]. tance of these channels r mouse knockout study by provided evidence that S expression of TTX-R curr. Sensory neurons from mic detectable TTX-R curre TTX-S sodium current co compensatory overexpress fibers of these animals (t enhanced electrical excit also exhibit small-but signi ly and mechanically evoke as delays in the develop thermal hyperalgesia. Fut into the respective contrib S channels to nocicepti significance of this molecu

Convergence and divergence at the

The afferent sensory ne capacity to detect a range uli and to re-set stimuli tissue injury or disease. suggested two molecular ing flexibility and diversit of the nociceptor (Figure

First, a given noxious sti excitability through a nur mechanisms. Protons, for al ion-channel targets, in receptors [29,39**,59]. Li larize sensory neurons thr VRL-1 [38,48*]. Such dive subtypes to respond to a thresholds or time courset lated by analgesic or proal,

Second, certain signal tr multiple stimuli, providi capacity to regulate nocice multiple physiological variab exemplified by VR1, wh tion from chemical and changes in nociceptor ex or disease [39**].

Conclusions

The peripheral limb of the ber of specialized cell t sophisticated sensory reper of neurophysiology, anat

relationships betv geneity among th this convergence understanding of nervous system harmful environn

Acknowledgements

This work was support The American Cancer Schizophrenia and Dep

References and

Papers of particular int have been highlighted

- of special interest
- of outstanding int

1. Meyer RA, Camp nociception. In *The* Edinburgh: Churchill
2. Nathans J: Molec 1987; 10:163-19
3. Jones DT, Reed R: involved in odora
4. Buck L, Axel R: A receptors: a mol 65:175-187.
5. McLaughlin SK, M cell-specific G-pr 1992; 357:563-5
6. Hoon MA, Adler E: Putative mamma GPCRs with disti
7. Nagy JJ, Hunt SP: neurones in dors containing subst 7:89-97.
8. Molliver DC, Wrig Yan Q, Snider WD dependence in e
9. Snider WD, Mach about nociceptor
10. Cao YQ, Mantyh F • Primary afferent to intense pain. / See annotation [11*].
11. De Felipe C, Herr Laird JM, Belmont analgesia and ag substance P. *Nat*. These two papers [10*, my, physiology and bel tions for a major signa
12. Woolf CJ, Mannio substance: elucic pharmacology. *N*
13. Malmberg AB, Ci pain and reduce *Science* 1997; 27
14. Stucky CL, Lewin •• nociceptors are 19:6497-6505. This study is one of the tional distinctions betv sensory neurons, and r and tetrodotoxin-resista
15. Dubner R, Price D of behavior in mc

functional hetero being clarified. As develop a better ough which the e of potentially

Institutes of Health, ation for Research on

Reading

al period of review,

al mechanisms of FD, Melzack R.

Annu Rev Neurosci

specific G protein 1989; 244:790-795.

code odorant on. *Cell* 1991;

Custducin is a taste t enducins. *Nature*

NJP, Zuker CS: of taste-specific 1999; 96:541-551.

atase-containing from those science 1982;

S, Doster K, Wen D, from NGF to GDNF 7; 19:849-861.

source: new Ideas

stein CJ, Basbaum AI: experience moderate

Doyle CA, Smith AJ, ed nociception, receptor for

combination with anat and surprising func the pain pathway.

is lacking genetic

Preserved acute ing PKC gamma.

negative 1999,

tools to look for func tive small-diameter in both heat-evoked

neural correlates sory-discriminative

- aspects of pain. In *Pain in the Trigeminal Region*. Edited by Anderson DJ, Kennedy MB. Amsterdam: Elsevier; 1977:57-66.
16. Brake AJ, Julius D: Signaling by extracellular nucleotides. *Annu Rev Cell Dev Biol* 1996, 12:519-541.
 17. Jahr CE, Jessell TM: ATP excites a subpopulation of rat dorsal horn neurons. *Nature* 1983, 304:730-733.
 18. Bleehen T, Keele CA: Observations on the algogenic actions of adenosine compounds on the human blister base preparation. *Pain* 1977, 3:367-377.
 19. Gu JG, MacDermott AB: Activation of ATP P2X receptors elicits glutamate release from sensory neuron synapses. *Nature* 1997, 389:749-753.
 20. Collo G, North RA, Kawashima E, Merlo-Pich E, Neidhart S, Surprenant A, North RA, Elde R: P2X3 is expressed by DRG neurons and properties of an extended family of ATP-gated ion channels. *J Neurosci* 1996, 16:2495-2507.
 21. Vulchanova L, Riedl MS, Shuster SJ, Stone LS, Hargreaves KM, Buell G, Surprenant A, North RA, Elde R: P2X3 is expressed by DRG neurons that terminate in inner lamina II. *Eur J Neurosci* 1998, 10:3470-3478.
- Highlights the restricted expression pattern of P2X3 in a subset of IB4-positive neurons. Provides a potential functional specification for this subclass of sensory neurons.
22. Chen CC, Akopian AN, Silvillotti L, Colquhoun D, Burnstock G, Wood JN: A P2X purinoceptor expressed by a subset of sensory neurons. *Nature* 1995, 377:428-431.
 23. Lewis C, Neidhart S, Holy C, North RA, Buell G, Surprenant A: Coexpression of P2X2 and P2X3 receptor subunits can account for ATP-gated currents in sensory neurons. *Nature* 1995, 377:432-435.
 24. Cook SP, Vulchanova L, Hargreaves KM, Elde R, McCleskey EW: Distinct ATP receptors on pain-sensing and stretch-sensing neurons. *Nature* 1997, 387:505-508.
 25. Jacobus W, Taylor GJ, Hollis DP, Nunnally RL: Phosphorus nuclear magnetic resonance of perfused working rat hearts. *Nature* 1977, 265:756-758.
 26. Steen KH, Reeh PW, Anton F, Handwerker HO: Protons selectively induce lasting excitation and sensitization to mechanical stimulation of nociceptors in rat skin, *in vivo*. *J Neurosci* 1992, 12:86-95.
 27. Krishtal OA, Pidoplichko VI: A receptor for protons in the nerve cell membrane. *Neuroscience* 1980, 5:2325-2327.
 28. Bevan S, Yeats J: Protons activate a cation conductance in a subpopulation of rat dorsal root ganglion neurones. *J Physiol (Lond)* 1991, 433:145-161.
 29. Waldmann R, Champigny G, Bassilana F, Heurteaux C, Lazdunski M: A proton-gated channel involved in acid sensing. *Nature* 1997, 386:173-177.
 30. Waldmann R, Bassilana F, Weille J, Champigny G, Heurteaux C, Lazdunski M: Molecular cloning of a non-inactivating proton-gated Na⁺ channel specific for sensory neurons. *J Biol Chem* 1997, 272:20975-20978.
 31. Hong K, Driscoll M: A transmembrane domain of the putative channel subunit MEC-4 influences mechanotransduction and neurodegeneration in *C. elegans*. *Nature* 1994, 367:470-473.
 32. Driscoll M, Chalfie M: The mec-4 gene is a member of a family of *Caenorhabditis elegans* genes that can mutate to induce neuronal degeneration. *Nature* 1991, 349:588-593.
 33. Lingueglia E, de Weille JR, Bassilana F, Heurteaux C, Sakai H, Waldmann R, Lazdunski M: A modulatory subunit of acid sensing ion channels in brain and dorsal root ganglion cells. *J Biol Chem* 1997, 272:29778-29783.
 34. Chen CC, England S, Akopian AN, Wood JN: A sensory neuron specific, proton gated ion channel. *Proc Natl Acad Sci USA* 1998, 95:10240-10245.
- Reveals that at least two splice variants of ASIC exist and exhibit differential distributions within sensory ganglia. Such findings could underline differential proton sensitivities among sensory neurons.
35. Drummond HA, Price MP, Welsh MJ, Abboud FM: A molecular component of the arterial baroreceptor mechanotransducer. *Neuron* 1998, 21:1435-1441.
 36. Szolcsanyi J: Actions of capsaicin on sensory neurons. In *Capsaicin in the Study of Pain*. Edited by Wood J. London: Academic Press; 1993:1-26.
 37. Szallasi A, Blumberg PM: Resiniferatoxin, a phorbol-related diterpene, acts as an ultrapotent analog of capsaicin, the irritant constituent in red pepper. *Neuroscience* 1989, 30:515-520.
 38. Caterina MJ, Schumacher MA, Tominaga M, Rosen TA, Levine JD, Julius D: The capsaicin receptor: a heat-activated ion channel in the pain pathway. *Nature* 1997, 389:816-824.
 39. Tominaga M, Caterina MJ, Malmberg AB, Rosen TA, Gilbert H, Skinner K, • • Raumann BE, Basbaum AI, Julius D: The cloned capsaicin receptor integrates multiple pain-producing stimuli. *Neuron* 1998, 21:1-20.
- This article further details the distribution of the capsaicin receptor (see [38]). It also shows that this channel can be activated by protons and provides evidence suggesting that it can function as an integrator of noxious thermal and chemical stimuli.
40. Michael GJ, Priestly JV: Differential expression of the mRNA for the • vanilloid receptor subtype 1 in cells of the adult rat dorsal root and nodose ganglia and its downregulation by axotomy. *J Neurosci* 1999, 19:1844-1854.
- By combining quantitative *in situ* hybridization and immunohistochemistry, these authors explore the distribution of VR1 and reveal complex patterns of overlapping molecular markers within sensory ganglia.
41. Guo A, Vulchanova L, Wang J, Li X, Elde R: Immunocytochemical localization of vanilloid receptor 1 (VR1): relationship to neuropeptides, the P2X3 purinoceptor and IB4 binding sites. *Eur J Neurosci* 1999, 11:946-958.
 42. Bevan S, Forbes CA, Winter J: Protons and capsaicin activate the same ion channels in rat isolated dorsal root ganglion neurones. *J Physiol (Lond)* 1993, 459:401P.
 43. Dickenson AH, Dray A: Selective antagonism of capsaicin by capsazepine: evidence for a spinal receptor site in capsaicin-induced nociception. *Br J Pharmacol* 1991, 104:1045-1049.
 44. Kirschstein T, Busselberg D, Treede RD: Coexpression of heat-evoked and capsaicin-evoked inward currents in acutely dissociated rat dorsal root ganglion neurons. *Neurosci Lett* 1997, 231:33-36.
 45. Vyklíček L, Vlachova V, Vitaskova Z, Dittert I, Kabat M, Orkand RK: Temperature coefficient of membrane currents induced by noxious heat in sensory neurones in the rat. *J Physiol (Lond)* 1999, 517:181-192.
 46. Nagy I, Rang H: Noxious heat activates all capsaicin-sensitive and • also a sub-population of capsaicin-insensitive dorsal root ganglion neurons. *Neuroscience* 1999, 88:995-997.
- This study provides physiological evidence for the existence of at least two classes of noxious thermal responses in cultured sensory neurons – high (52°C) and low (43°C) thermal thresholds – and relates these responses to capsaicin sensitivity and cell size.
47. Reichling DB, Levine JD: Heat transduction in rat sensory neurons by calcium-dependent activation of a cation channel. *Proc Natl Acad Sci USA* 1997, 94:7006-7011.
 48. Caterina MJ, Rosen TA, Tominaga M, Brake AJ, Julius D: A capsaicin • receptor homologue with a high threshold for noxious heat. *Nature* 1999, 398:436-441.
- This study identifies a vanilloid receptor homologue that appears to provide a molecular basis for the findings of Nagy and Rang [46*].
49. Meyer RD, Campbell JN: Myelinated nociceptor afferents account for the hyperalgesia that follows a burn to the hand. *Science* 1981, 213:1527-1529.
 50. Caffrey JM, Eng DL, Black JA, Waxman SG, Kocsis JD: Three types of sodium channels in adult rat dorsal root ganglion neurons. *Brain Res* 1992, 592:283-297.
 51. Rush AM, Elliot JR: Phenytoin and carbamazepine: differential inhibition of sodium currents in small cells from adult rat dorsal root ganglia. *Neurosci Lett* 1997, 226:95-98.
 52. Scholz A, Appel N, Vogel W: Two types of TTX-resistant and one TTX-sensitive Na⁺ channel in rat dorsal root ganglion neurons and their blockade by halothane. *Eur J Neurosci* 1998, 10:2547-2556.
 53. Sangameswaran L, Fish L, Koch B, Rabert D, Delgado S, Ilnicka M, Jakeman L, Novakovic S, Wond K, Sze P et al.: A novel tetrodotoxin-sensitive, voltage-gated sodium channel expressed in rat and human dorsal root ganglia. *J Biol Chem* 1997, 272:14805-14809.

54. Akopian AN, Souslova V, England S, Okuse K, Ogata N, Ure J, Smith A, Kerr BJ, McMahon SB, Boyce S *et al*: The tetrodotoxin-resistant sodium channel SNS has a specialized function in pain pathways. *Nat Neurosci* 1999, 2:541-548.
The authors take a genetic approach to dissect the role of a TTX-R sodium channel subtype (SNS) in nociception. Using a broad range of techniques, they demonstrate that while this molecule is not essential for the generation of action potentials, its absence leads to loss of TTX-R currents in cultured sensory neurons, an increase in C fiber excitability, and changes in acute thermal and mechanical nociception.
55. Akopian AN, Silvilotti L, Wood JN: A tetrodotoxin-resistant voltage-gated sodium channel expressed by sensory neurons. *Nature* 1996, 379:257-262.
56. Sangameswaran L, Delgado S, Fish L, Koch B, Jakeman L, Stewart G, Sze P, Hunter J, Eglon R, Herman R: Structure and function of a novel voltage-gated, tetrodotoxin-resistant sodium channel specific to sensory neurons. *J Biol Chem* 1996, 271:5953-5956.
57. Dib-Hajj SD, Tyrrell L, Black JA, Waxman SG: Na_v1, a novel voltage gated Na channel, is expressed preferentially in peripheral sensory neurons and downregulated after axotomy. *Proc Natl Acad Sci USA* 1998, 95:8963-8968.
See annotation [58*].
58. Tate S, Benn S, Hick C, Trezise D, John V, Mannion R, Costigan M, Plumpton C, Grose D, Gladwell Z, Kendall G, Dale K, Bountra C, Woolf CJ: Two sodium channels contribute to the TTX-R sodium current in primary sensory neurons. *Nat Neurosci* 1998, 1:653-655.
Together, these two studies [57*,58*] reveal the existence of a second TTX-R sodium channel subtype (SNS2/PN3) that is electrophysiologically distinct from SNS/PN3, and detail the differential expression patterns of these subtypes.
59. Li C, Peoples RW, Weight FF: Enhancement of ATP-activated current by protons in dorsal root ganglion neurons. *Eur J Physiol* 1997, 433:446-454.